Electronic Theses and Dissertations

Theses, Dissertations, and Major Papers

2004

Characterization of mammalian WDR1 during dynamic actin rearrangement events.

Tenley E. Noone
University of Windsor

Follow this and additional works at: https://scholar.uwindsor.ca/etd

CHARACTERIZATION OF MAMMALIAN WDR1 DURING DYNAMIC ACTIN REARRANGEMENT EVENTS

By Tenley E. Noone

A Thesis

Submitted to the Faculty of Graduate Studies and Research through the Department of Biological Sciences in Partial Fulfillment of the Requirements for the Degree of Master of Science at the University of Windsor

Windsor, Ontario, Canada

2004

© 2004 Tenley E. Noone

Library and
Archives Canada

Bibliothèque et
Archives Canada

Published Heritage
Branch

Direction du
Patrimoine de l'édition

395 Wellington Street
Ottawa ON K1A 0N4
Canada

395, rue Wellington
Ottawa ON K1A 0N4
Canada

Canada

CHARACTERIZATION OF MAMMALIAN WDR1 DURING DYNAMIC ACTIN REARRANGEMENT EVENTS

Submitted by

Tenley E. Noone

APPROVED BY:

_____

Dr. Sirinart Ananvoranich
Department of Chemistry & Biochemistry

Dr. Adnan Ali
Department of Biological Sciences

Dr. Andrew Hubberstey, Advisor
Department of Biological Sciences

Dr. John Hudson, Chair of Defense
Department of Biological Sciences

Friday, September 24th, 2004

Abstract

The actin cytoskeleton functions within processes such as cell extension, migration, and neurogenesis; yet the mechanisms of actin regulation are not completely understood. WD repeat proteins (WDR1) have recently been shown to interact with actin and regulate cortical actin dynamics through interactions with cofilin in a number of species. However studies on mammalian WDR1 have not been reported. Further studies in chick systems have also indicated several cofilin-independent functions of WDR1 within cytokinesis and cell migration.

We investigated the human homologue of yeast WDR1 and identified the expression of two isoforms, a full length 60 kDa protein and an N-terminal truncated 50 kDa protein. Analysis of WDR1 expression in transformed and non-transformed cell lines indicated that the two isoforms were differentially expressed. Sequence analysis revealed the WD motifs were homologous to kelch motifs found within *Drosophila* kelch. Kelch containing proteins are believed to mediate protein-protein interactions. Protein interaction experiments demonstrated WDR1 bound actin and formed hetero-multimeric complexes; however no interaction with cofilin was observed. Localization studies showed WDR1 localized to actin filaments (similar to vinculin) and to areas undergoing actin rearrangement with cofilin and CAP1. Interestingly, WDR1 was shown to remain attached to glass coverslips as part of a WDR1 aggregated complex (WAC) after trypsin mediated cell detachment. Latrunculin A and cytochalasin D treatments indicated WDR1 may stabilize actin filaments during depolymerizing events.

iii

Therefore, these results have provided an initial characterization of the important role of hWDR1 within the critical cellular processes of attachment and migration, and have provided experimental avenues for future pursuit.

iv

Acknowledgements

I would like to thank my Supervisor Dr. Andrew Hubberstey for his patience, support, and the opportunity he gave me to explore this project. I would like to thank my committee members, Dr. Adnan Ali and Dr. Sirinart Ananvoranich, and the chair of my committee, Dr. John Hudson who have given me so much support and encouragement through my degree. I would like to thank the entire complement of faculty of biological sciences for their wisdom and guidance, for which I am very grateful to have shared. I thank the staff for their support and encouragement which made everyday enjoyable. I would like to acknowledge the past and present members of the Hubberstey lab for their help and humor. I would also like to thank my friends and fellow graduate students for their support and for making my experience at Windsor so enjoyable. I would also like to thank my parents, my godparents, my family, and Jason Johnston for all of their support and patience. Finally, I would like to thank the faculties of Science, Chemistry and Biochemistry, and Biology for my experience at Windsor.

V

Table of Contents

Chapter One: Introduction

Chapter Four: Conclusions and Future Directions

List of Figures

x

Chapter Three: Determination of WDR1 Proteins Functions during Cell Migration, Attachment, & Neurogenesis

List of Tables

List of Abbreviations

W- tryptophan
D- aspartic acid
H- histidine residue
G- glycine residue
WDR1- tryptophan and asparatic-acid residue repeat protein one
CAP1- cyclase-associated protein one
Aip1- actin interacting protein one
PCR- polymerase chain reaction
DEPC- diethyl pyrocarbonate
GST- glutathione-S-transferase
SB- sample buffer
MOPS- N-morpholinopropanesulfonic acid
RNA- ribbonucleic acid
DNA- deoxynucleic acid
GAPDH- glyceraldehydes phosphate dehydrogenase
PBS- phosphate buffered saline
ICC- immunocytochemistry
REF- rat embryonic fibroblast
HEK- human embryonic kidney
SDS- sodium dodecyl sulphate
aa- amino acid
kDa- kilo Dalton
bp- base pair
kb- kilobase
PAGE- polyacrylamide gel electrophoresis

Chapter 1

Introduction

The eukaryotic cytoskeleton is responsible for initiating and affecting many important cellular processes such as cell division, adhesion, cell migration, endocytosis/ exocytosis, neurogenesis, cell morphology and vesicle transport (Cooper, 2000). Loss of cytoskeletal regulation occurs in such prevalent diseases as cancer, Alzheimer's disease, and heart disease, therefore understanding the complex mechanisms regulating these processes is critical for the progress of both cellular biology and the production of improved medical therapies. The cytoskeleton is comprised of three major filament types; microfilaments, approximately 7 nm in diameter consist primarily of polymerized actin monomers; microtubules which are the thickest filaments (approximately 25 nm diameter) composed of mainly tubulin isoforms and intermediate filaments which unlike the previous two classes are comprised of a large variety of protein types (e.g. keratin and lamin) (Cooper, 2000). Each filament type performs discrete functions within the cell; however filament types are able to function synergistically to orchestrate complex cellular behaviours.

Our current understanding of the many proteins regulating the function and integration of cytoskeletal filaments is not yet complete, but is essential for the design of effective targeting of many prevalent diseases of the neurological, circulatory, digestive, and muscular systems. The focus of this thesis is to provide further insight into proteins regulating the actin cytoskeleton through the characterization of a recently identified

1

mammalian protein belonging to the WDR1 family of proteins, which are known to effect actin (Konzok et al., 1999; Mohri and Ono, 2003; Okada et al., 1999; Rodal et al., 1999). Actin microfilaments are thin flexible fibers composed of polymerized actin monomer proteins (filamentous or F-actin). F-actin can be ordered into complex structures of dense bundles and loose three-dimensional actin mesh-works consisting of additional proteins, such as myosin, which each participate to provide a means for cellular motility, cell extension/ neurogenesis, cytokinesis, cell surface tension and dynamic membrane functions (Bamburg et al., 1999). Microtubules differ from microfilaments in that they are hollow cylindrical rods of considerable diameter composed primarily of alpha and beta tubulin proteins which function to regulate cell shape, various cell movements, neurogenesis, intracellular organelle transport, and chromosome separation during mitosis (Goode et al., 2000). Intermediate filaments are distinct from the previous two classes of filaments in several ways, the first being their proteomic composition, which is highly variable depending on both their location and function (Pollard & Earnshaw, 2002). In addition, these filaments are not directly involved in cell motility or migration (Cooper, 2000). Intermediate filaments are comprised of intertwined protofilaments consisting of anti-parallel protein dimers which provide structural support to the cell through the provision of a scaffold to which organelle structures are able to integrate with dynamic cytoskeleton components (Pollard & Earnshaw, 2002).

Actin

The existence of actin was initially hypothesized in 1904 and first identified by Straub (1942) as a contractile element with myosin (Cooper, 2000). It has since been shown to form homogenous microfilament fibers conserved within all eukaryotic cells

(non-muscle actin) (Bamburg, 1999). Actin is one of the most abundant cytoskeletal proteins, typically accounting for 5- 20% of total cellular protein (Cooper, 2000). Actin is highly conserved across eukaryotic vertebrate and non-vertebrate organisms such as yeast, slime mold, worm, insect, frog and mammal and is predicted to associate with >60 binding proteins in higher eukaryotes (Cooper, 2000). The genome of *Saccharomyces cerevisiae* encodes one actin protein while the human genome encodes a total of six actin proteins with only two isoforms expressed within a tissue type (Kedes et al., 1985). The four muscle isoforms include α-cardiac, α-skeletal (both located within the sacromeric muscles of the skeletal and cardiac systems), α, γ (both expressed within smooth muscle), β and γ isoforms (both unique to non-muscle cells including immune cells, epithelial cells, and neural cells) (Kedes et al., 1985). This reflects a correlation between the relative complex capabilities of cellular function with the presence of a more complex actin cytoskeleton. Additionally, actin is able to interact with several other proteins such as fimbrin, tropomyosin, and myosin to expand its functional capabilities (Pollard et al., 2000).

The six mammalian actin genes remain highly conserved (~90% amino acid homology to the yeast actin gene) and transcribe a 43 kDa globular (G-actin) protein containing four domains which form a weak adenosine tri-phosphatase (ATPase) cleft structure that is capable of head-to-tail binding to other actin monomers (Otterbein et al., 2001; Pollard et al., 2000). The G-actin protein is able to alter its binding affinity for adenosine tri- or di-phosphate (ATP or ADP respectively) depending on the cytosolic salt concentration, cellular pH, cation availability and accessory protein binding (Otterbein et al., 2001; Pollard et al., 2000). The four domains, consisting primarily of α-helices and a

3

few β sheets, fold with direction from bound water molecules to encircle a central ATP binding cleft and periphery protein binding sites on the lateral loops (Otterbein et al., 2001). Each of the four domains interacts with a divalent cation (predominantly magnesium following the relative cytosolic availability, and to a lesser extent calcium) (Otterbein et al., 2001). The divalent ion bound centrally in the third domain is critical for the catalytic hydrolysis of ATP to ADP and is termed the catalytic ion (Blanchoin and Pollard, 2002). The catalytic cleft is comprised of two highly conserved β-hairpins within subdomain-1 which fold to interact with two homologous domains in subdomain 3 to generate the hydrolysis activity of the protein, which is coupled to the protein's conformational change but is not required for its polymerization (Otterbein et al., 2001). The protein binding loops predominantly located in subdomains 2 and 4 allow the association of actin with proteins such as gelsolin, profilin, and deoxyribonuclease (DNase) I and undergo the most pronounced conformational alterations upon hydrolysis (Otterbein et al., 2001). G-actin spontaneously interacts *in vitro* at cellular conditions through subdomain 2 (in the DNase I binding site) and is able to dimerize and further polymerize into F-actin. However, this process is highly regulated through many monomer, dimer, trimer and polymer binding proteins *in vivo* (Pollard & Earnshaw, 2002).

Filamentous Actin

In order to assemble F-actin filaments *in vivo,* two actin monomers must dimerize and further trimerize to effectively facilitate their head-to-tail binding to other actin dimers to yield short multimer fragments which are then incorporated to generate the extending filament (Figure 1.1) (Oosawa & Asakura, 1975). In the absence of actin

4

binding proteins, the stability of actin dimers and trimers is dramatically reduced and thus presents insurmountable difficulties for the direct study of dimer/ trimer interactions, however the use of *in vitro* polymerization assays has added to the current understanding of actin dynamics (Blanchoin and Pollard, 2002; Pollard et al., 2000).

Spontaneous polymerization will occur *in vitro* when the monomer concentration exceeds ~ 0.1 µM under physiological conditions; however within the cell the G-actin concentration is maintained at ~ 100 µM owing to the presence of actin associated proteins (discussed below) (Pollard et al., 2000). Actin was first characterized in association with myosin (a muscle motor protein) and so the terms for the ends of the filament are derived from the appearance of an actin-myosin filament with the pointed end equating to the minus (slow growing) end and the barbed end referring to the plus (fast growing) end (Figure 1.1) (Straub, 1942). The rate limiting step of actin polymerization is the initiation (nucleation) of the multiple dimer and trimer bindings (Oosawa & Asakura 1975). As stated, the hydrolysis of the ATP molecule bound within the actin protein is not required for filament polymerization or filament nucleation (Blanchoin and Pollard, 2002). The conformational state of ATP-bound actin is more favorable for maximizing accessibility of the actin binding site by other monomers; however ADP-bound actin may still remain bound, although the bond strain is increased thus typically inhibiting ADP- filament nucleation (Otterbein et al., 2001). The cell utilizes the additional strain of the ADP-actin-actin bond within filaments to aid accessory proteins in the removal of monomers because the altered conformation changes the availability of protein binding sites as well as the reduced actin bond strength

5

Figure 1.1 Regulation and function of actin within dynamic cellular processes.

The polymerization dynamics of actin generate force for cell migration and neurite extension. A, the regulation of actin polymerization by pointed-end capping proteins (purple ovals), barbed-end capping proteins (blue ovals), monomer sequestering proteins (pink diamonds) and monomer recycling proteins (gray ovals) is depicted. The hydrolyzed (GDP-bound) actin is shown in blue while the ATP-bound actin is shown in red. Actin is removed from the pointed-end of the filament and incorporated at the barbed-end. B, branched cortical actin meshwork at the edge of the cell. C, (adapted from (Sarmiere and Bamburg, 2004) actin within an extending neurite within the P domain is located at the neurite tip (blue bracket), the T domain behind the tip in the neurite pad (red bracket), and the C domain within the neurite extension (purple bracket). D, (adapted from (Condeelis et al., 2001; Critchley, 2000; Dawe et al., 2003; Medley et al., 2003)the leading lamellipodia of a migrating cell demonstrating an extending filopodia. E, (apdapted from Minamide et al. 2003; Medley, Buchbinder et al. 2003) FA complex within the tip of the attaching filopodia. The EC signal (blue circle) binds the cell surface receptor (gray dimer) and signals through the membrane receptor (yellow) to the FA proteins (pink).

6
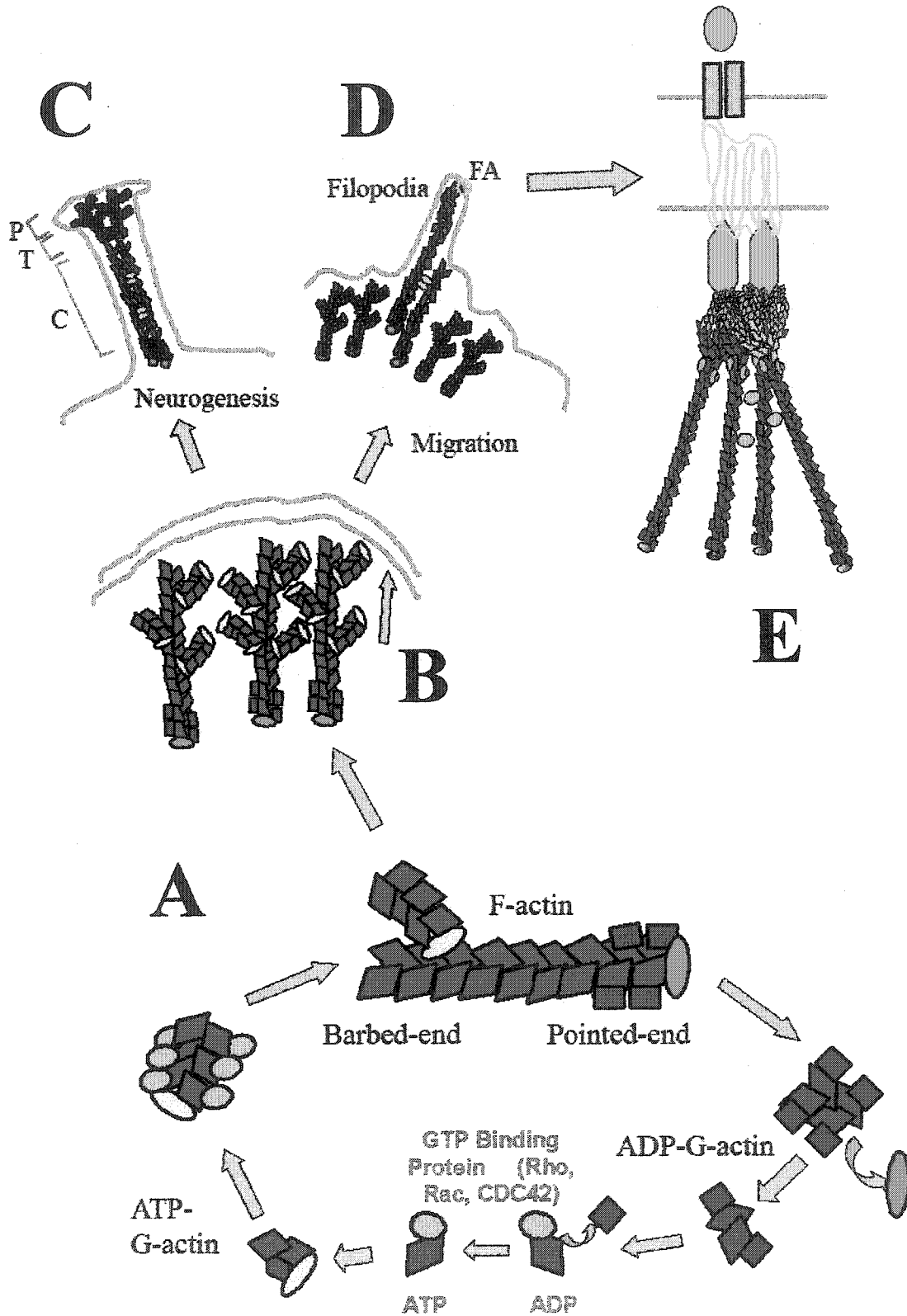
Figure 1.1

(Blanchoin and Pollard, 2002). Therefore, as would be expected, in stable fibers the concentration of ADP-actin is increased at the pointed end while the barbed end consists of primarily ATP-actin (Cooper and Schafer, 2000). Some actin filaments with ADP-barbed ends are observed but it is thought the hydrolysis allows actin-binding proteins to identify and depolymerize older fragments and so these filaments are much less common in the cell (Cooper and Schafer, 2000). The actin proteins in a filament are rotated by approximately 166° relative to each other which accounts for both the unique double helix filament structure and the dynamic capabilities of the filaments (Pollard et al., 2000). The double-helix structure allows rapid filament compression and stretch by bond rotation while the degree of twist within the filament determines the position of the incorporated monomers exposed protein binding sites for regulatory and supporting proteins which are able to regulate filament generation and degradation directly through their interactions with the bound monomers availability of protein binding sites (Paavilainen et al., 2004; Pollard et al., 2000). Additionally, the twist in the filament influences the rate of ATP hydrolysis thereby further effecting filament stability (Cooper, 2000).

As mentioned previously the hydrolysis of bound ATP ultimately alters the stability of the filament thus facilitating removal of short multimer ADP-fragments by actin accessory proteins such as ADF/cofilin. The fragments are further degraded into dimers then monomers which are sequestered by monomer binding proteins such as CAP1 and profilin (Figure 1.1) (Paavilainen et al., 2004). The protein-bound liberated ADP-actin monomers readily undergo nucleotide exchange catalyzed by the bound accessory protein (such as profilin) and thus enter a large reserve pool (~ 100 µM)

8

remaining poised for re-incorporation back into the filament at the barbed end (Pollard et al., 2000). This process of actin protein recycling, as the monomers are removed from one end and added to the other, is termed treadmilling and is responsible for generating a polarized force for such processes as cell motility, growth, division and neurogenesis (Figure 1.1) (Pollard et al., 2000).

F-actin Types

In the cell there are two main pools of F-actin fibers that function together in the eukaryotic cell; a responsive, dynamic highly branched meshwork termed the cortical actin layer and a more stable fibrous filament network (Pollard et al., 2000). The cortical actin pool localizes to areas of dynamic cytoskeletal rearrangement and is responsible for processes such as leading edge motility, endocytosis/exocytosis, and lamellipodia/filopodia formation and often associates with actin-associated proteins involved in directing actin treadmilling and branching such as ADF/cofilin, profilin and Arp2/3 proteins (Pollard et al., 2000). The more stable filaments are typically observed within the main body of the cell and associate with stabilizing proteins such as tropomyosin to yield structural strength and scaffold support to the cell, as observed with the occurrence of stress fibers in cultured fibroblast cells (Pollard et al., 2000). Both populations of fibers share certain actin-associated protein binding relationships; however both fiber pools interact with different actin binding proteins which function to regulate the fibers differing functional abilities (Paavilainen et al., 2004; Pollard et al., 2000).

9

Actin-Based Cellular Processes: Migration

The quiescent cell may be regarded as possessing a uniform cytoskeleton consisting of strong actin-myosin contractile fibers (stress fibers) strengthening the interior while maintaining a flexible actin meshwork at the periphery (Critchley, 2000; Pollard and Borisy, 2003). The initiation of motility is directed through the activation of cell surface receptors by extra-cellular ligand binding such as growth factors or other chemotactic signals which stimulate the actin cytoskeleton to undergo rapid rearrangement that polarizes the cell by generating a polymerizing and disassembling actin gradient (Condeelis et al., 2001; Kuhn et al., 1998; Medley et al., 2003). This process had been classified into three distinct stages; the protrusion of the leading edge of the cell, the formation of stable adhesions to the extra cellular matrix (ECM) and the release and retraction of the lagging edge (Critchley, 2000; Kuhn et al., 2000; Small et al., 2002). The leading edge or leading lamella (lamellipodium) formation begins with alteration of the local actin meshwork into a more dynamic flexible array which accommodates the incorporation of actin protein addition and polymerization (Chen et al., 2000; Condeelis et al., 2001). Small filament assembly and branching begins, initiated through actin polymerizing and branching proteins such as profilin, and Arp2/3 proteins which enable actin to provide the driving force to stretch the cell forward (Hahne et al., 2001; Machesky and Hall, 1997; Small et al., 2002). The small filaments, termed microspikes are approximately 1-5 μm in length (equaling the breath of the lamellipodia) which push the edge forward while larger protrusion of bundled actin filaments termed filopodia extend segments of the membrane considerably further (Small et al., 2002). The filopodia initiate the second stage of motility through extension beyond the cell into the

10

ECM and establishing a strong contractile focal adhesion (FA) complex (Figure 1.1) (Abe et al., 2003; Critchley et al., 1999; Rodriguez et al., 2003). It is currently unknown if filopodia generation *de novo* filaments or bundle existing filaments, however the filopodia extend and establish physical interactions between extra-cellular membrane receptors and actin cytoskeletal proteins which allows the cell to anchor securely to the ECM and exert force through the actin contractions and dynamics (Mohri et al., 1998; Rodriguez et al., 2003; Small et al., 2002; Turner et al., 2000). The FA complex is critical for motility and requires the binding of ECM ligands to cell adhesion integrins resulting in the clustering of additional integrin receptors and subsequent activation of cellular signaling cascade molecules such as Rac and focal adhesion kinase (FAK) (Critchley, 2000; Medley et al., 2003; Turner, 2000). The ultimate result of the activated signaling cascades is the recruitment of actin stress fibers to region of the integral receptors through the association of linking proteins such as talin (activated by FAK), vinculin, α-actinin (which are both activated though Rho) and filamin (responsive to Cdc42) that bind and localize the fibers to the inner membrane (Critchley, 2000; Medley et al., 2003).

The final stage of motility is initiated at the opposite side of the cell (the rear edge or uropodia) by dissociation of the FA and actin cytoskeleton (Rodriguez et al., 2003). This final process is initiated by the physical pull of the membrane which disrupts the interaction of proteins linking the fiber to membrane and activates signals pathways such as LIM kinase which activate actin depolymerizing proteins such as cofilin to initiate liberation of free monomers (Gungabissoon and Bamburg, 2003; Small et al., 2002).

11

Neurogenesis: Neurite Formation and Extension

The process of neurite extension is initially similar to motility leading edge dynamics in that it requires the formation of an actin rich lamellipodium; however the lamellipodia for neural extension are evenly dispersed around the cell at set intervals without the presence of an uropodia (Figure 1.1) (Kaverina et al., 2002a; Sarmiere and Bamburg, 2004). The lamellipodia then undergoes a segmentation represented by the recruitment of dense patches of microtubules which polymerize to extend the lamellipodia out and away from the cell which creates a neural outgrowth (Adams and Schwartz, 2000; Sarmiere and Bamburg, 2004). The actin-rich lamellipodium remains intact at the periphery domain (P domain) of the extension while the central region (C domain) of the neurite contains dense patches of microtubules, actin and organelles (Sarmiere and Bamburg, 2004). An additional transition area (T domain) separates the P and C domains and serves as the primary location of actin turn over, as growing barbed ends face the terminus of the P domain, the retrograde flow of actin towards the pointed ends approaches the T domain where it is broken down and recycled by actin associated proteins (Figure 1.1) (Gungabissoon and Bamburg, 2003; Sarmiere and Bamburg, 2004). The P domain, also termed the growth cone, characteristically appears splayed and consists of a lamellipodium edge complete with microspikes and numerous filopodia extensions (Gungabissoon and Bamburg, 2003; Sarmiere and Bamburg, 2004). The filopodia, as in motile cells, consist of parallel actin bundles and are thought to determine the direction of neuron growth (Nakayama and Luo, 2000; Sarmiere and Bamburg, 2004). Additionally, true nerve cells form dendritic spines; dense regions of actin extending from the C domain which function in neural signaling, and axonal processes

12

which occur from the conversion of a neurite extension from a stimulus sensory region to a signal transmittance region, however in the model system used in this thesis these processes are absent (Sarmiere and Bamburg, 2004).

Actin Binding Proteins

Cytoskeletal remodeling requires the coordinate interaction of a multitude of actin-interacting proteins which regulate polymerization, branching, depolymerization, and bundling of filaments. Each process requires a distinct class of effector including barbed and pointed end capping proteins, filament bundling/cross-linking proteins, monomer and binding/sequestering proteins (Table 1.1). Identification of the proteins functioning within these processes is critical to expanding our knowledge of actin-based events. Recently, a novel family of actin-interacting proteins termed WD repeats proteins (WDR) was identified yet their precise role remains to be discovered.

WDR1 Protein Structure:

The Mammalian WDR1 gene encodes a 601 aa protein containing nine tryptophan and aspartic acid (WD) repeats and an N-terminal truncated 534 aa protein which is thought to contain only seven WD repeats, yet six unidentified additional isoforms are proposed to exist (www.ncbi.nlm.nih.gov Homologue gene #6628). The WD motifs in both proteins are comprised of approximately 30-40 conserved amino-acid residues bracketed by an amino-terminus non-polar glycine and a basic histidine (GH) repeat and a carboxyl-terminus non-polar tryptophan and a negatively charged aspartic acid (WD) pair which interact to form a β-propeller structure. From the retrieved

13

Table 1.1 Characterization of selected actin interacting proteins

Barbed-Capping	Pointed-Capping	Bundling/ Cross linking	Monomer Binding
Gelsolin	Arp2/3	Filamin	Profilin
Capping Protein	Tropomodulins	α-actinin	CAP
Formin		Fascin	Cofilin

Table 1.2 Function and size of selected kelch proteins

Protein	Function	Size (kDa)
Ral2	Ras effector	~60
β & α Scruin	F-actin binding	~95
IPP	Actin cytoskeletal modulator	~65
Kelch	F-actin binding	~70
Mayven	Neural actin binding	~60

crystallized structure of the yeast and *C. elegans* WDR1 proteins and prediction based on

protein sequence the orientation of the propellers blades is such that each of the encoded

WD repeats folds into 4-anti parallel beta sheets which in turn forms one blade of the

propeller protein (Ono, 2003; Voegtli et al., 2003). These structural motifs are prevalent

in eukaryotic cells, as 1% of the *S. cerevisiae* genome is predicted to encode WD

proteins; however these motifs are unique among eukaryotes (Pollard & Earnshaw,

2002). The pre-mRNA transcript of WDR1 is approximately 42.78 kb long and generates

a 3.3 kb mRNA transcript that is thought to undergo alternative splicing to produce the

full length 60 kDa protein which contains nine blades and the truncated 50 kDa protein

predicted to contain seven blades (www.ncbi.nim.nih.gov/IEB/Research/Acembly). The

structure of both the yeast and *C. elegans* proteins reveal the propellers are divided and

twisted into two domains with each containing 7 propellers, however as both the yeast

and *C. elegans* proteins contain 14 propellers; the prediction by structure is the number of

blades is evenly dispersed between the two protein domain halves (Voegtli et al., 2003,

Ono, 2003). Interestingly, the mammalian proteins are predicted to contain an un-even

number of propellers comparison among these structures will be quite informative.

WDR1 Family Homology

The WD motif encodes four anti-parallel beta sheets which give rise to an

elaborate tertiary structure of a beta-propeller and was first identified in the beta-subunit

of the trimeric guanine nucleotide binding protein (G- protein Beta-transducin) which

acts to mediate signaling between membrane signaling proteins and intracellular

pathways (Adler et al., 1999). Importantly this motif is also abundant in the p40 subunit

15

of Arp2/3 complex which is known to be a predominant modulator of cortical actin rearrangement through the nucleation of actin elongation and branching (activated through Wiskott - Aldrich syndrome Protein (N-WASP) (Uruno et al., 2003). This motif also bears strong homology to the Drosophila kelch protein motif, denoted by conserved C-terminal WD and N-terminal GH repeats, which are found in a variety of beta-propeller proteins performing a wide range of functions including actin binding and rearrangement while the most conserved function of this domain is the regulation of mediating protein-protein interaction (Table 1.2) (Adams et al., 2000; Kim et al., 1999; Soltysik-Espanola et al., 1999). Notable Drosophila actin associated kelch proteins include Ral2, intracisternal A particle-promoted polypeptide (IPP), β- & α-Scruin, kelch, and Mayven (Adams et al., 2000; Robinson and Cooley, 1997; Soltysik-Espanola et al., 1999; Way et al., 1995). Interestingly Kelch β-propellers are able to comprise one protein of multiple blades or a larger propeller comprising many WD repeat blades which one or two domains similar to the predicted structure of hWDR1 (Adams et al., 2000).

The function of WDR1 orthologues (Aip1, UNC-78, and SCF1) in other species

The mammalian WDR1 was formerly termed Aip1 after the yeast protein actin interacting protein (Aip1p). However owing to the subsequent the identification of multiple WD motifs, Aip1 was later termed WDR1 (Adler et al., 1999; Rodal et al., 1999). WDR1 orthologs are present in a large number of eukaryotic organisms and have been classified from *Arabidopsis, Physarum polycephalum, Dictyostelium, Drosophila melanogaster,* yeast, *Xenopus,* chicken, rat, mouse, and human (Adler et al., 1999; Iida

16

and Yahara, 1999; Konzok et al., 1999; Okada et al., 1999; Ono, 2001; Rogers et al., 2003). As expected no prokaryotic orthologs have been reported.

Saccharomyces cerevisiae:

Actin interacting protein or suppressor of temperature sensitive (*ts-*) cofilin1 (Aip1p/ SCF1p) was originally identified in *S. cerevisiae* as a 67 kDa actin binding protein through a yeast two-hybrid screen performed by Amberg et al., (1995) as a protein able to interact with the yeast actin protein. Rodal et al., (1999) later confirmed this interaction using the same technique however they also observed a novel reciprocal interaction between cofilin-Aip1p proteins. Cofilin was the first member identified of the Actin Depolymerizing Factor family by Bamburg et al., (1980) and since been shown to be of critical importance in yeast for the regulated break down of F-actin into G-actin proteins, however no additional binding partner had been previously identified (Bamburg et al., 1991). Cofilin binds actin in dynamic areas of actin breakdown such as the cortical actin patches and the termini of the more stable actin cables (Bamburg, 1999). Rodal et al., (1999) generated anti-Aip1p antibodies to examine the distribution of Aip1p and confirmed a pattern similar to that of cofilin and strengthened the two-hybrid data suggesting the existence of either a direct or indirect interaction with actin and cofilin. Data obtained using mutant yeast cells defective in either cofilin activity, Aip1p activity or actin polymerization abilities have elucidated that loss of Aip1p does not severely impair cell growth or cortical actin architecture (Rodal et al., 1999). However the expression of both cofilin and Aip1p proteins is required for their correct localization to areas of cortical actin as the combination of ΔAip1p with either mutant cofilin or G-actin

17

is synthetically lethal in yeast cells (Rodal et al., 1999). These data coupled with the identification of only cofilin-Aip1p and Aip1p binding sites on actin and distinct Aip1p and actin binding sites on cofilin supported the existence of a regulatory ternary complex of the actin-cofilin-Aip1p (Rodal et al., 1999). The nature of the regulatory mechanism of the complex interaction was proposed by Iida & Yahara (1999) through the observations of long cofilin-decorated actin rods in cells lacking Aip1p and the ability of Aip1p expression to rescue the temperature sensitivity phenotype of Δcofilin cells. This data suggested that Aip1p regulates cofilin's activity through its unique ability to enhance the actin depolymerizing abilities of cofilin (Iida & Yahara, 1999).

This model was challenged by two-hybrid screening data obtained by Drees et al., (1999) which showed Aip1p was able to interact strongly with the actin binding protein Srv2p (Suppressor of Ras^{val14}, homologue to the mammalian Cyclase-Associated Protein, CAP1) (Freeman and Field, 2000; Hubberstey and Mottillo, 2002). The protein Srv2p was identified by Field et al., (1990) as an actin-binding effector of the Ras pathway of adenylyl-cyclase signaling and has since been shown to associate with cofilin-actin complexes during active actin remodeling (Moriyama and Yahara, 2002). The reported interaction of Srv2p with Aip1p suggested an additional function of Aip1p and further proposed that the binding of actin or cofilin by Aip1p may not necessarily be a direct interaction (Freeman and Field, 2000).

The accomplished work of Balcer et al., (2003) generated the current model of a bi-functional role for cofilin during cortical actin dynamics through the identification of a interaction between a high-molecular-weight 1:1 complex of six G-actin and Srv2p proteins, and an F-actin barbed-end protein capping complex consisting of cofilin and

18

Aip1p proteins. Balcer et al., (2003) also observed the Aip1p-cofilin barbed end capping complex prevents re-annealing of severed fragments and allows their further depolymerization by cofilin. It was also verified that Srv2p was able to competitively interact with cofilin bound ADP-G-actin and catalyze the actin nucleotide exchange cooperatively with profilin by replacing cofilin binding, hence liberating cofilin and increasing the ATP-actin reserve (Balcer et al., 2003).

This model is well supported with evidence obtained thus far in both yeast and higher eukaryotes and serves as the template for the further study of functioning of CAP1, WDR1, cofilin proteins in higher eukaryotic organisms.

Xenopus laevis:

Xenopus Aip1 (xAip1) was first identified as a 65 kDa protein by Okada et al., (1999) using an affinity chromatography column of *Xenopus* cofilin (xAC) and actin. Interestingly, several other large polypeptides (94, 90, 65, 63, 60, and 55 kDa) were eluded from the column however antiserum generated to the xAC fraction detected primarily the 65 kDa protein, which through sequence data was identified as xAip1 (Okada et al., 1999). The cloned cDNAs of the 65 kDa protein obtained from a stage 30 embryonic library revealed two transcripts, one full length and the other lacking part of the N-terminus, however antibodies raised against the protein were specific and did not detect a second truncated protein (Okada et al., 1999). Okada et al., (1999) reported that xAip1 localized with cofilin to the dynamic embryonic cleavage furrow within early embryos. Further investigation revealed xAip1 localized within cells at the blastula stage to cortical actin regions, mitotic apparatus and nuclei. The developmental significance of

this pattern of expression was investigated through microinjections of xAip1 protein into one cell of two-cell stage blastomeres which resulted in abnormally large, round blastomeres exhibiting eventual arrested development (Okada et al., 1999). Upon closer inspection of the cells Okada et al., (1999) described the apparent loss of correct cortical actin and cofilin staining, instead replaced by diffuse and broad protein localization which is in contrast to the effects of the over expression of cofilin on actin that typically resulted in large filamentous aggregates.

Further detailing of the molecular relationship of xAip1 with cofilin and actin using DNAse1-actin affinity columns, xAC affinity columns, and gel filtration techniques demonstrated that xAip1 was unable to bind G-actin in the presence or absence of cofilin, but was able to bind F-actin only in the presence of cofilin but not induce significant twist in the filaments (Okada et al., 1999). These data supported a role for xAip1 has an enhancer of actin depolymerization through a cooperative interaction with cofilin (Okada et al., 1999). Supporting data for the interaction was obtained from light scattering studies, sedimentation and polymerization assays which showed that the affinity of xAip1 for F-actin was dependent upon cofilin expression, and the presence of xAip1 protein was able to slightly increase the ability of cofilin to depolymerize filaments, however further localization studies were required to clarify the precise mechanism (Okada et al., 2002; Okada et al., 1999). Gold-labeling immuno-electron microscopy experiments described an association of xAip1 with F-actin which was dependent upon the presence of cofilin and the ability of xAip1 to exclusively bind the barbed-ADP ends of the cofilin-severed F-actin filaments (82% fragment binding) (and to a lesser degree the sides of filaments (38%)) (Okada et al., 2002). However no affinity of xAip1 for ATP-barbed synthesized

20

in vitro was observed, which was in agreement with the results of depolymerization assays (Okada et al., 2002). Together, these results generated a model in which xAip1 is able to cooperatively bind to barbed end of filaments with cofilin and also interact with cofilin-severed short filaments which effectively increases the amount of pointed filament ends available for cofilin severing and thereby enhances cofilin's depolymerizing activity (Okada et al., 1999, Okada et al., 2002). Yet this model did not account for their observations that although xAip1 was able to bind filamentous actin the addition of the protein had little effect on the rate of either polymerization or depolymerization, which suggested the mechanism of *Xenopus* depolymerization may be more complex then postulated (Okada et al., 2002).

Dictyostelium discoidium:

The *Dictyostelium* WDR1 ortholog gene (DAip1) was originally identified from a screen searching for a p21-activated kinase gene as being 33% homologous in sequence to the yeast Aip1 gene (Konzok et al., 1999). Konzok et al., (1999) investigated the localization of DAip1 through the production of antibodies raised against bacterially derived recombinant proteins and reported DAip1 localized with cofilin, although did not overlap cofilin within the cortical actin region of cells. DAip1 also appeared abundant in areas undergoing active F-actin rearrangement such as the lamellipodia of motile cells, the filopodia and pseudopodia, the phagocytic cup, and the poles of dividing cells (Konzok et al., 1999). Further work using a green-fluorescent-protein labeled DAip1 demonstrated DAip1 was shuffled between those dynamic structures undergoing rapid actin rearrangement (Konzok et al., 1999). DAip1-null cells were generated to assay *in*

21

vivo protein function and determined that unlike cofilin, DAip1 is not essential for viability and loss of expression generated several interesting actin-based phenotypes (Aizawa et al., 1999; Konzok et al., 1999). The most striking impairment of the DAip1-null cells was the defect in cytokinesis which resulted in larger slow-growing multi-nucleated cells typically exhibiting hyperactive and exaggerated lamellipodia, filopodia and pseudopodia formation and extensions (even throughout cytokinesis) (Aizawa et al., 1999; Konzok et al., 1999). These null cells were also dramatically impaired for several actin-dependent processes such as the constitutive uptake of fluids (macropinocytosis), ligand-induced phagocytosis, and cell motility (Konzok et al., 1999). However these cells remained able to form multicellular fruiting bodies and demonstrated normal cofilin localization, suggesting that although DAip1 may regulate may actin processes it is not essential for cell survival, multi-cellular behaviour or correct cofilin localize to actin (Konzok et al., 1999). These mutant phenotypes were specific to the loss of DAip1 activity since the introduction of DAip1 back into null cells completely restored the defective motility and macropinocytosis to wild-type rates, and increased the rate of phagocytosis to nearly 50% more then exhibited by the wild type cells; however the mutants displayed only a partial restoration of normal cytokinesis (Konzok et al., 1999).

To determine which region of the protein was responsible for activity, this group also compared the rescue ability of the C and N termini of DAip1 through the fusion of either end to GFP-protein tag within the DAip1-null cells (Konzok et al., 1999). Konzok et al., (1999) found that although the C-terminus-GFP protein was able to localize to the expected areas such as the lamellipodia and filopodia, only the N-terminus-GFP protein was able to restore partial function to the defective processes, suggesting the active

22

domain resides within the C-terminus while the N-terminus function to localize the protein within the cell (Konzok et al., 1999).

The ability of DAip1 to partial restore cytokinesis to expressing cells is consistent with results reported from work performed by Aizawa et al., (1999) who showed that over-expression of DAip was able to impair cytokinesis and generated multi-nucleated cells. The function of DAip1 during cytokinesis was further investigated by Gerisch et al., (2004) through the visualization of cellular mitotic events *in vivo* within DAip1-null mutant cells, cortexillin-null cells (an actin bundling protein of *Dictyostelium*), and myosin-II null cells expressing green-fluorescent-protein (GFP) labeled tubulin. Gerisch et al., (2004) confirmed the previous description of the mutant cells and demonstrated the large multi-nucleated nuclei of both the DAip1-null and cortexillin-null contained polyploid chromosome numbers and were due to an abundance of constitutively active centrosomes which directed multiple synchronous mitotic events in the absence of cytokinesis. The phenotypes of the two null mutants were comparable yet differed from those observed from the myosin-II mutants enabling Gerisch et al., (2004) to conclude the phenotypes observed from the DAip1-null cells were primary due to the presence of extra centrosome structures and not due to a deficiency in cytokinesis suggesting DAip1 may be involved in centrosome or mitotic regulation but not likely in the induction of cytokinesis.

Together, these results strongly suggested DAip1 is a critical regulatory protein during cytokinesis and may function as an actin bundling protein able to colocalize with cofilin and maintain regulation of the actin cytoskeleton during processes of F-actin remodeling such as endocytosis, lamellipodia and filopodia formation (Konzok et al.,

23

1999, Gerisch et al., 2004). These results were not able to indicate any protein interaction with cofilin and actin and the Daip1-null mutant cells displayed contrast phenotypes to the cofilin over-expressing cells characterized by the presence of dense fibrous bundles of cytoplasmic actin (Aizawa et al., 1999).

Evidence was reported by Aizawa et al., (1999) used electron micrographs as well as actin polymerization and light scattering assays to demonstrate that DAip1 was able to bind actin filaments *in vitro* and enhance the depolymerization activities of cofilin, however in the absence of cofilin the affinity of DAip1 for actin was reduced and the binding of DAip1 was not able to induce a twist or depolymerization. These data suggested that DAip1 cooperatively bound the barbed end of filaments and lengths of filament and enhanced the severing ability of cofilin through twist induction (Aizawa et al., 1999).

Konzok et al., (1999) suggested the function of DAip1 was more complex then proposed from the model of Aizawa et al., (1999) and provided supporting data through the closer investigation of the DAip1-null mutant cells. Konzok et al., (1999) examined the mode of DAip1 actin regulation using actin disrupting agents of known mechanism to contrast the phenotypes observed in the DAip1-null cells. The treatment of the null cells with the actin depolymerizing agent latrunculin-A and the barbed-end capping agent cytochalasin-A resulted in phenotypes opposing those displayed by the over-expressing DAip1 suggesting DAip1 exerted its effects through other mechanisms then barbed-end capping or filament severing (Konzok et al., 1999).

The current model of DAip1 supports a strong interaction with cofilin at the cell cortex within processes requiring rapid F-actin rearrangement and depolymerization

24

currently accomplished through unknown mechanisms and also suggests a novel role regulating cytokinesis perhaps independent of the established interaction with cofilin (Aizawa et al., 1999, Konzok et al., 1999, Gerisch et al., 2004).

Caenorhabditis elegans:

The *C. elegans* gene uncoordinated-78 (UNC-78) was originally described by Waterston et al., (1980) to be essential for correct body wall muscle formation and muscle motility, but it was the sequence comparisons with established WDR1 sequence data performed by Ono (2001) which led to the identification of UNC-78 as the *C. elegans* WDR1 ortholog gene. In order to determine the function of UNC-87 the gene was cloned from a *C. elegans* library and the recombinant UNC-78 protein was expressed in *Escherichia coli* (Mohri and Ono, 2003).Upon assaying protein function it was reported that despite the bacterial origins of the protein, UNC-78 displayed the ability to enhance the depolymerizing activity of the *C. elegans* muscle-cofilin protein (UNC-60B) on rabbit F-actin and demonstrated little affinity for F-actin in the absence of UNC-60B (Mohri and Ono, 2003). This suggested that UNC-78 could bind actin with UNC-60B and UNC-78 may function to maintain the cytoskeletal regulation by cofilin. A surprising result obtained during the depolymerization assays was the inability of UNC-78 to depolymerize filaments in the presence of *C. elegans* non-muscle cofilin isoform, UNC-60A which suggests the interaction of UNC-78 is isoform specific (Mohri & Ono, 2003). Complementary to this finding was the identification of two existing UNC-78 genes encoded within the *C. elegans* genome as the isoform gene K08F9.2 which shares 68% homologous sequence to the gene encoding the 65 kDa UNC-78 protein (Mohri & Ono,

25

2003). This is in striking contrast to the WDR1 gene found in other organisms which all appear to contain only one WDR1 ortholog gene within their genomes (Mohri & Ono, 2003). To distinguish between the two isoforms, antibodies against a synthetic peptide sequence derived from a region unique to the UNC-78 protein which bound specifically to the 65 kDa protein during assays were produced (Mohri & Ono, 2003). Protein localization using the antibody demonstrated that during early embryo development, UNC-78 expressed only within a small subset of cells which corresponded at later stages to an expression pattern restricted only to body wall muscle, the pharynx, and the spermatheca (Mohri and Ono, 2003). Further immuno-staining revealed UNC-78 was localized in developing worms within muscle cells with myosin adjacent to muscle myofibrils (Mohri & Ono, 2003). In adult worms UNC-78 displayed a striated pattern which instead corresponded to the actin filament arrangement peripheral to the myofibrils, and matched the expression pattern of UNC-60B identically (Mohri & Ono, 2003). As this data supported a muscle-specific localization of UNC-78 with UNC-60B and actin, further investigation into the function of UNC-78 within these cells was accomplished using recombinant worms. Ono (2001) generated several null and mutant UNC-78 and UNC-60B worms to elucidate the role of UNC-78 during actin rearrangement (Ono, 2001). UNC-78 expression was shown to be critical for proper body wall muscle structure and function as previously reported, but it was observed to be essential for correct actin organization in muscle cells and required for UNC-60B localization to the periphery of myofibrils (Ono, 2001). It was further determined the loss of UNC-60B expression did not disrupt UNC-78 localization to actin filaments

26

suggesting UNC-60B was not required for the binding of UNC-78 to actin filaments (Ono, 2001).

Together these data strongly support a regulatory interaction between UNC-60B and UNC-78 in the generation and maintenance of the actin cytoskeleton in muscle cells; however the molecular mechanism remained unknown (Mohri and Ono, 2003; Ono, 2001; Ono, 2003). Therefore to address this issue Mohri & Ono (2003) used their recombinant UNC-78 and UNC-60B proteins for further *in vitro* polymerization protein perfusion assays. Mohri & Ono (2003) first assayed the effects of UNC-78 as a barbed end capping protein by comparing the effects of two known strong barbed-end capping agents, gelsolin and cytochalasin D (CD) with UNC-60B on actin depolymerization rates. The first set of experiments challenged the barbed end capping mechanism through which UNC-78 was thought to enhance UNC-60B filament depolymerization ability (Mohri and Ono, 2003). The experiment was based on the assumption that if UNC-78 caps the barbed filament end then the rate of depolymerization by UNC-60B with UNC-78 should be comparable with other capping agents (Mohri and Ono, 2003). Mohri & Ono, 2003 reported the effects of either CD or gelsolin were similar to each other but determined the rate of depolymerization to be the highest with UNC-78 and UNC-60B and was unaffected by the addition of either agent. Additionally they reported that despite their observations of the addition of UNC-78 in either the presence or absence of the capping agents impaired no effect on actin dynamics; both capping agents were able to inhibit the activity of UNC-60B and produced longer filaments (Mohri and Ono, 2003).

The observations reported by Mohri & Ono, 2003 were critical to understanding the role of UNC-78 and UNC-60B because they were able to demonstrate UNC-78

27

functioned with UNC-60B through a novel actin-dependent and barbed-end capping independent mechanism. These results were further verified using rhodamine-actin polymerization assays to definitively test the successful capping of the barbed end by UNC-78 (Mohri and Ono, 2003). If the barbed end capping was complete then the protein cap would prevent the incorporation of G-actin onto the existing filament as Mohri & Ono, 2003 experimentally demonstrated for both the gelsolin proteins and cytochalasin D agents; however UNC-78 was not able to prevent the polymerization of the label actin proteins, and further evidence confirmed the presence of both UNC-78 and UNC-60B increased depolymerization but yet did not impact the rate of novel polymerization. To further verify their data Mohri & Ono, 2003 repeated the localization experiment performed by Okada et al., 1999 using different *in vivo* techniques and reported UNC-78 binding along the length of the filament in addition to the barbed end, thus further supporting their *in vitro* polymerization data.

Taken together these results demonstrate the inability of UNC-78 to cap the barbed filament end and confirm the F-actin-dependent association of UNC-78 with UNC-60B. This interaction has been shown to be critical for proper actin cytoskeleton arrangement and regulation in *C. elegans* provides a well-founded model for the function of WDR1 homologues identified in other eukaryotic species.

WDR1 Studies from Other Species:

The results from the detailed study of *S. cerevisiae, Dictyostelium, C. elegans* and *Xenopus* have elucidated preliminary functions of WDR1 as a potential regulatory protein able to potentially interact and cooperate with cofilin to influence actin depolymerization

28

dynamics and additionally control aspects of complex actin cytoskeletal processes such as cytokinesis, endocytosis, and cell motility (Adler et al., 1999; Mohri and Ono, 2003; Okada et al., 2002; Rodriguez et al., 2003). Preliminary studies in several organisms including *Drosophila* and human systems have generated some evidence supporting these proposed roles (Rodriguez et al., 2003; Rogers et al., 2003). Recently work in *Drosophila* S2 cells has implicated WDR1 (with cofilin) for critical actin processes such as forming the lamellipodia for cell migration and actin regulation for cytokinesis (Kelso et al., 2002; Pollard and Borisy, 2003; Rodriguez et al., 2003; Rogers et al., 2003). These results have been partially supported by studies of human smooth muscle cell substrate-dependent attachment and proliferation which demonstrated WDR1 expression is maintained in quiescent, static cells but is increased >5 fold during active cell proliferation and motility, thus indicating the observed functions within *Drosophila* and *Dictyostelium* appear to have remained conserved within the more complex human system (Ichii et al., 2001).

Interestingly, another line of study has suggested that in other species such as *P. polycephalum*, chick, and mouse the main function of WDR1 ortholog proteins is a stress-response protein (Lomax et al., 2001; Matsumoto et al., 1998; Oh et al., 2002; Verma et al., 2004b). The *P. polycephalum* WDR1 ortholog gene, p66 was identified by Matsumoto et al., (1998) as a heat shock protein up-regulated in response to elevated heat (independently of cofilin) able to interact with both actin and cofilin during remodeling of the actin cytoskeleton to enable the rapid generation of cytoplasmic actin rods during microcyst formation. More recently Oh et al., (2002) have reported observing an increase in WDR1 expression, also independent from cofilin expression, in chick cochlea organs following excessive noise damage within the actin-rich basal homogene and cuboidal

cells without any change of cofilin expression. A complementary observation was reported from the study of nickel-induced transformation mouse embryo cells which generated data indicating an immediate transcriptional up-regulation of WDR1 in response to elevated calcium concentrations induce by the carcinogenic nickel effects, hence supporting a stress-induced response (Verma et al., 2004a).

Various orthologues of WDR1 proteins have been studied in many organisms to varying degrees with the attempts of yielding some insight into the function of WDR1 proteins, however more detailed studies should work to yield the precise functioning of WDR1 proteins in higher organisms and clarify our current understanding of the mechanisms control the diverse range of functions of our mammalian actin cytoskeleton.

Additional actin binding proteins: Barbed end capping proteins:

Gelsolin, Capping Protein, Formin

The barbed (fast growing) end of the filament is the dominant regulator of actin rearrangement dynamics both in stable and transient filament types and is characteristically orientated towards the cell membrane (Table 1.1) (Bailly et al., 2001; Pollard et al., 2000). The barbed-end associated proteins control the rate of filament extension by tightly binding to the end of a growing filament and either facilitating or inhibiting filament extension (Bamburg, 1999). The barbed-end capping proteins are also able to influence the activity of pointed end capping proteins, as the dissociation of the barbed-capping protein decreases the binding affinity of the pointed-capping protein for the pointed-end, although this relationship is not well understood as current models are derived from primarily *in vitro* polymerization studies (Condeelis et al., 2001; Pollard

30

and Borisy, 2003). The removal of barbed capping proteins is accomplished by interactions with polyphosphoinositides either through direct contact with the cell membrane or cytosolic signaling pathways, yet removal may also be influenced by the presence of actin-associated proteins and the activity of ATP-hydrolysis, although the mechanisms of these processes require further study (Kowalczynska and Nowak-Wyrzykowska, 2003; Paavilainen et al., 2004). Within the cell it has been deduced from *in vitro* polymerization assays that the concentration of barbed-ends are very low and are a key regulator of actin polymerization since *in vitro* ATP-actin polymerizes readily at a free barbed end, and in the absence of barbed capping proteins this would quickly deplete the cell's monomeric actin pool (Pollard et al., 2000). Without the presence of cytosolic barbed ends the actin dynamics would be static, however upon increased free barbed end availability the balance of severing and polymerization commences (Belmont and Drubin, 2001).

Gelsolin is a conserved barbed-capping protein known to regulate barbed end dynamics through its ability to both tightly cap barbed ends and block the filament extension and sever long polymers (Cooper and Schafer, 2000; Pollard et al., 2000). The promotion of filament severing occurs in response to high cytosolic (Ca^{2+}) and is initiated by its localization along the length of the polymer thereby resulting in the dissociation of multimer actin fragments which are rapidly capped (at their newly generated barbed ends) by gelsolin and further depolymerized through the binding and activity of additional proteins (Cooper and Schafer, 2000; Pollard et al., 2001). The removal of the gelsolin cap allows rapid filament growth and is regulated through contact with polyphosphoinositides (Cooper and Schafer, 2000; Pollard and Borisy, 2003).

Capping protein (CP) is a highly conserved and abundant barbed capping protein with various isoforms including a muscle (CapZ) and non-muscle (CapG) form (Blanchoin et al., 2000; Mohri et al., 2004; Paavilainen et al., 2004). CP is a dimer consisting of an alpha and beta subunit which associate together to bind the actin terminus and are removed from the barbed end through interaction with polyphosphoinositides, which allows for rapid actin polymerization (as with gelsolin) (Falck et al., 2004; Kong and Kedes, 2004). CP is unique in that this protein is able to bind the ADP-monomer binding protein twinfilin and although twinfilin does not actively participate in elongation, its association with CP is essential for correct spatial organization of cortical actin yet the nature of this relationship is presently unclear and requires further study (Falck et al., 2004, Paavilainen et al., 2004).

The formin family of proteins is a unique and exciting class of barbed-end capping proteins conserved from yeast to human which are able to bind both the barbed end and the membrane and hence serve to physically anchor the barbed end to the cell's inner membrane (Chang and Peter, 2002; Pruyne and Bretscher, 2000). Interestingly, formins have been shown to be essential for long stable fiber formation (through barbed end binding) and function to directly transduce Rho G-protein signals (via Cdc42 –see below) to facilitate cytoskeletal rearrangement (Chang and Peter, 2002; Evangelista et al., 2002; Pollard, 2004). However they have also recently been shown to form large multi-protein complexes, such as that of the Arp2/3 complex, Bud6, and profilin, and facilitate pointed end capping and nucleate branching, thus indicating an increasing regulatory potential of formins in cytoskeletal dynamics (Evangelista et al., 2002; Pollard, 2002; Pollard, 2004).

32

Pointed end capping proteins:

Actin-related-protein (Arp) proteins and tropomodulins

The pointed (slow growing) end is the furthest end of the actin filament from the membrane, facing towards the inner part of the cell (Blanchoin et al., 2000; Pollard et al., 2000). The regulation of the pointed end by capping proteins is not as dramatic as the barbed-end capping proteins and the two classes are thought to work synergistically as the presence of barbed-end capping proteins are postulated to serve a regulatory role for the pointed end capping proteins and their ability to influence the rate of actin disassembly, filament branching and protein dissociation (Blanchoin et al., 2000; Uruno et al., 2003). Pointed end capping is essential for *de novo* filament assembly, and is the rate limiting step for *in vitro* polymerization assays (Cooper and Schafer, 2000; Pollard et al., 2000). The binding of the pointed capping protein *in vivo* regulates multimer subunit dissociation rates as the hydrolyzed ADP-actin are high, and therefore this terminus is less stable and prone to attack by actin depolymerizing proteins, such as ADF/ Cofilin (Blanchoin et al., 2000; Pollard and Borisy, 2003). Contrary to expectation, the dissociation of proteins at the pointed end has little impact of the volume of reserve ADP/ATP monomers as the pool of G-actin is relatively large, but activation of pointed capping proteins initiates nucleation of ATP monomers and additional activation stimulates the branching of cortical actin networks (Pollard et al., 2000). Cortical actin populations are localized to dynamic areas (such as the leading edge of motility) and provide a three-dimensional scaffold of short actin branches which polymerize to push the membrane forward and generate force (Goode et al., 2000; Pollard et al., 2000). The

33

branches of this meshwork are situated at 70 degree angles to maximize strength and construction efficiency (Pollard et al., 2000). Pointed capping proteins orchestrate the branching by nucleating short filaments which are then localized to the periphery of existing filaments, a process that is regulated through pointed capping protein activation via accessory proteins (Belmont and Drubin, 2001; Goode and Rodal, 2001; Pollard, 2001).

The best understood class of pointed capping proteins is the Actin-Related-Protein (Arp) 2/3 complex of proteins, which is a group of seven conserved proteins known to bind and nucleate filament polymerization, and direct actin branching through activation by the Wiskott-Aldrich Syndrome protein (WASp) family (Paavilainen et al., 2004, Pollard et al., 2000). The Arp2/3 is comprised of two known actin related proteins, Arp2, Arp3, and five currently unclassified proteins, p18, p14, p19, p35, and p40 which interact in sequential order to nucleate actin assembly and branching (Paavilainen et al., 2004). The WASp protein family (including WASp family verprolin [WAVE] homologous family) are activated by the Rho G-proteins Cdc42 and Rac-1 which transduce cytoskeletal rearrangement signals by accelerating monomer shuttling to the barbed end (Bishop and Hall, 2000; Higgs and Pollard, 2001; Xu et al., 2003). This in turn activates the formation of nucleating proteins and initiates branching through the Arp2/3 complex (Paavilainen et al., 2004). Upon activation by WASp proteins, the Arp2/3 nucleates fiber formation until actin incorporation is blocked by the binding of capping proteins (Pollard et al., 2000). Additionally, interaction with selected WASp proteins can result in Arp2/3 complex binding at the periphery at existing filaments and nucleating branches (Pollard et al., 2000).

Tropomodulins, contrary to the Arp2/3 complex localizes primarily within stable filament complexes (stress fibers) and is most abundant in muscle cells in actin fibers associated with tropomyosin (Kong and Kedes, 2004). Tropomodulins proteins nucleate fiber stable formation and are not associated with branching, yet function to facilitate fiber interaction with other elements of the cytoskeleton, such as myosin proteins (Kong & Kedes, 2004).

Filament Bundling/ Cross-Linking proteins:

Filamin, α-Actinin and Fascin

Bundling/cross-linking proteins are localized in dynamic F-actin regions (cortical actin at the leading edge, and filopodia) and function to yield strength and flexibility to the actin network hence providing structural support and rapid response to deformations in cell shape (Pollard, 2003; Tseng et al., 2002). Bundling proteins are unique in that they typically dimerize to produce both branched meshworks and are able to bundle long F-actin fibers into parallel arrays and thus generate strength to facilitate extension and can also confer flexibility through the compressibility of short branched fibers (Peraud et al., 2003; Tseng et al., 2004). The flexibility of cortical actin patches owes to the structure of bundling proteins as these proteins form homodimers which function as a hinge, with one arm binding the existing filament and the other associating with the short filament branch from which further branches can extend (Tseng et al., 2004). The strength is conferred through the angle the branches are bound at by the bundling protein dimer which aligns each branch at 70° relative to each other in the array so as external deforming forces will be resisted until the hinge connecting the two bundling proteins bends causing the

35

meshwork to compress and accommodate the stress (Krendel and Bonder, 1999; Tseng et al., 2004).

Fascin is a highly conserved actin bundling protein which is unique in its ability to generate firm and flexible actin arrays without cooperation from other actin proteins (Brieher et al., 2004). Fascin has been shown to be the sole requirement by the intracellular bacterial pathogen *Listeria monocytogenes*, which enters the cell and hijacks actin and actin-associated proteins for motility (Adams and Schwartz, 2000; Brieher et al., 2004). This species utilizes two phases for transport; the first involves the Arp2/3 complex of proteins to generate motility, yet recent studies have shown the second is Arp2/3 independent and requires only fascin proteins to design long hollow cylindrical for the production of cytosolic elongation-based motility (Brieher et al., 2004). Additionally, fascin has been shown to be one of only a small number of actin associated proteins essentially required for oncogenic motility and invasiveness thus demonstrating the unique ability of these proteins to interact solely with actin to perform the critical bundling function (Peraud et al., 2003).

The actinin proteins are widely distributed actin bundling protein, conserved from yeast to their four classes in human and localizes predominantly to dynamic areas of cortical actin patches (Kowalczynska and Nowak-Wyrzykowska, 2003; Tseng et al., 2002; Virel and Backman, 2004). Interestingly, *in vitro* studies have shown the predominant non-muscle isoform of α-actinin is able to function in a similar method as fascin, although it is able to confer more rigidity to actin arrays then fascin, and further in vivo studies have demonstrated α-actinin is able to respond directly and quickly to

36

integrin signaling thus making these proteins unique among the bundling proteins (Chen et al., 2000; Virel and Backman, 2004).

The best characterized bundling protein is filamin which is highly conserved from lower eukaryotes to humans and functions both within loosely branched networks (preferentially at low concentrations) and strong, tensile-force resistant densely bundled meshworks at high filamin concentrations (Critchley et al., 1999; Tseng et al., 2004). Filamin has been shown to contain an N-terminal actin binding site and undergo dimerization to cross-link similar to both fascin and α-actinin (Tseng et al., 2004). However, filamin is unique among bundling proteins in that it is able to provide elasticity within both strong actin arrays and flexible dynamic branching actin networks (Tseng et al., 2004; Tseng et al., 2002). It is currently postulated that filamin proteins, although redundant in their responsive cortical actin binding, uniquely provide the cell with a means to rapidly regulate resistance to deforming stresses and hence serve a critical function (Tseng et al., 2004).

Monomer binding/ Sequestering proteins:

Profilin, CAP, Cofilin

Monomer binding proteins are vital modulators of actin dynamics (Paavilainen et al., 2004). This is due to their regulatory ability to control G-actin availability within the cell and consequently represent one of the most widely studied families (Blanchoin et al., 2000; Paavilainen et al., 2004; Sagot et al., 2002). Sequestering proteins preferentially associate with either ADP- or ATP-G-actin in a 1:1 binding ratio to sequester the monomer from dynamic areas into the cytosolic reserve actin pool, until they are

37

stimulated to release their monomer either for polymerization or nucleotide exchange (Pollard & Earnshaw, 2002). Numerous studies have shown actin will spontaneously polymerize under cellular conditions when the G-actin concentration exceeds the critical concentrate of ~ 0.1 μM proteins, however the cellular G-actin pool is estimated at ~ 100 μM concentration thus demonstrating the importance and the high degree of regulation of monomer sequestering proteins by actin associated proteins (Pollard et al., 2000). Sequestering proteins are vital for the regulation of actin polymerization as they are not only able to rapidly bind newly dissociated proteins, but also catalyze the ATP nucleotide exchange (Paavilainen et al., 2004). This effectively re-activates the monomer for additional polymerization and further delivers the protein to actively polymerizing barbed ends (Paavilainen et al., 2004). A relative comparison of abundance of actin and actin-associated proteins in the cytosol of un-activated (un-coagulated) human platelet cells reflects the critical function of these proteins (Paavilainen et al., 2004; Pollard et al., 2000). Pollard et al., 2000 quantitatively reported F-actin accumulates to ~330 μM, G-actin totals ~220 μM, the sum of the capping proteins Arp2/3, gelsolin, CP is merely ~19 μM, while the sum of ADF/cofilin, profilin and thymosin-$\beta 4$ equates to ~580 μM emphasizing the important cytoskeletal regulatory role of these proteins (Pollard et al., 2000; Pollard and Borisy, 2003).

Profilin is highly conserved across eukaryotic species as the smallest G-actin binding protein (12-16 kDa) which preferentially associates with ATP-actin monomers and this binding is essential for major processes such as cytokinesis and polarized actin polymerization (Bamburg, 1999; Bamburg and Wiggan, 2002; Paavilainen et al., 2004). In yeast, profilin is essential for actin recycling as it interacts with cofilin bound ADP-

38

actin and is thought to catalyze the actin nucleotide exchange which further causes the monomer to dissociation from cofilin (Bamburg et al., 1999; Rosenblatt et al., 1997). The recharged ATP-monomer remains bound by profilin and upon initiation of active polymerization is escorted by profilin to polymerizing barbed ends (Birkenfeld et al., 2003; Chan et al., 2000). A current debate exists regarding the precise nature of the profilin-ATP-actin binding relationship as it was postulated profilin catalyzed the nucleotide exchange by initiating the dissociation of ADP from bound G-actin for the more favorably actin-bound ATP (Moriyama and Yahara, 2002; Paavilainen et al., 2004). However studies with yeast demonstrate profilin null phenotype could be restored with the expression of *Arabidopsis* profilin which lacks the typical profilin exchange factor binding site (Paavilainen et al., 2004). Therefore further studies are required to clarify the exact role for profilin in actin binding.

The CAPs (Cyclase-Associated Protein) represent a unique family of actin associated proteins which were first characterized in yeast as an effector of the adenylyl cyclase signaling pathway for actin rearrangement and have since been shown to be highly conserved from yeast to higher eukaryotic systems such as mammals (Freeman and Field, 2000; Hubberstey and Mottillo, 2002; Paavilainen et al., 2004). CAP proteins were originally thought to function homologously with profilin proteins owing to their ability to catalyze nucleotide exchange on ATP-depleted cofilin bound monomers and localize ATP-monomers to actively polymerizing cortical barbed ends (Hubberstey and Mottillo, 2002; Moriyama and Yahara, 2002). However recent studies have since revealed CAP proteins are able to form large multi-proteins complexes as homodimers and proteins such as cofilin, actin, and actin-interacting protein (Aip1/ WDR1) which

39

may yield additional functions for CAP proteins (Balcer et al., 2003; Moriyama and Yahara, 2002). Previous studies have shown CAP was able to form large protein complexes although it was thought these heterogeneous complexes consisted primarily of CAP and actin proteins, and so future studies will hopefully investigate the capabilities of CAP proteins and work to elucidate its complex functioning (Hubberstey et al., 1996; Hubberstey and Mottillo, 2002; Moriyama and Yahara, 2002).

Cofilin was originally identified as an F-actin binding protein and was named for its formation of co-filamentous structures with actin (co-filin), however further analysis revealed it was a member of a previously categorized family of monomer binding Actin Depolymerizing Factor (ADF) proteins which are named for their ability to spontaneously disassemble actin filaments, and are currently referred to as the ADF/Cofilin (AC) family of proteins (Bamburg et al., 1999; Dawe et al., 2003; Sarmiere and Bamburg, 2004). AC proteins are the predominant regulators of filament dissociation, yet they typically do not influence the reserve pool of G-actin (as it is too abundant) (Bamburg, 1999; Gungabissoon and Bamburg, 2003). These proteins are essential for dynamic fiber retraction and dramatically impair many major cellular processes when removed from the cell (Bamburg, 1999; Bamburg and Wiggan, 2002). AC proteins cooperatively bind to ADP-filaments and induce an un-stable twist in the fiber resulting in the liberation of small actin multimers which cofilin further disassembles into the single monomer, which remains bound by cofilin (or ADF) in a 1:1 stoichiometric ratio (Bamburg, 1999; Ojala et al., 2001). AC proteins remain bound to ADP-monomers until the interaction with additional actin associated proteins catalyzes the monomer's nucleotide exchange (ADP for ATP) which then results in AC

40

dissociation from the monomer, and upon further activation (de-phosphorylation) through the LIM kinase pathway (an effector of Rac and Rho) is able to continue filament degradation (Bamburg, 1999; Birkenfeld et al., 2003; Mohri et al., 2000; Sarmiere and Bamburg, 2002). It has been shown that CAP may participate with cofilin to increase monomer nucleotide exchange; however the first ever identified binding partner of cofilin was recently reported in yeast to be Actin-Interacting-Protein (Aip1, homologue to the mammalian WDR1 protein) and cofilin has since been implicated in large protein complexes with CAP, Aip1, and actin thus suggesting the presence of a novel regulatory mechanism for actin (Amberg et al., 1995; Dawe et al., 2003; Kuhn et al., 2000; Rodal et al., 1999).

Control Over Actin Remodeling Pathways:

Guanine tri-phosphatases (GTPases or G-proteins) represent a broad class of molecular switches through which a cell initiates morphological responses to extra-cellular signals (ECS). ECS are perceived through three main pathways, the first being direct entry of the ECS into the cell through the membrane (as is the case of steroid hormones), the binding of a surface ligand to initiate pinocytosis or endocytosis (e.g. viral invasion) or through the production of intracellular messenger molecules, stimulated by the binding of specific ligands on the surface of the cell which then initiate signal transduction cascades through either the phosphorylation (addition of a phosphate group), prenylation (addition of 20 carbons), or farnesylation (addition of 15 carbons) of effector proteins (Adjei, 2001; Bishop and Hall, 2000). The activation of signal transduction cascades occurs through the activation (phosphorylation) of cell surface receptors which

41

span the membrane to transduce the ECS to membrane-localized cytosolic proteins (adaptor proteins) which in turn activate additional (more mobile) cytosolic effector proteins (Adjei, 2001).

Actin Signaling Through G-proteins

The Rho GTPase Family comprises a unique class of G-proteins that primarily localize away from the membrane within the cytosolic during their quiescent state but bind the cytosolic C-terminal domain if activated integrin membrane receptors (Adjei, 2001; Hall, 1998b). Rho GTPases mediate their signals through guanine exchange factors and guanine dissociation inhibitory proteins through which they are able to induce a variety of cellular responses which include endocytosis, exocytosis, cell proliferation, neurogenesis and cell motility (Blangy et al., 2000; Hall, 1994; Hall, 1998a).

The Rho family of G-proteins encompasses three subfamilies: Rho, Rac, and Cdc42 proteins (Bishop and Hall, 2000; Clayton et al., 1999; Hall, 1995). The Rho subfamily of G-proteins were the first classified by Ridley & Hall, 1992 through their ability to direct the assembly of contractile myosin-actin filaments (stress fibers) and initiate the assembly of focal adhesion structures for mediating cell attachment (Hall and Nobes, 2000; Nobes et al., 1998; Olivo et al., 2000). The Rho family has been expanded to include many proteins such as Rho A (with p160 ROCK), Rho B, C, L, and Rnd 1, 2, 3 (Bishop and Hall, 2000; Blangy et al., 2000; Drechsel et al., 1997; Hall and Nobes, 2000; Kroeze et al., 2003). Subsequent studies have shown the stress fiber formation induced by Rho does not involve *de novo* filament assembly but is instead triggered through the activation of bundling proteins to assemble strong filament bundles (Hall, 1998b; Kroeze

42

et al., 2003; Ridley and Hall, 1994). Interestingly, Rho has also been implicated in neurogenesis and is currently thought to be the dominant regulator of neurite retraction and cellular rounding by directing the assembly of contractible fiber formation (Hall, 1998b; Kuhn et al., 2000; Nobes and Hall, 1995). Complementary to these findings Rho has also been shown to be a dominant regulator of the first Gap phase (G_1) of the cell cycle, and further interacts with other regulators (such as Rac) later during cytokinesis and cell division (Cotteret and Chernoff, 2002; Nobes and Hall, 1999; Verma and Ihler, 2002). Rho is thought to impart this effect through the recruitment of focal adhesion proteins and assembly of contact mediated FA structures (Critchley, 2000; Hall, 1998b; Machesky and Hall, 1996). Rho signaling is not only critical for FA formation but also FA maintenance, as studies have demonstrated that within 15 minutes of blocking Rho activity integrin receptors dissociate from the FA which disrupts the adhesion dependent signaling that is critical for progression through the cell cycle and cell viability (Hall, 1998b; Ridley and Hall, 1994). Interestingly, the signals responsible for integrin clustering are also required for correct FA formation but not for stress fiber formation or for FA protein (such as vinculin) localization to the ends of the fibers, suggesting a cooperation of pathways is needed to induce FA assembly (Bailly, 2003; Bailly et al., 2003; Machesky and Hall, 1997; Medley et al., 2003).

The next subfamily of Rho proteins to be identified was the Rac family of G-proteins which was shown to activate actin dynamics at the leading edge of motile cells and is known to include the Rac proteins Rac1, 2, 3 (Blangy et al., 2000; Cotteret and Chernoff, 2002; Hall, 1995; Kuhn et al., 1998; Verma and Ihler, 2002). The Rac proteins differ from the Rho proteins primarily in their regulatory mechanism of actin proteins, as

43

Rac family is able to induce active actin polymerization, not just actin filament bundling (Adjei, 2001; Machesky and Hall, 1997). However Rac, like Rho has been shown to induce FA formation, although the FA structures formed by the Rac proteins are typically smaller and unlike true FA structures, are only present in the actively growing lead edge of motile cells (Machesky and Hall, 1997). These small FA structures consist of concentrated polymerizing actin filaments and are termed microspikes and are responsible for generating motility by driving the leading edge forward (Adams and Schwartz, 2000; Little et al., 2004; Small et al., 2002). The Rac family was shown to interact closely with the third Rho subfamily of Cdc42 proteins at the leading edge of cells and subsequent study reveal Cdc42 proteins localize to areas of active Rac proteins to regulate microvilli and filopodia extensions through a large number of effector proteins including Cdc42, G25K, Chp, Rho D, G, H and TC10 (Bishop and Hall, 2000; Drechsel et al., 1997; Hall and Nobes, 2000).

As the Rac proteins polymerize actin to push the cell edge forward the Cdc42 proteins produce microvilli and filopodia extensions of the cell membrane which facilitate substrate attachment and progression of motility (Hall, 1998b; Ho and Bretscher, 2001; Rodriguez et al., 2003). The mechanism of actin rearrangement within the filopodia is currently unknown, whether it be through bundling or *de novo* filament generation, however filopodia has been shown to exist in N-WASp defective fibroblast cells suggesting the Arp2/3 complex is not required which may suggest bundling protein activity (Bishop and Hall, 2000; Higgs and Pollard, 2001; Nakagawa et al., 2001). The mechanism of actin associated protein activated by Cdc42 is under current study.

Further studies examining activation, localization and protein targets have revealed many redundancies amongst these three families and have led to much debate about the correct categorization of family members, and even families since an increasing number of researchers group the preceding two families of Rac and Cdc42 families into one large class (Adjei, 2001; Bishop and Hall, 2000; Hall, 1998b).

Summary:

The main objective of this thesis was to identify and examine the role of mammalian WDR1 in actin rearrangement that occurs during cell adhesion, migration and neurogenesis.

The thesis is divided into two major chapters. Chapter two outlines the initial characterization of human WDR1 and analyses of the expression of WDR1 mRNA and protein in a variety of cells and tissues. Chapter 3 examines the localization of WDR1 proteins during dynamic actin remodeling processes such as cell retraction, migration, adhesion, and neurite extension during PC12 differentiation.

The results of this thesis provide further insight into the expression and potential role of mammalian WDR1 proteins during actin remodeling.

Chapter Two

Isolation and Characterization of Mammalian WDR1

Introduction:

Understanding the signal transduction pathways generating the multitude of cellular behaviours utilized by the cell is critical for the design of novel and innovative medical therapies and disease treatments. The human actin cytoskeleton regulates many vital cellular processes such as migration, endocytosis, exocytosis, mitosis/ cytokinesis, and neurogenesis. However a complete understanding of the mechanisms governing actin remodeling still remains elusive despite the involvement of actin in several prevalent diseases such as Alzheimer's disease, heart disease, and cancer. Currently, several families of regulatory proteins have been identified and their functions have been reported however most actin-interacting proteins and pathways that control actin remodeling remain unknown.

One family of recently identified actin interacting proteins has been classified according to a highly conserved motif of 30-40 amino acids bracketed by an N-terminal glycine-histidine (GH) residue pair and a C-terminal tryptophan-aspartic acid (WD) pair (Amberg et al., 1995; Gettemans et al., 2003; Rodal et al., 1999; Voegtli et al., 2003). Each motif encodes four anti-parallel β-sheets which interact to form one beta-propeller blade structure (Gettemans et al., 2003; Rodal et al., 1999; Voegtli et al., 2003). Proteins containing beta-propellers are typically involved in mediating protein interactions

46

(Amberg et al., 1995; Gettemans et al., 2003). These proteins are termed WD proteins and are conserved throughout eukaryotic species such as *Arabidopsis, Physarum, Dictyostelium, Drosophila,* yeast, *Xenopus,* chicken, rat, and mouse (Adler et al., 1999; Konzok et al., 1999; Oh et al., 2002; Ono, 2003; Rogers et al., 2003). WD proteins have been shown to interact with the actin depolymerizing protein cofilin and actin to enhance filament depolymerization in yeast (Okada et al., 2002; Ono, 2001; Rodal et al., 1999). However several reported observations of both *Drosophila* and *Dictyostelium* systems have recently supported a novel cofilin-independent function for WDR1 proteins during cytokinesis (Gerisch et al., 2004; Konzok et al., 1999; Rogers et al., 2003). Loss of WDR1 regulation has been shown to impact several actin-based processes such as endocytosis, exocytosis, cell migration and lamellipodia dynamics yet the most severe effects included induction of unregulated synchronous carcinogenic mitotic events (Aizawa et al., 1999; Gerisch et al., 2004; Konzok et al., 1999; Rogers et al., 2003). Recent studies of avian WDR1 demonstrated elevated protein expression during basal hair cell regeneration independent of cofilin (Adler et al., 1999; Oh et al., 2002). Preliminary studies on human endothelial cells have additionally implicated WDR1 to function within cell attachment and support the role of WDR1 during cell proliferation (Ichii et al., 2001). Despite the established study of WDR1 proteins in other eukaryotic organisms the human WDR1 gene remained uncharacterized. To help elucidate the function of human WDR1 proteins we have cloned and characterized the full length human WDR1 gene. During the cloning of full length WDR1, a second amplicon was discovered and through the use of WDR1 antibodies we have confirmed two forms exist in mammalian cells, a 50 kDa isoform (devoid of the final ~73 C-terminal amino acids) and the full length 60 kDa protein.

47

Materials and Methods:

WDR1 Isolation and HA-tagged Vector Construction:

The isolation of the full-length human WDR1gene (hWDR1) was accomplished using polymerase chain reaction (PCR) with primers #133F & #139R (Sigma) (Appendix A) designed using the human WDR1 sequence reported in the GenBank database as a template (www.ncbi.nlm.nih.gov). A human brain cDNA library was used as the template and an amplicon of 1821 bp corresponding to the full length gene was isolated and purified using a gel-purification kit (Sigma). The PCR product was subjected to restriction enzyme digestion with Eco RI and Not I which cleaved at sites embedded within the forward and reverse primers respectively. The purified digested product was ligated into the mammalian protein expression cloning vector pCI-HA (Promega) (Hubberstey et al., 1996) using T4 DNA ligase (MBI Fermentas) and transfected into DH5α *Escherichia coli* cells (by calcium chloride transformation). The C-truncated isoform of WDR1 (WDN534) was amplified using the primers (#132R & #133F) (Appendix A) and was digested with Not I and Eco RI enzymes (Promega). The WDN534 cDNA was then ligated into the pCI-HA and expression vector using T4 DNA ligase and transfected into DH5α cells.

Construction of HA-tagged Cofilin:

The human cofilin gene was cloned from a human brain cDNA library using PCR and primers designed against the human cofilin sequence available on the GenBank database (www.ncbi.nlm.nih.gov). The primers #143F and #141R were designed to contain an Eco RI and a Not I restriction enzyme site (respectively) which were used to

48

cleave the 501 nt amplicon for column purification and ligation into the pCI-HA vector (Hubberstey et al., 1996).

Production of the MYC-tagged proteins:

The production of MYC-tagged WDR1, WDN534 and cofilin was accomplished through the ligation of the inserts into the pCI-MYC mammalian expression vector (as described for the HA-constructs) (Hubberstey et al., 1996).

Gene Sequence Analysis:

All of the HA-tagged cDNA clones were completely sequenced at the York University core-facility to confirm sequence integrity. Further sequence comparisons and searches were performed using the NCBI BLAST on-line software program (http://www.ncbi.nlm.nih.gov/BLAST/).

Tissue Culture and Transfection:

Human embryonic kidney (HEK 293) and rat embryonic fibroblast (REF52) cell lines were maintained in Dulbeco's media (DMEM-Sigma) supplemented with 10% fetal bovine serum (Sigma) and 100 units/ml of penicillin/streptomycin (Sigma). The cells were grown at 37° C with an atmosphere of 5% CO_2, until ~90% confluency at which point the cells were spilt using 1X trypsin/EDTA (Sigma) and continued to be grown on either 10 cm, 6 cm, or 3.5 cm tissue culture dishes (Sarstedt) as appropriate for the experiment.

49

Western Blot Analysis:

The constructed plasmids were transfected into HEK 293 cells using Lipofectamine 2000 transfection reagent as outlined in the manufacturer's protocol (Invitrogen) using 1 μg of the DNA vector. The transfected cells were allowed to express the proteins for approximately 36-48 hours prior to protein extraction.

Total cytosolic protein extracts from the transfected and un-transfected control cells were collected by scraping the cells from their dishes in RIPA buffer (20mM Tris pH 7.5, 150 mM NaCl, 10 mM KCl, 1% NP-40 (IGEPAL CA-630), 10% glycerol) containing a protease-inhibitor (Roche Complete mini protease inhibitor cocktail tablets). The cells were then sonicated (power 3 for 2X 15 seconds on ice) and the cytosolic extracts were purified by centrifugation at 500 RPM for 8 minutes at 4° C. The total extracts were then denatured by boiling in 1X Laemmli protein sample buffer (SB) for 4 minutes and approximately 20 μg of protein was separated on a 10% SDS-PAGE gel and subjected to western blot analysis using a Bio-Rad blotting apparatus and Tris-glycine-methanol transfer buffer. After blotting onto nitrocellulose, identification of the HA- of MYC tagged proteins of interest were detected using a mouse-anti HA antibody (1:1000 in TTBS) or anti-MYC antibody (1:500) (a gift from Dr. Dallan Young, University of Calgary) for 1 hour at RT followed by a secondary incubation with horseradish peroxidase-conjugated (HRP) goat anti-mouse antibody (Chemicon) (1:4000 in TTBS). The blot was rinsed three times for 10 minutes in 1X TTBS and the tagged proteins were visualized using the LUMI-Light chemiluminescent kit (Roche). The size determination of the proteins was determined by the relative distance the proteins migrated compared to a protein ladder marker (MBI Fermentas).

50

Immunocytochemical Analysis of Cellular Protein Localization:

The cellular localizations of both endogenous and heterologous proteins were determined by immunocytochemical (ICC) analysis. Prior to plating cells, round glass coverslips (CS) (16 mm, Fisher) were prepared by heating in 500 ml of 1 M HCl at 50-60°C for 4-6 hours. The solution was cooled, rinsed three times with H_2O and sonicated for 15 minutes (1 complete cycle on the GE portable sonicating water bath) in three washes of ddH_2O, one wash of 50% and 70% ethanol and a final 30 minute wash of 95% ethanol. Mammalian cells were seeded onto the washed CS and grown until the cell density was ~50% confluent and then transfected as described previously with either one of the two HA-WDR1 vectors or the two control HA-tagged CAP1 (Hubberstey et al., 1996) and HA-tagged cofilin constructs. After 36-48 of protein expression, the cells were fixed onto the CS in 3.7% formaldehyde in 1X phosphate-buffered saline (PBS- 14 mM NaCl, 2.7 mM KCl, 10 mM Na_2HPO_4, 1.75 mM KH_2PO_4) for 10 minutes, and permeabilized for 10 minutes in 0.5% Triton X-100 in 1X PBS. The cells were then incubated with 100 μl of primary anti-HA mouse antibody (12CA5) diluted 1:500 in 1X PBS for 1 hour at 37° C, after which the excess unbound antibody was removed and the CS were washed in 0.05% Tween-20 in 1X PBS for 10 minutes followed by a 5 minute 1X PBS wash to removed excess detergent. The cells were once again hybridized for 1 hour at 37° C with an appropriate secondary Alexa fluor-conjugated goat anti-mouse antibody (Molecular Probes) and washed in 0.05% Tween-20 in 1X PBS. The coverslips were then rinsed three times in double distilled water and placed face down on a glass microscope slide coated with Slow-Fade Light anti-fade reagent (Molecular Probes) and sealed with clear nail polish prior to confocal microscopy analysis. The confocal analysis

51

was performed using an MRC 1024 laser scanning confocal microscope and the confocal-assistant software (Bio-rad). Further image manipulations were performed with either Adobe Photoshop or CorelDraw software.

GST-WDR1 Protein Production:

To generate bacterially expressed recombinant GST-WDR1 novel forward and reverse primers were designed (#144F and 145R) encoding the restriction sites Eco RI and Xho I respectively (Appendix A). The PCR was performed using one nanogram of pCI-HA-WDR1 as template and the amplicon was purified from a restriction digest using a plasmid purification column kit. The product was cloned into the pBlueScript /SK II (Stratagene) vector and further subcloned into the glutathione S-transferase (GST)-tag containing inducible vector pGEX-KG. The resulting GST-WDR1 vector was expressed in DH5α, XL1 Blue, and DH10β *E. coli* cells each grown at either 25° C, 30° C or 37° C and isolated using glutathione-agarose immobilized beads (Sigma). Briefly, the overnight plasmid-expressing bacterial cultures were diluted ~1:100 in fresh LB media and grown to an optical density (OD_{600}) of ~0.45 before recombinant protein expression was induced by the addition of isopropylthio-β, D-galactopyranoside (IPTG- Fisher) (1 mM final concentration). The cultures were induced for approximately 2-3 hours before they were centrifuged at 8000 rpm for 15 minutes and washed briefly in cold 1X PBS before the iced culture was lysed by sonication (3X on setting 3). The lysed cells were incubated in ~1.0% Triton X-100 for 30 minutes on ice and then centrifuged at 10,000 rpm for 15 minutes. After centrifugation 5 ml of supernatant was retrieved and nutated with 50 μl of a 50% slurry of 1X PBS and glutathione-beads for thirty minutes at 4° C. The beads and bound

52

proteins were washed three times in 1X PBS before boiling for 4 minutes in 1X SB to disrupt the glutathione-GST bond allowing the GST-fusion protein to be analyzed on a 10% SDS-PAGE gel and visualized using Coomassie Blue protein stain. Analysis of the GST-WDR1 recombinant protein demonstrated the fusion protein was not stable and was degraded by the *E. coli* cells. Therefore, two additional primers sets were designed from the WDR1 sequence to produce two smaller N-terminal (GSTWDN) (#144F & #146R) or C-terminal truncated (GSTC190) GST-fusion proteins (#145R & #147F) (Appendix A). The bacterial expression and protein analysis were performed on both the N- and C-terminal constructs as described above and resulted in the production of only one partially stable recombinant protein (GSTC190). To increase protein stability GSTC190 was expressed as two smaller products. Additional primer sets complementary to the C190 fragment and were designed which produced both an N-terminal 146 aa GSTC158 (#147F & #162R) and a C-terminal 130 aa GSTC136 (#163F & #145R) recombinant protein (Appendix A). The purification of the two recombinant proteins was performed as described above using a 100 ml 1:100 diluted LB culture except following the post-triton incubation centrifugation half of the pellet was washed three times in thrombin cleavage buffer (20 mM Tris pH 8, 150 mM NaCl, 2.5 mM CaCl$_2$) and subjected to a 30 minutes incubation in the thrombin cleavage buffer containing 3-4 units of thrombin (~3 units/ 1 µl thrombin enzyme). The thrombin cleavage reaction was stopped by the addition of phenylmethylsulphonyl fluoride (PMSF) (Sigma) (1 mM final concentration).

53

WDR1 Antibody Production and Purification:

Rabbit antibodies were raised against a synthetically generated 17 residue peptide sequence corresponding to a highly conserved and stable hWDR1 epitope as predicted by software computations (acetyl-TEDSKRIAVVGEGREKC-) (SynPep Corporation). The N-terminal hWDR1 epitope is present in both the full length and truncated N534 proteins. The peptide was conjugated to a KLH tri-peptide and injected into two female NZW (SPF) rabbits (named Fluffy and Bananas) for 28 days prior to the first of three collections of antibody containing serum by SynPep Corp.

The serum of both rabbits was assayed for antibody titer against the WDR1 peptide by SynPep following each extraction and was verified upon reception using western blot analysis of HA-tagged proteins WDR1, WDN534, cofilin, and CAP1. The blot was probed initially with the anti-WDR1 serum, then stripped using Restore stripping buffer (Pierce) and reprobed with the anti-HA antibody to verify antigenic specificity. The serum was subjected to further purification using ammonium-sulfate precipitation and dialysis. The ammonium-sulfate reaction was performed using 10 ml of serum to which 10 ml of a cold saturated ammonium sulfate solution was added drop-wise and mixed at 4° C for one hour before centrifugation at 3000 x g for 20 minutes. The pellet was resuspended in 10 ml of sterile 1X PBS and the ammonium-sulfate was removed over night at 4° C through dialysis using three changes of 1X PBS buffer (Pierce dialysis cassettes). The specificity of the antibody was again assayed as described above and the purified rabbit serum was then centrifuged at 3000 x g for 4 minutes and aliquoted for storage.

The cofilin polyclonal rabbit antibody and the vinculin monoclonal mouse antibody were both purchased from Cytoskeleton Inc. while the hCAP1 was previously produced by Dr. A. Hubberstey (Swiston et al., 1995). The ICC 594 nm red and far-red 647 nm phalloidin dyes and the secondary anti-mouse and anti-rabbit Alexa 488 nm (or 594 nm) fluor-conjugated antibodies were all purchased from Molecular Probes. The anti-G-actin monoclonal antibody was purchased from Chemicon while the anti-β-tubulin monoclonal mouse antibody was obtained from Sigma. The HRP-conjugated secondary goat anti-mouse or anti-rabbit antibodies for western blot analysis were also purchased from Molecular Probes.

The endogenous localization patterns of WDR1, F-actin, cofilin, CAP, vinculin and β-tubulin proteins were examined using the ICC technique described above in both HEK 293 cells and REF 52 cells. The 1X PBS dilutions of the antibodies used were anti-WDR1 (1:200), anti-cofilin (1:100), anti-CAP1 (1:100) and anti-β-tubulin (1:500) and an anti-F-actin 568 phalloidin stain (1:50).

The simultaneous staining of two target proteins was performed as described previously with the exception that two primary antibodies were added together, washed and incubated for 1 hour at 37° C with both of the two corresponding secondary antibodies. For the preparation of the triple labeled CS the two targeted proteins were prepared as described above with the exception of the second antibody hybridization which included a 1:30 dilution of Alexa 684 phalloidin (blue) to stain F-actin. The visualization of protein localization was performed using ICC confocal analysis as described.

<u>Immunoprecipitation Analysis</u>:

To determine binding partners of WDR1, immunoprecipitation (IP) experiments were performed using Protein-A agarose conjugated HA-antibody columns targeted against the exogenous HA-tagged proteins. The HA-affinity columns were prepared by chemical linking ~1.0 mg (300 μl) of 12CA5 anti-HA antibody to 1.5 ml of Protein-A beads (Sigma) washed in sterile 1X PBS. The 12CA5 antibody heavy chain was covalently linked to the amino groups of the Protein-A beads using 20 mM imidoester containing dimethylpimelidate in a 0.2 M sodium borate solution (sterile 1X PBS) for one hour. The reaction was stopped by the addition of 0.2 M ethanolamine (pH 8). The beads were then washed with 1X sterile PBS and following analysis on SDS-PAGE gel, and the gel was stained with Coomassie blue to verify the covalent cross-linking reaction was complete. The beads were then stored at 4° C in a 50% slurry in sterile 1X PBS until further use.

HEK 293 cells at 50-60% confluency on 60 mm plates were transfected as described previously using Lipofectamine 2000 with either the HA- constructs or co-transfected with both HA- and MYC- vectors. After 36-48 hours, the cells were sonicated and total cytosolic protein was collected in either 1 ml or 0.5 ml of protease-inhibitor containing RIPA buffer (as described previously except with 0.1% NP 40, 15 mM NaCl and 1% glycerol). A portion of the extract was retained and prepared in 1X SB to assay protein expression (transfection efficiency) using western blot analysis while the remaining total protein extract was incubated with 40 μl of the affinity column slurry for one hour. The column was then washed three times with 0.5 ml of RIPA buffer before boiling for 4 minutes in 1X SB and resolving on a 10% or 12% SDS-PAGE gel for

western blot analysis using either anti-actin, anti-MYC and anti-HA antibodies for protein detection.

Reverse Transcriptase Polymerase Chain Reaction (RT-PCR):

Total human RNA from lung, kidney, liver, heart, brain and trachea (Ambion) was used to synthesize cDNA templates in a reaction containing 1 µg of each sample, 0.5 µg of oligo dT (Promega), and 10 µM of dNTPs and heated for 15 minutes at 65° C followed by the addition of 5X reverse transcriptase buffer, 2 nmol of DTT, and 1µl of RNAse Out (Invitrogen). Each reaction was heated initially for two minutes at 42° C before the addition of 1 µl of Superscript II reverse transcriptase (Invitrogen) and incubated for 50 minutes, followed by a 15 minute 70° C incubation. The cDNA reaction was cooled on ice, briefly centrifuged and stored at -20° C expression of WDR1 and WDN534 transcripts within each tissue were analyzed using PCR Supermix (Invitrogen) and primers directed against a commonly shared 400 bp N-terminal domain using the primers #133F & #155R and a unique 600 bp sequence within the C-terminal domain of WDR1 (#156F & #139R) (Appendix A). The constitutively expressed glycolytic enzyme glyceraldehyde-3-phosphate dehydrogenase (GAPDH) was additionally amplified to serve as an internal control for both the reverse transcriptase reactions and PCR reactions (#149F & #150R) (Appendix A). This experiment was also repeated using rat cerebellum, frontal cortex, post cortex, pons, spinal cord, medulla, and hippocampus RNA samples for cDNA template generation to non-quantitatively determine the expression of WDR1 within several isolates of neural tissue.

57

<u>Northern Blot Analysis</u>:

Total RNA was collected from a variety of cell lines including HEK 293, REF 52, rat pheochromocytoma (PC12), human breast adenocarcinoma (MCF7), human brain astrocytoma (U87), human lung cancer (Calu), and human prostate cancer (DU145) cells maintained in 10% FBS DMEM with 1% P/S (as defined previously with the exception of the PC12 cells which contained an additional supplement of 5% horse serum) on 10 cm plates. To avoid RNAse contamination all distilled water for either solution preparation or equipment pre-washing was treated with 0.1% (v/v) diethyl pyrocarbonate (DEPC, Sigma) followed by 2-3 multiple autoclaving cycles. Laboratory equipment was additionally presoaked in RNAse-Out solution (Ambion) and washed three times with DEPC-H$_2$O. The total RNA was collected using TRIzol (Invitrogen) as per supplied instructions with the exceptions only 0.5 ml of 75% ethanol was used for the final washes and the pellet was resuspended in only 30 µl of RNAse free water to increase the concentration of the RNA. The samples were prepared by adding ~10 µg of RNA to a solution of 15 µl formamide, 3 µl 5X MOPS pH 7 (2.0 g N-morpholino propane sulfate, 80 ml DEPC- H$_2$O, 5 mM sodium acetate) and 5 µl formaldehyde and were heated to 65 ℃ for 15 minutes before the addition of 2 µl northern 5X SB. The samples were then loaded onto a 1.2% agarose formaldehyde gel (8 ml 5X MOPS, 7.15 ml 37% formaldehyde, 25 ml DEPC-H$_2$O and 0.5g agarose) pre-run for 5 minutes at 39 volts in 1X MOPS running buffer. The samples were run at 50-55 volts for 4-5 hours until the bromophenol blue dye front migrated approximately 7 cm into the gel. The gel was then soaked in three rinses of DEPC- H$_2$O for a total time of 1 hour to remove excess formaldehyde and then soaked in sterile 20X SSC buffer pH 7 (175.3 g NaCl, 88.2 g sodium citrate, 800 ml DEPC- H$_2$O)

58

for 45 minutes to 1 hour. The RNA samples were then transferred over night to a positively charged nylon membrane (Osmotics) solid support using capillary transfer. Following the overnight transfer of RNA, the nylon membrane was soaked for 5 minutes in 6X SSC prior to the immobilization of the RNA by covalent cross-linking using shortwave UV light of 254 nm for 1 minute using a Bio-rad crosslinker followed by dehydration of blot under vacuum for 1 hour at 80° C in a Bio-rad gel dryer. The membrane was then placed in 10 ml of ULTRAhyb hybridization buffer (Ambion) at 55° C for one hour before the addition of the [^{32}P]-dCTP isotope-labeled DNA probe which hybridized with the membrane for 12-14 hours. After hybridization the radioactive membrane was briefly washed at RT twice for 5 minutes and once for 10 minutes using 0.1% (w/v) SDS 2X SSC, and finally for 20 minutes with 0.1% SDS 1X SSC before the membrane was wrapped in Saran wrap and exposed to blue Kodak film using a BioScience intensifying screen in a Kodak film cassette. The cassette was stored at -80° C for two to four days before the film was removed and developed using Kodak developer and fixer.

Probe synthesis for Northern Blot Analysis:

The synthesis of the WDR1 DNA probe was performed using magenta DNA Klenow polymerase (Stratagene) and 50 ng of purified PCR generated WDR1 cDNA for 10 minutes at 37° C using the Stratagene Prime-It labeling kit and [α-P^{32}] cytosine tri-phosphate (Amersham). The probe synthesis reaction was terminated by the addition of 5 mM EDTA and immediately purified using a Sephadex column (Amersham). During the probe synthesis reaction 1 μl samples were taken to assay both reaction efficiency and

59

probe activity using scintillation β-particle counting analysis (Packard Bell). Following elution of the labeled probe from the column, the probe was denatured by boiling for 3 minutes at 100° C, quickly centrifuged and added directly to the pre-hybridized membrane. The synthesis of the GAPDH probe was performed as described above using 50 ng of purified PCR generated GAPDH template using the primers #149F and #150R (Appendix A).

To reprobe the northern blot, the hybridized DNA probe was stripped prior to the next pre-hybridization by immersion of the membrane in two 150 ml washes of boiling 0.1% SDS 0.1 X SSC solutions. Excess liquid was removed and the membrane was incubated in the pre-hybridization buffer prior to subsequent hybridization.

Results:

The Cloning of hWDR1 and Sequence Characterization:

The cloning of the human WDR1 (hWDR1) gene from a human brain library resulted in the isolation of an 1821 bp cDNA which corresponded to the full length WDR1 gene transcript and encoded nine WD motifs. At that time no complete full length sequence existed, however several reported partial cDNA sequences were used to compile the entire sequence which was used to design the PCR primers. Using the human genome database sequence we confirmed that the human WDR1 gene resides on chromosome 4 (4p16.1) (Adler et al., 1999).

In addition, a database search for WDR1 homologs indicated that a C-terminal truncated isoform also existed in some species. Therefore, primers were designed to amplify a truncated WDR1 transcript that lacked the final 287 nucleotides (nt) of the full

Table 2.1 Comparisons of WDR1 orthologs

Species	Size	#WD Motifs	% Seq. Identity
Human	60.6 Kd	9 WD	100%
Mouse	60 Kd	NA	95%
Chick	67 Kd	9 WD	88%
Xenopus	65 Kd	7 WD	78%
C. elegans	65 Kd	9 WD	38%
Yeast	67 Kd	8 WD	28%

Figure 2.1 Comparisons of WDR1 orthologs.

The sequences of WDR1 orthologs were compared. The sequence of proteins from human (top line), mouse (second line), chick (third line), *Xenopus* (fourth line), *C. elegans* (fifth line) and yeast (bottom line) were analysed. The star (*) indicates residues that are conserved within the species, (:) denotes residues displaying conserved substitutions while (.) identifies semi-conserved residue substitutions. The locations of the hWDR1 WD motifs are as reported in GenBank, and shown in the blue text.

62

Figure 2.1

Figure 2.2 Examination of the kelch-like WDR1 motifs.

The WD motifs of WDR1 are similar to motifs identified from the *Drosophila* kelch protein. The typical kelch motif is shown (top). The essential (red), the hydrophobic (green), the large (blue), the small (pink), and polar (gray) amino acid groups are shown. Comparisons of sequences of hWDR1, *S. cerevisiae*, and *S. pombe* WD motifs are displayed and mismatched residues are indicated in yellow.

64

Kelch Motif Consensus

N-terminus   GH--...----s-lhhhGG-s---...-----p----Y------W-----...---WD   C-terminus

WDR1 Kelch-like Motif Comparisons

(Number indicates the first G in GH, the first G in the GG, the Y and W in the final WD)

hWDR1

#1 N-Terminus	GH---...--kVCALGGsK ---...--D----YaisW----...---WD				
	145	227	238	263	
#2	GH---...--LtVHKNGGkS---...--dG----YWD				
	218	332	358	359	
#3	GH---...--NeHFASGGmD---...--D----YvW---...------WID-----WT				
	530	550	557	584	603

S. cerevisiae Aip1p

#1 N-Terminus	GH--...--DqEPYQGGi--...---D----YWD				
	158	254	279		
#2	GH--...--YnPLISGSyD---...---S----YSSISWD				
	338	353	388	393	
#3	IH--...--EdLVATGSID---...--A---YNNLLWE--...---AD---WN				
	529	559	586	591	601	610

S. pombe Aip1p

#1 N-Terminus	GH--...--EiDAHKGSi---...--T----YSCKIWD				
	144	231	253	258	
#2	GH--...--AtHFYTASYDGTVLSWD				
	313	333	342		
#3	IH--...--StHLATASIDT----E----YiamknahslgatqveWY				
	520	540	567	573	

s = small residue (A, G, S and sometimes N, D, C, P, T, V)
l = large residue (R, E, Q, H, I, L, K, M, F, Y, W and sometimes N, D, C, P, T, V)
h = hydrophobic residues (A, G, I, L, M, F, P, W, Y, V, and sometimes C & K)
p = polar residues (R, N, D, C, E, Q, H, K, S, T)
R = highly conserved kelch amino acids
Y = amino acid inconsistent with kelch homology
- = non-conserved amino acid residue
... = unspecified number of amino acids

Figure 2.2

length WDR1 sequence. Table 2.1 compares the sequence of hWDR1 and the reported nucleotide sequences of other WDR1 genes, the number of predicted WD motifs and the percent homology to the hWDR1 gene. Figure 2.1 displays sequence comparisons of the WDR1 genes and the predicted location of the WD motifs. The comparison of the gene sequences displays evolution of the WDR1 gene as the human gene is approximately 28% homologous to yeast and 95% similar to rat gene sequences.

This indicates that WDR1 may serve an essential function within vital cytoskeletal processes. The WD motif of the hWDR1 gene was noted to show strong homology to a motif described in the *Drosophila* Kelch protein family identified through a conserved kelch motif containing an N-terminal GH dipeptide and a C-terminal WD dipeptide. These conserved residues flank a central core containing one large amino acid preceding three hydrophobic acids followed by two glycines and finally terminating downstream with a tryptophan residue six amino acids downstream from a conserved tyrosine residue, typically preceded by a polar acid as shown in Figure 2.2 (Adams et al., 2000; Gettemans et al., 2003; Kim et al., 1999). The kelch motif typically consists of 44-56 residues encoding four anti-parallel beta-sheets which fold and form one blade of a beta-propeller structure. Proteins containing β-propellers typically mediate protein interactions and are used by a large percent of the kelch proteins to bind and modulate actin (Adams et al., 2000; Kim et al., 1999; Soltysik-Espanola et al., 1999; Way et al., 1995).

The hWDR1 protein contains three kelch-like motifs located within the beta-propeller motifs at residues (GH 145) 224-242 (WD263) in the fifth WD motif, (GH 218) 338-359 (WD 359) in the sixth WD motif and at (GH 530) 546-559 (WD 584) in the eighth WD motif as indicated in Figure 2.2. The kelch-like motifs of hWDR1 display the

conserved di-glycine peptides, the aromatic tyrosine and tryptophan reported in more then 90% of known kelch proteins. However these motifs notably lack the conserved six amino acids spacing between the Y and W residues typically observed within ~70% of the identified kelch proteins (Adams et al., 2000; Kim et al., 1999). The yellow residues in Figure 2.2 indicate amino acid types not typically exhibited within ~70% of the kelch proteins examined, however the remaining coloured residues indicate the high homology between the kelch motif and the WDR1 kelch-like sequences which suggest WDR1 may be classified as a kelch-like protein. The presence of presumptive kelch motifs within WDR1 further suggests that WDR1 serves a critical function in mediating protein interactions involved in actin rearrangement.

Expression of WDR1 in Mammalian Cells:

To examine potential proteins interacting with WDR1, HA- and MYC-tagged WDR1, WDN534, and cofilin vectors were used to over-express these proteins in mammalian cells. Western blot analysis revealed that the cloned WDR1 MYC- and HA-tagged proteins (Figure 2.3, lanes 1 & 5) were found to both produce a 60 kDa protein, consistent with the sizes of previously reported WDR1 proteins. A small discrepancy in size between the HA- and MYC-WDR1 proteins was observed with MYC-WDR1 protein appearing slightly larger in size. This difference was attributed to the presence of the larger MYC epitope tag as this result was consistently observed between the WDN534 (Figure 2.3, lanes 2 & 6), and cofilin (Figure 2.3, lanes 3 & 7). The expression of the HA- and MYC-tagged WDN534 generated a C-terminal truncated 50 kDa protein (Figure 2.3, lanes 2 & 6). The expression of the HA- and MYC-tagged cofilin is shown in Figure 2.3

67

Figure 2.3 Expression of HA- and MYC- tagged WDR1, cofilin and CAP1 vectors.

Verification of correct exogenous protein expression in HEK 293 cells was performed using SDS-PAGE analysis. The expression of both HA- (lanes 1-4) and MYC- (lanes 5-7) was assayed. HA-WDR1 (lane one), HA-WDN534 (lane two), HA-cofilin (lane three), HA-CAP1 (lane four) were constructed with MYC-WDR1 (lane five), MYC-WDN534 (lane six), and MYC-cofilin (lane seven).
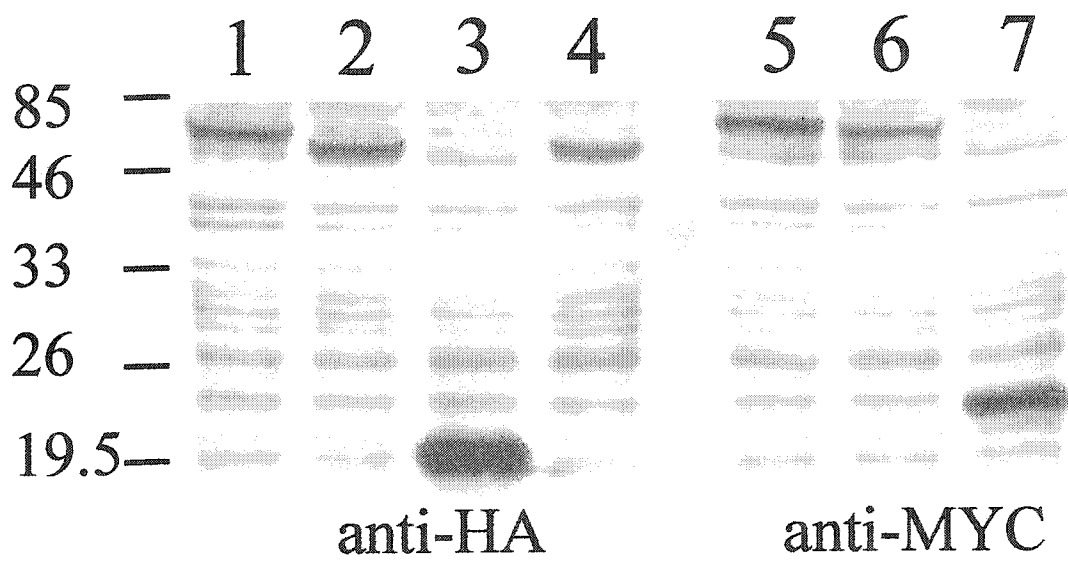
Figure 2.3

(lanes 3 & 7) and yielded proteins approximately 19 kDa and 22 kDa respectively (owing to the MYC epitope tag size difference) which is consistent with the established size of 19 kDa for full length cofilin (Bamburg, 1999).

Since no data exists on the expression of WDR1 in various tissues, an analysis of WDR1 transcript levels was performed using human RNA. RT-PCR analysis was performed on human cDNA that had been produced using human total RNA as template. Three amplicons were produced, two expressing either the N or C-terminus of WDR1 and a third 800 bp fragment reflecting the control gene glyceraldehyde-3-phosphate dehydrogenase (GAPDH). The strong expression of the GADPH fragment in each lane confirmed the quality of the cDNA. The two WDR1 gene fragments that were amplified attempted to distinguish between the full length and the truncated WDR1 transcripts (Figure 2.4A). A C-terminal 600bp fragment corresponding to only the full length WDR1 gene was observed (Figure 2.4B, lane 2-7). An N-terminal fragment which would amplify both the full length and truncated transcripts was also observed in all tissues (Figure 2.4B, lanes 2-7). The same expression pattern was also observed within rat cerebellum, frontal cortex, post cortex, pons, spinal cord, medulla and hippocampus samples (Figure 2.4C, lanes 2-8). Although the RT-PCR was not quantitative, the results indicated that WDR1 was expressed in a variety of human tissues; however the relative N-terminal and C-terminal amplicon intensities varied amongst samples, suggesting that at least two isoforms of WDR1 exist in tissues.

To further investigate the presence of alternate WDR1 transcripts, northern blot analysis of WDR1 expression in the human cell lines DU145, MCF7, HEK 293, Calu, U87 and the two rat cell lines of REF 52 and PC12 cells resulted in the identification of a

70

Figure 2.4 RT PCR analysis of WDR1 and WDN534 tissue expression.

The expression of both WDR1 and WDN534 within selected rat and human tissues was investigated using RT PCR. A, schematic representation (top) of the N- (400 bp) and C-terminal (600 bp) WDR1 amplicons. Additionally, the co-amplification of the constitutive 800 bp GAPDH was used for an internal control. B, expression of hWDR1 within lung (lane two), liver (lane three), kidney (lane four), heart (lane five), brain (lane six), and trachea (lane seven). C, expression of WDR1 within rat brain extracts of cerebellum (lane two), frontal cortex (lane three), post cortex (lane four), pons (lane five), spinal cord (lane six), medulla (lane seven), and hippocampus (lane eight) tissues.
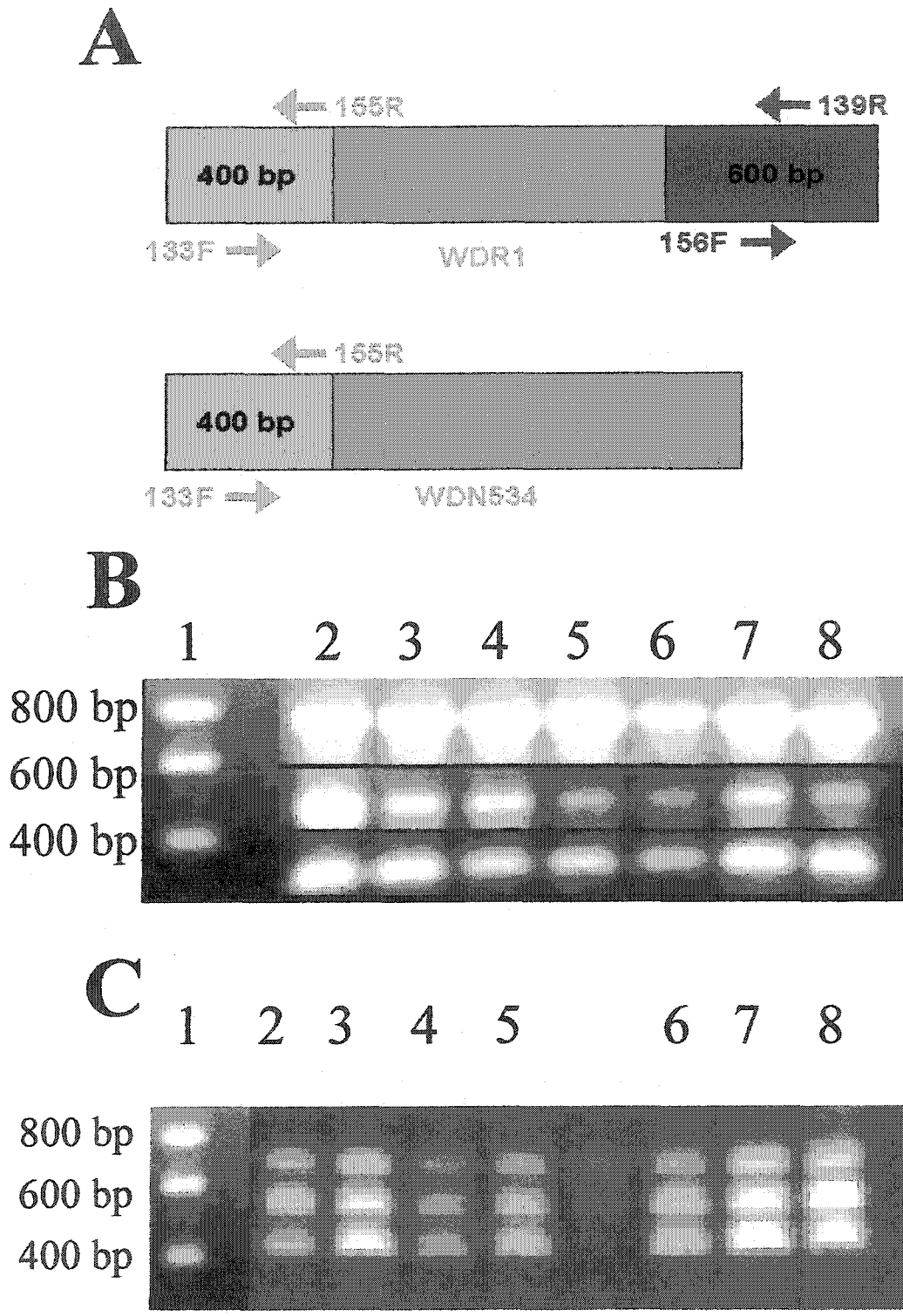
Figure 2.4

Figure 2.5 WDR1 transcript expression analyses.

The endogenous expression of mammalian WDR1 was examined within a variety of cell lines using northern blot analysis. A, northern blot identifying the primary 3.0 kb WDR1 transcript (arrow), and the less intense 2.2 kb WDR1 band (arrow). B, northern blot verifying the presence of the 1.3 kb control transcript of GAPDH (arrow). C, the methylene blue staining of the 2.4 kb 18S and the 6.3 kb 28S RNA bands on the nylon membrane (arrows).

73
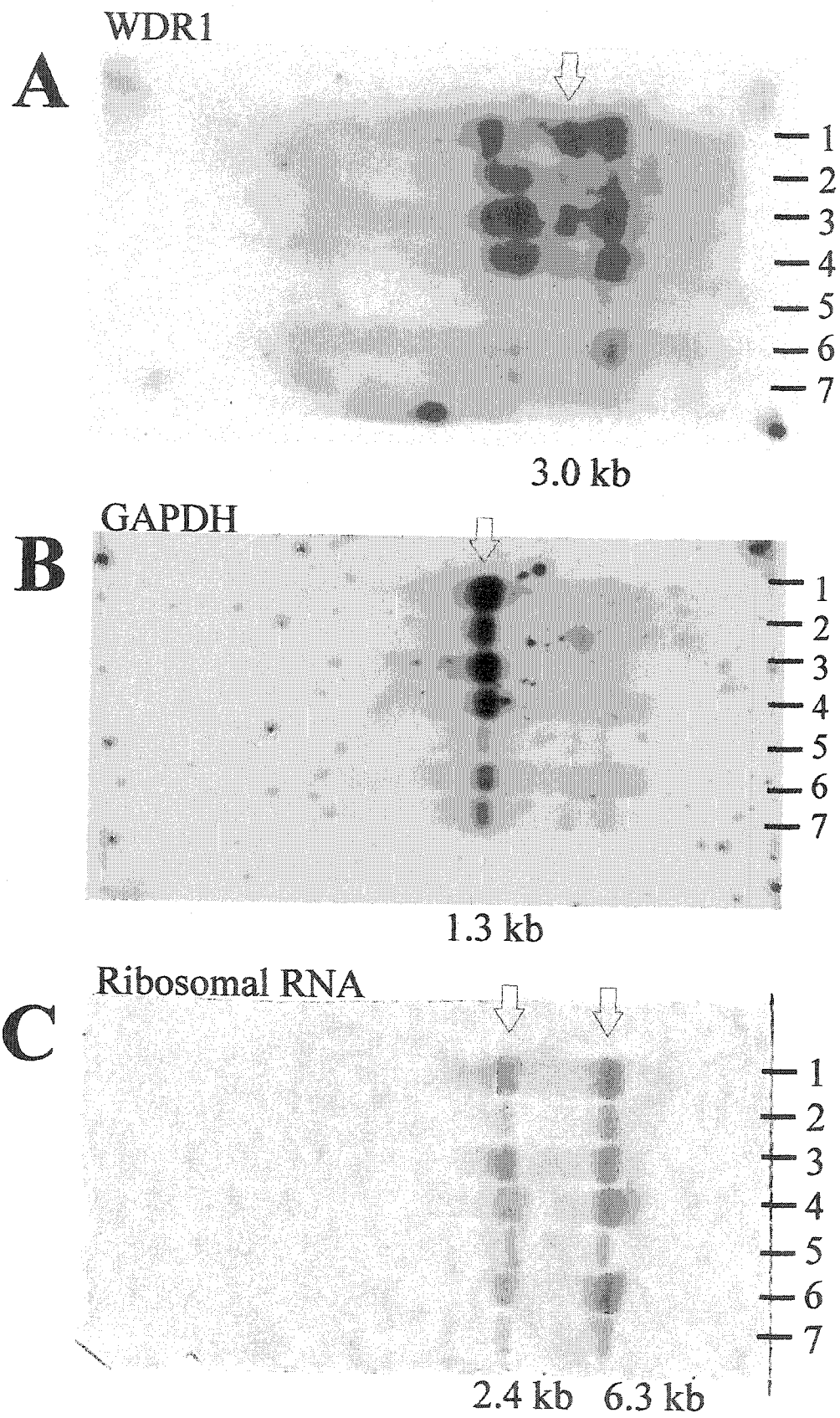
Figure 2.5

prevalent WDR1 transcript of approximately 3.0 kb (Figure 2.5A, lanes 1-7). However in some tissues a smaller truncated transcript of approximately 2.2 kb was also observed (Figure 2.5A, lanes 1-7). Additionally observed was some cross-reaction of the hWDR1 probe with ribosomal band fragments; however these results further support the RT-PCR data and suggests that at least two WDR1 transcripts may exist in some tissues. The quantity and quality of the RNA on the blot was then assayed using the 1.3 kb transcript of GAPDH as a positive control (Figure 2.5B, lanes 1-7). The GAPDH control hybridization pattern intensity corresponded to the WDR1 hybridization pattern which suggested the faint WDR1 expression in lanes 5-7 (Figure 2.5A) reflects a lower concentration of RNA. The RNA on the nylon membrane was further quantified using a bromophenol blue stain to visualize the ribosomal RNA 28S and 18S subunit transcripts (Figure 2.5C, lanes 1-7) and confirmed to be of inconsistent concentrations corresponding to the intensity of WDR1 hybridization. Therefore, the results of these experiments suggest WDR1 is widely expressed across many cell lines and that the WDR1 isoform may also be differentially spliced from the 3.0 kb full length transcript as predicted by Verma et al., (2004) and Adler et al., (1999).

WDR1 Antibody Production and Protein Expression

In order to generate anti-WDR1 antibodies, different fragments of hWDR1 were cloned into a GST expression vector in DH5α *E. coli*. Other reports had suggested that bacterial expressed WDR1 recombinant proteins were unstable (Oh et al., 2002) therefore various regions of hWDR1 were selected to provide the GST-fusions. The production of the 90 amino acid C-terminal recombinant WDR1 protein (GSTC190) was produced in *E.*

75

Figure 2.6 Recombinant WDR1 protein expression.

The production of recombinant GST-WDR1 in DH5α cells was assessed using SDS-PAGE analysis. The identification of GST-C190 (lane one, arrow), and the subsequent result of the two hour thrombin cleavage (lane two, arrow) and six hour cleavage (lane three, arrow). Within these lanes the cleaved GST fragments are visible (~28 kDa), and degradation products of incomplete cleavage reactions. The two consistently present bands indicated with two arrows in lane three are nonspecific interactions.

76
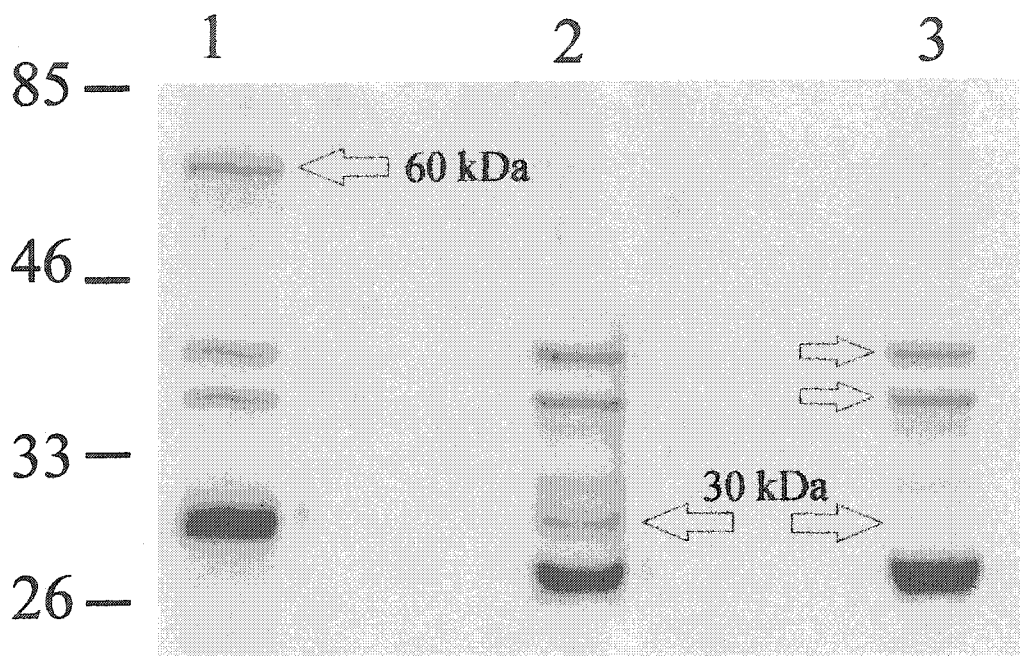
Coomassie Blue Stain

Figure 2.6

coli and analyzed on a 10% SDS-PAGE gel. It was observed that although the complete 60 kDa fusion protein was produced, it was significantly less abundant then the 28 kDa GST fusion tag (Figure 2.6, lane 1, arrow). The subsequent purification of the WDR1 protein required thrombin cleavage of the protein from the GST-tag which was performed for either two or six hours (Figure 2.6, lane 2 & 3 respectively). The two hour digest resulted in the liberation of small amount of C190 (as indicated by the arrow), and cleaved GST (~28 kDa), however complete C190 protein degradation was observed after six hours (Figure 2.6, lane 3, arrow) indicating that although the cleaved protein was stable enough for expression, it was not stable enough for purification. To maximize protein stability two smaller recombinant proteins were designed against the GSTC190 C- and N-termini (GSTC136 and GSTC158, Appendix A) predicted to encode 13 kDa and 14.6 kDa proteins respectively. However expression analysis demonstrated that neither of the two proteins was stable in sufficient abundance for purification and so it was decided that a synthetically derived peptide was to be used instead of the bacterially expressed protein.

To generate polyclonal antibodies against WDR1, a synthetically derived conserved 17 aa epitope in the N-terminus was synthesized *in vitro* and used to inject into rabbits. Purified serum was assessed for WDR1 specificity using over-expressed proteins in HEK 293 cells. As shown in Figure 2.7A all proteins were expressed in equal amounts and detected using anti-HA antibodies. However, only the WDR1 proteins in lanes 1 & 2 and not the cofilin or CAP1 proteins in lanes 3 & 4 were detected on a western blot using the anti-WDR1 antibody (Figure 2.7B).

Figure 2.7 Anti-WDR1 antibody specificity assays.

The specificity of the un-purified WDR1 polyclonal antibodies raised against synthetic WDR1 peptides was examined by western blot using HEK 293 cell extracts. A, the immunoprecipitated HA-tagged WDR1 (lane one), HA-WDN534 (lane two), HA-cofilin (lane three), HA-CAP1 (lane four), are shown with the total extracts of exogenously expressing HA-WDR1 (lane five), HA-WDN534 (lane six) and HA-CAP1 (lane seven) positive controls. B, the specificity of the un-purified anti-WDR1 antibody was assayed and found to detect only the IP extracts of HA-WDR1 (lanes one & five) and the total extracts of HA-WDN534 (lanes two & six).

79
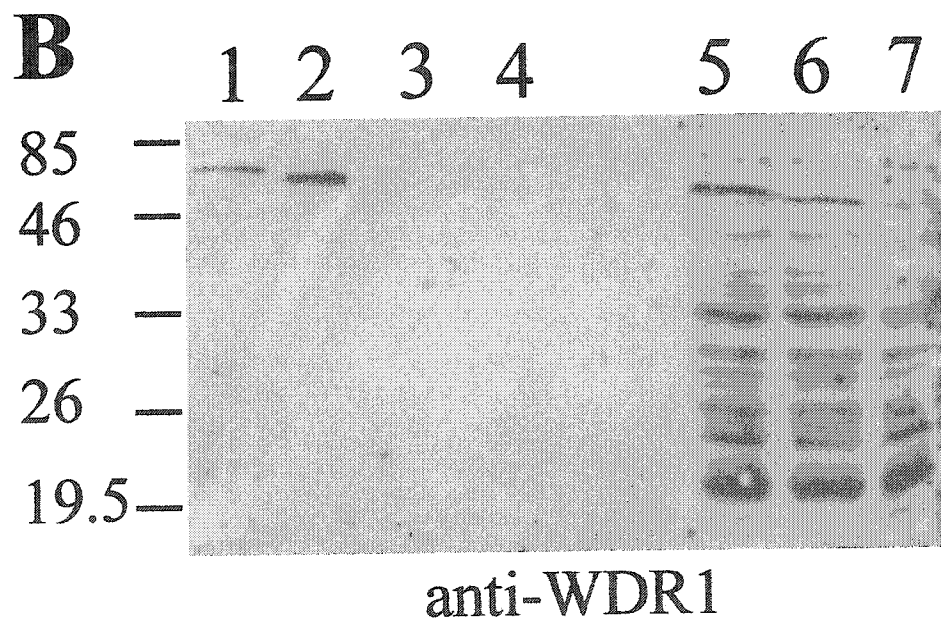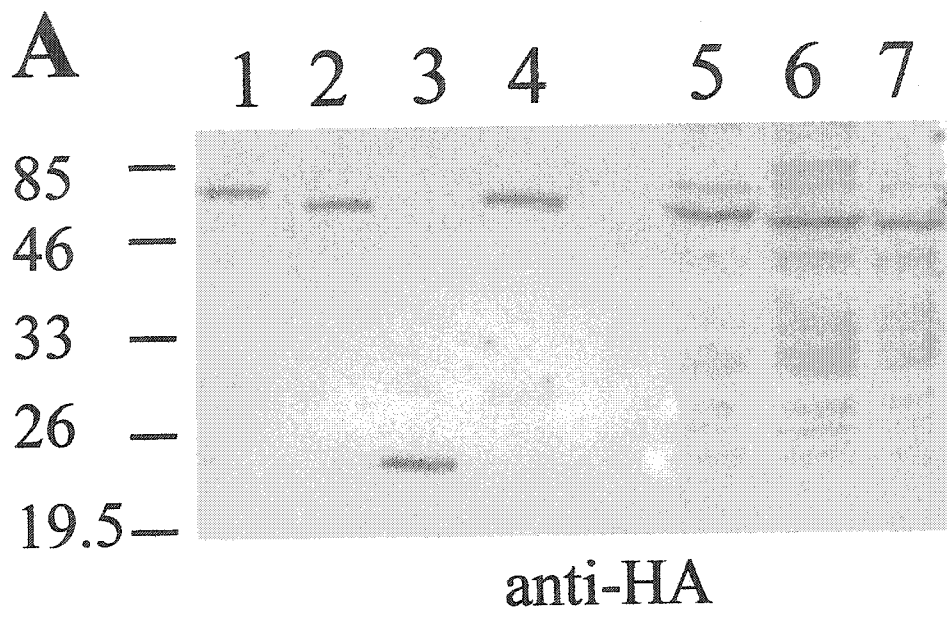
Figure 2.7

Figure 2.8 *In vivo* localization of endogenous WDR1.

The endogenous pattern of WDR1 localization was investigated using ICC confocal analysis of REF 52 fibroblast cells. Images A (400X total), G (600X), K (600X) display the endogenous WDR1 staining patterns. B (400X), E (600X), M (600X) indicate F-actin phalloidin staining. D (600X), H (600X), L (600X) show the localization of vinculin. C (400X), F (600X), I (600X), M (600X) display the merged images.

81
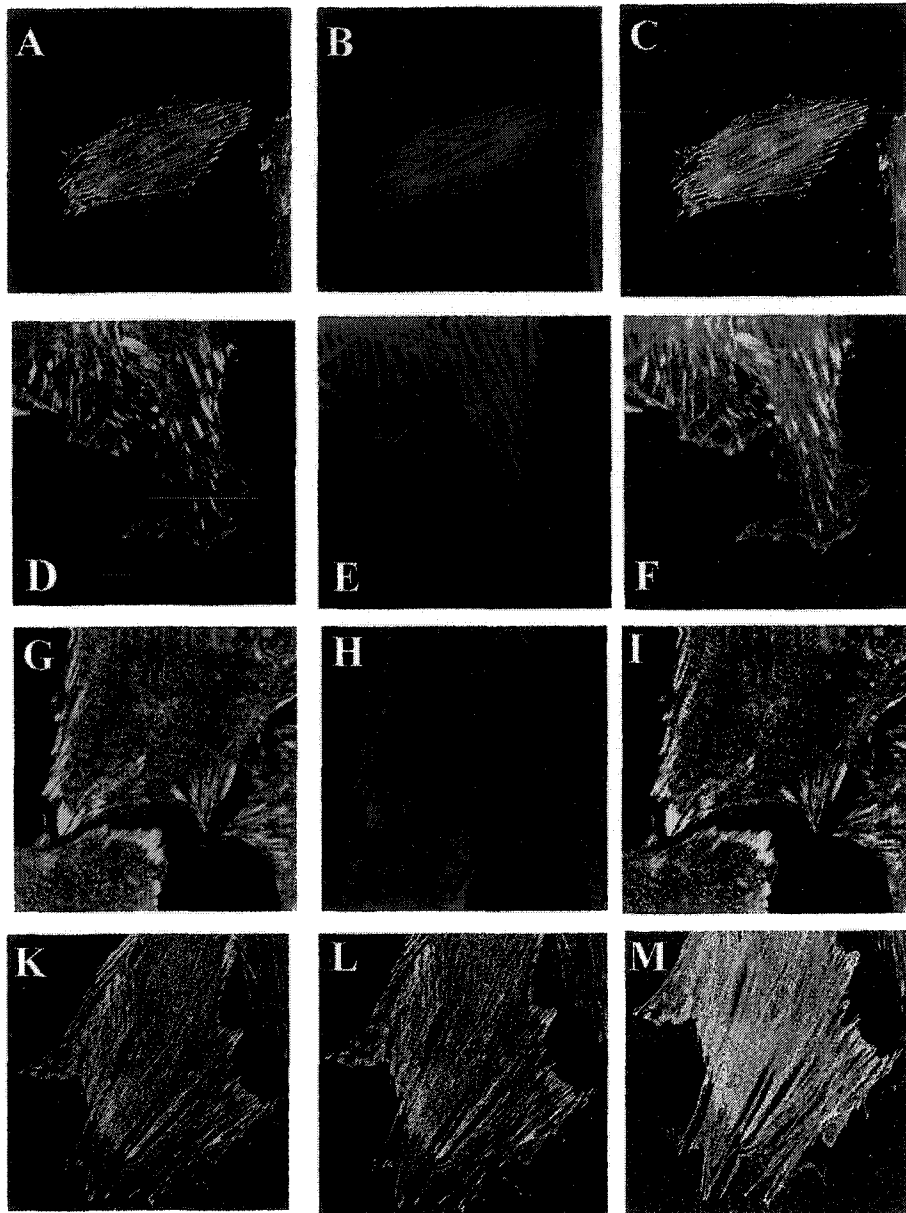
Figure 2.8

Determination of Endogenous Localization of WDR1 within REF 52 Cells:

To detect the presence and localization of endogenous WDR1, the WDR1 antibody was utilized in ICC confocal analysis of REF 52 cells. Interestingly, it was observed that WDR1 proteins localized to the end of actin filaments in a pattern similar to the FA protein vinculin (Figure 2.8, A-C, D-F). The localization of vinculin to the FA with actin was first established (Figure 2.8, D-F) and was contrasted to the endogenous expression pattern of WDR1 (Figure 2.8., A-C). The results demonstrate a similar pattern of localization for both WDR1 and vinculin, as WDR1 appeared to co-localize with vinculin at the barbed ends of actin filaments (Figure 2.8, G-I, K-M). The localization pattern of cofilin was also compared to vinculin (as cofilin and WDR1 cannot be simultaneously detected since both are rabbit antibodies). It was observed that the pattern of cofilin localization was quite distinct from that of WDR1 and vinculin, and was general and diffuse however higher amounts of cofilin were co-localized to both filament termini and lamellipodia with vinculin (Figure 2.9, A-C). A similar pattern of general diffuse staining was observed for CAP1 with increased intensity within cortical actin regions (Figure 2.9, D-F).

The localization of WDR1 with β-tubulin was also investigated with confocal analysis as tubulin is an element of the FA complex; however no evidence to support an interaction was collected as the two proteins do not appear to localize together (Figure 2.9, G-I).

Figure 2.9 *In vivo* localization of additional actin interacting proteins.

The endogenous expression patterns of cofilin, CAP1, and β-tubulin proteins were examined in REF 52 cells with confocal analysis. A (1200X) displays the staining pattern of cofilin. D (1200X) shows endogenous CAP1 expression. B (1200X) & E (1200X) detail the pattern of vinculin localization. G (400X) demonstrates WDR1 staining. H (400X) indicates β-tubulin localization. C (1200X), F (1200X), I (400X) are the merged images.

84
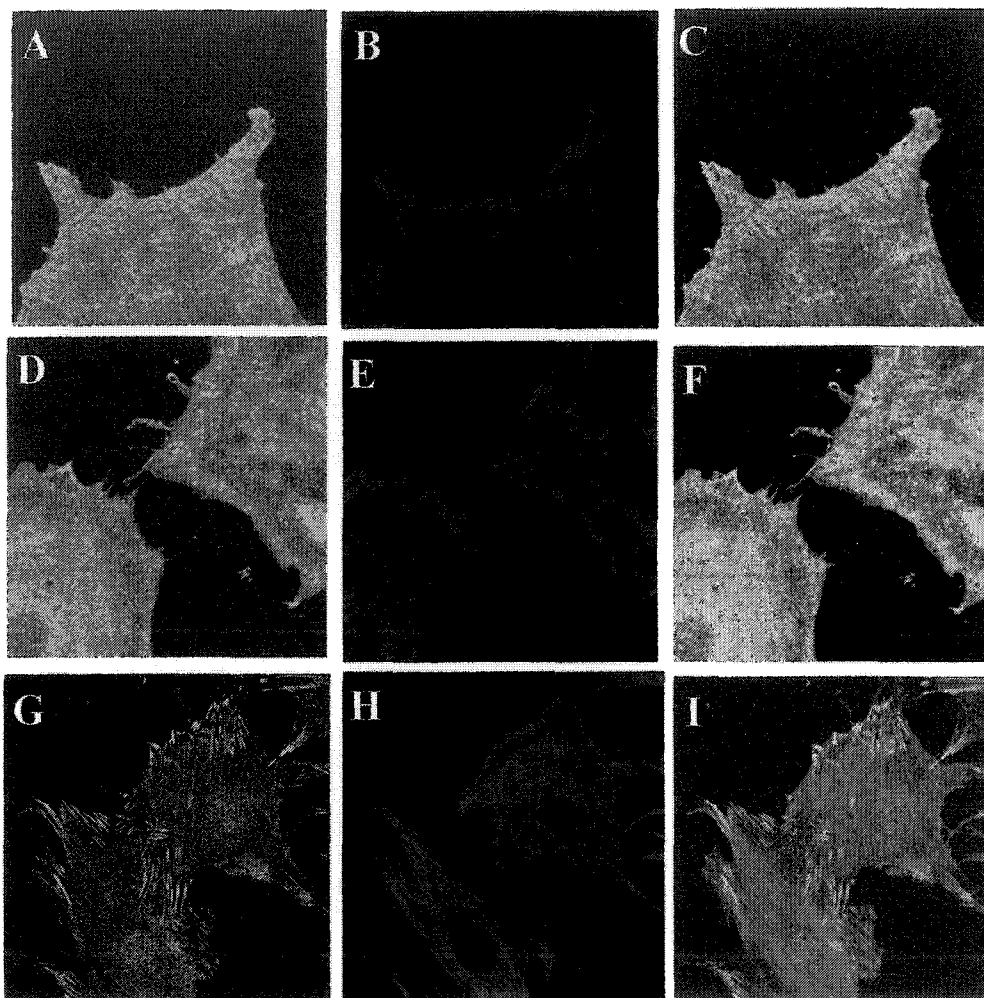
Figure 2.9

Figure 2.10 Interactions of WDR1 with actin.

The interactions of WDR1 with actin were investigated using immunoprecipitation analysis of transfected HEK 293 cells. A, the expression of HA-tagged WDR1 (lane one), WDN534 (lane two), cofilin (lane three), and CAP1 (lane four) was confirmed as shown. B, the blot was then striped and reprobed for actin. The presence of actin was observed within the immunoprecipitated extracts of HA-WDR1 (lane one), HA-WDN534 (lane two), and the two positive controls HA-cofilin (lane three), and HA-CAP1 (lane four).

86
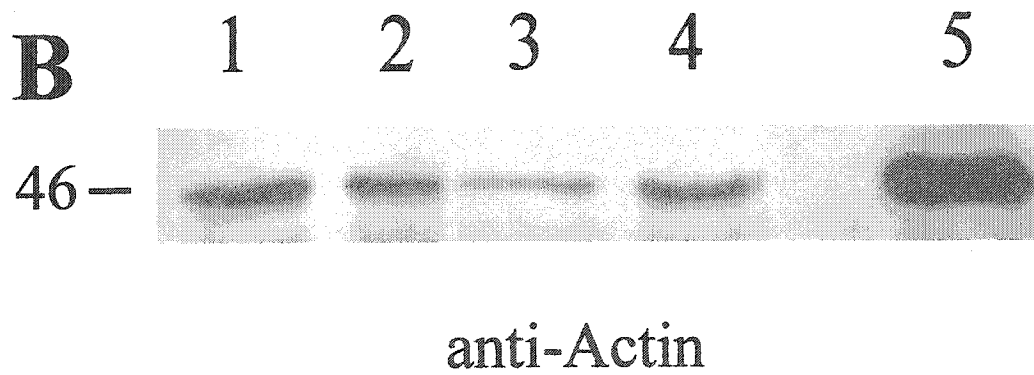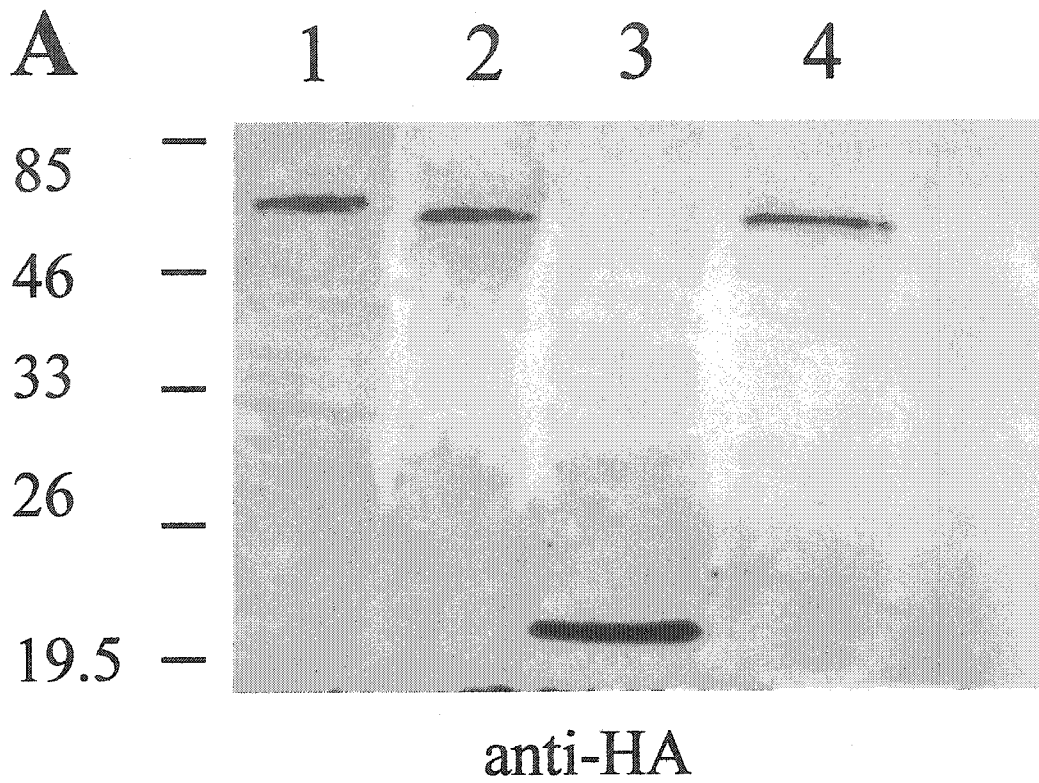
Figure 2.10

Determination of WDR1 Protein Interactions:

Previous studies have suggested that WDR1/ Aip1 proteins interact with elements of the actin cytoskeleton (Amberg et al., 1995; Konzok et al., 1999; Okada et al., 2002; Ono, 2001). Therefore the ability of WDR1 to interact with actin was tested using co-precipitation experiments. The presence of actin in the immunoprecipitated protein extracts of exogenously expressed HA-tagged WDR1 and WDN534 from REF 52 cells demonstrated that both WDR1 proteins were able to interact with actin (Figures 2.10A & 2.10B, lanes 1 & 2). The actin binding abilities of two established actin interacting proteins, cofilin and CAP1 were assayed as positive controls and were confirmed to interact with actin (Figure 2.10B, lanes 3 & 4). Total cellular actin was used in lane 5 as a positive marker (Figure 2.10B). Therefore, this confirms that both human isoforms of WDR1 can interact with actin.

The ability of HA-tagged WDR1 to bind other actin binding proteins was tested using co-expressed MYC-epitope proteins and immunoprecipitation experiments. Therefore, the ability of HA-WDR1 to bind MYC-cofilin, MYC-CAP1, MYC-WDN534, or other MYC-WDR1 proteins was tested in HEK 293 cells using anti-HA IP reactions and analyzed using anti- HA and anti-MYC western blots. Interestingly the WDR1 proteins were found to bind both themselves and each other (Figure 2.11A & 2.11B, lanes 1 & 3) and a combination of the two (Figure 2.11A & 2.11B, lane 2). However, using the previous IP conditions no interaction with cofilin was detected (Figure 2.11B & 2.11C, lane 4) or with CAP1 (data not shown).

The apparent similar localization of endogenous WDR1 and vinculin within cells led to an investigation of whether WDR1 could physically interact with vinculin.

Figure 2.11 Interactions of WDR1 with additional actin interacting proteins.

The interactions of WDR1 with selected actin proteins were examined in HEK 293 cells using double IP experimental technique. A, the verification of immunoprecipitated HA-constructs of WDR1 (lanes one, two and four), WDN534 (lane three), CAP1 (lane five). B, the identification of MYC-tagged protein presence within the IP extracts of WDR1 (lane one), WDN534 (lanes two and three), and CAP1 (lane four). C, the conformation of the expression of MYC-tagged constructs of WDR1 (lane one), WDN534 (lane two and three), cofilin (lane four), and CAP1 (lane five) within the total extracts.

89
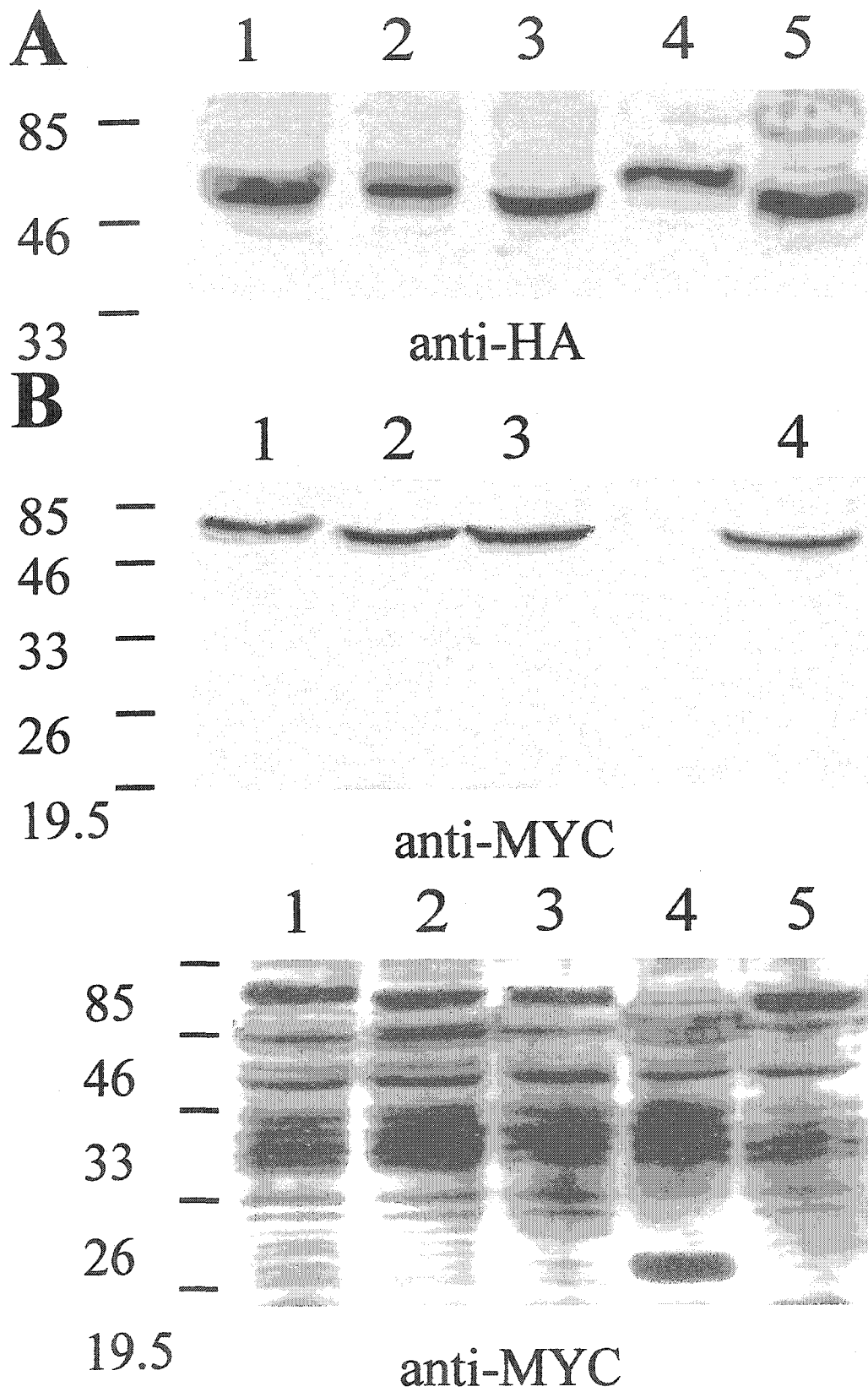
Figure 2.11

Figure 2.12 Interactions of WDR1 with vinculin.

The interaction of WDR1 with the FA protein vinculin was examined in REF 52 cells using IP experiments and western blotting analysis. A, the presence of vinculin was indicated within positive vinculin control (lane five), however not in lanes one-three. B, the identification of HA-WDR1 (lanes one, two and three) and HA-WDN534 proteins within REF 52 total cell extract was verified.

91

A

1　　2　　3　　4　　5

118 —

85 —

anti-Vinculin

B

1　　2　　3　　4

85 —

46 —

anti-HA
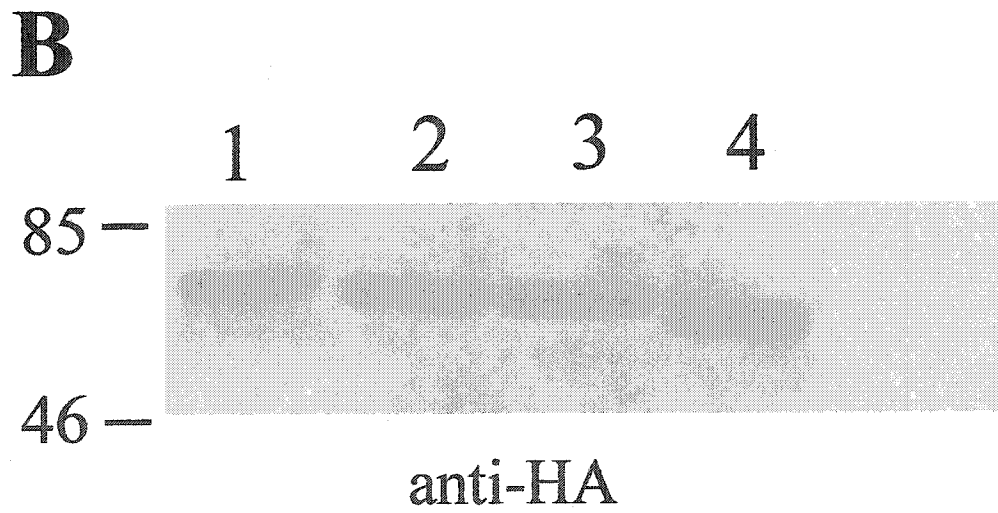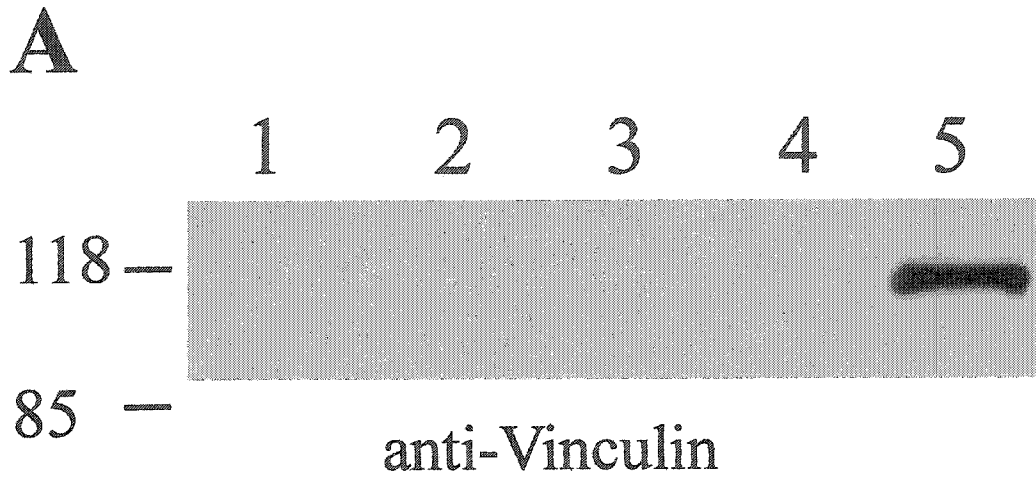
Figure 2.12

Therefore, the potential interaction between vinculin and each of the exogenously expressed HA-WDR1 and HA-WDN534 proteins was assayed using IP and western blot analysis. Under the experimental conditions used no apparent interaction was observed between either WDR1 (Figure 2.12A & 2.12B, lanes 1-3) or WDN534 (Figure 2.12A & 2.12B, lane 4). A sample of REF 52 cell extract was used as a positive vinculin control (Figure 2.12A, lane 5).

WDR1 Protein Expression within Human and Rat Cell Lines:

The conserved evolution of WDR1 orthologs suggests an essential and conserved cellular function of WDR1 proteins. To determine the conserved nature of hWDR1 proteins the endogenous patterns of WDR1 expression in several different human cell lines and a rat cell line were compared. The patterns of endogenous WDR1 expression within a variety of transfected and non-transfected cells were examined. Western blot analysis was performed on the total protein extracts of MCF7, DU145, REF, Calu, U87, and HEK 293 cells (Figure 2.13, lanes 1-6) cells in addition to HEK 293 cells expressing exogenous HA-WDR1 and WDN534 proteins (as positive controls) (Figure 2.13A-B, lanes 7& 8, 2.13C, lanes 1 & 2). The anti-HA WDR1 control extracts were used to determine relative WDR1 protein size (Figure 2.13C, lanes 1 & 2). The anti-WDR1 staining revealed the presence of bands ranging from 46-70 kDa, however it was observed the DU145, Calu, and U87 cells lines (Figure 2.13A, lanes 2, 4, 5) all expressed both the full length 60 kDa WDR1 and a typically amount of the truncated 50 kDa proteins. The U87 cell line was also observed to express a 65 kDa band (Figure 2.13A, lane 5). Interestingly, the MCF7 and HEK 293 cells expressed only the truncated isoform in significant quantity (Figure 2.13A, lanes 1 & 6). Additionally, the MCF7 cells were shown

93

Figure 2.13 Expression of WDR1 within human and rat cell lines.

The expression pattern of WDR1 within several human and rat cell lines was examined using anti-WDR1 SDS-PAGE analysis of total cell protein extracts. A, the expression of WDR1 proteins was examined within MCF7 (lane one), DU145 (lane two), REF 52 (lane three), Calu (lane four), U87 (lane five), HEK 293 (lane six) using a positive controls of both WDR1 and WDN534 (lane7), and a WDN534 (lane 8). B, expression analysis of vinculin (lanes one to eight) on the same blot containing the same cell lines described above. C, Verification of WDR1 size determinations using HA-WDR1 and HA-WDN534 (lane one), and HA-WDN534 (lane 2).

94

anti-WDR1

anti- Vinculin

Anti-HA
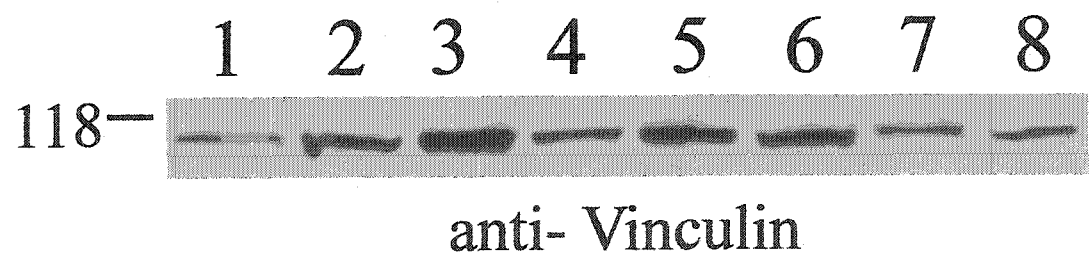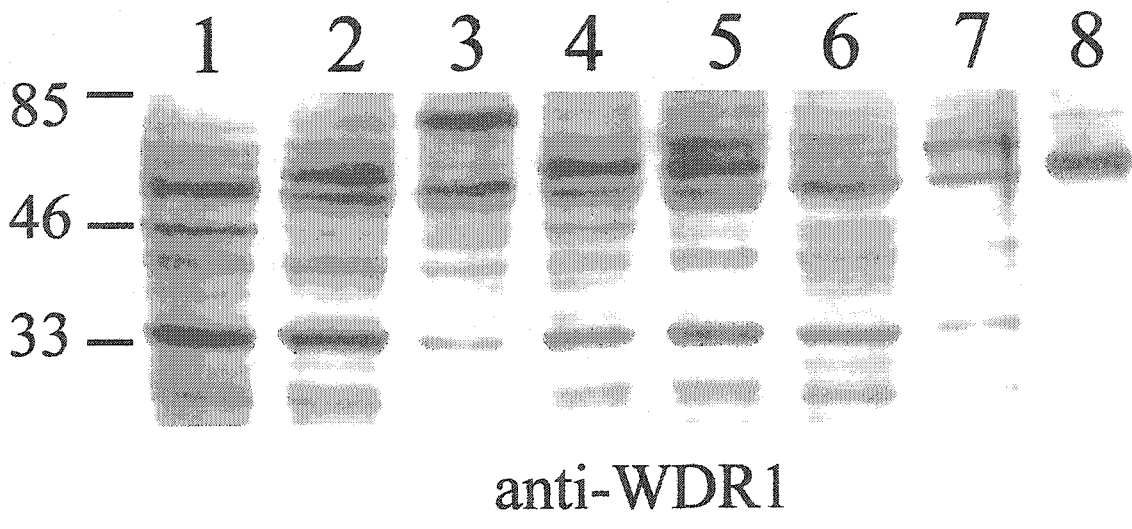
to express a 46 kDa band (Figure 2.13A, lane 1). The REF 52 cell line also demonstrated expression of the truncated isoform; however this cell line also significantly expressed a larger ~70 kDa protein (Figure 2.13A, lane 3). The identity of the 46, 65 and the 70 kDa proteins are still unknown. The apparent display of differential protein expression between the non-transformed and carcinoma cell lines may be an indication of an apparent difference in the cellular functions of WDR1 and WDN534 during cell growth, division and attachment. Additionally, the ICC data demonstrating the co-localization of WDR1 and vinculin proteins may suggest a role for WDR1 within the FA complex, so vinculin expression was also assayed as a marker of FA activity. The protein extracts found to express a relatively consistent amount of vinculin protein as only a slight difference of amounts could be observed between cell lines (Figure 2.13B, lanes 1-8).

Together these results indicate that hWDR1 is expressed in a variety of human tissues and can associate with the actin cytoskeleton. The results also suggest WDR1 may form oligomeric complexes with itself which may influence its function and potential binding partners in both transformed and non-transformed cells.

Discussion:

The mammalian actin cytoskeleton directs numerous vital cellular processes, and yet complete characterizations of the many proteins effecting actin remodeling remain unknown. WD proteins have been reported to interact with both cofilin and actin to enhance filament depolymerization in several organisms (Konzok et al., 1999; Okada et al., 2002; Okada et al., 1999; Rodal et al., 1999). To identify and describe mammalian WDR1 both the full length 1821 bp cDNA gene and a 1534 bp C-terminal truncated

96

isoform (WDN534) was amplified using primers designed against compiled cDNA fragments. The 1821 bp WDR1 cDNA showed 22% and 95% sequence homology to the reported WDR1 yeast and rat sequences. The identification of the truncated isoform WDR1 appears unique amongst other WDR1 transcripts confirmed within other species. The complex genome of *Xenopus* has been observed to express a possible isoform transcript lacking a portion of the N-terminus WT sequence, although it was reportedly a product of genome tetraploidy and was not considered to be of genuine expression (Okada et al., 2002; Okada et al., 1999). Organisms such as *C. elegans* have been reported to contain two WDR1 genes both expressed in a tissue specific manner; however this pattern is currently unique to this species (Mohri and Ono, 2003; Ono, 2001).

Sequence analysis of WDR1 and truncated WDN534 fragments described the presence of nine and seven repeated WD motifs respectively. These motifs are known to encode four anti-parallel beta-sheets able to interact and produce a beta-propeller blade tertiary structure ((Adams et al., 2000; Gettemans et al., 2003)). Typically WDR1 orthologues have been reported to contain between eight and fourteen WD motifs, however structure analysis of both yeast and *C. elegans* WDR1 described fourteen WD motifs producing two-seven blade domains (Ono, 2003; Voegtli et al., 2003). Structural identification of hWDR1 will be intriguing due to the odd number of WD motifs. Further analysis of WD motif sequences of hWDR1, *S. cerevisiae* and *S. pombe* identified three WD motif domains exhibiting 82.5%, 91.2%, and 84.5% amino acid homology to the *Drosophila* kelch protein motif (Figure 2.2). Interestingly, of the three WD motifs of hWDR1 displayed the most homology to Kelch motifs are primarily characterized by the presence of conserved C-terminal WD and N-terminal GH repeats bracketing a 44-56

97

conserved amino-acid known to encode a beta-propeller consisting of four anti-parallel beta-sheets. Although the position and number of kelch motifs is variable within kelch proteins, they are typically known to mediate protein interactions and several have been shown to interact with actin (Adams et al., 2000; Gettemans et al., 2003; Kim et al., 1999). The two *Drosophila* kelch proteins kelch and actinfilin each contain 6 C-terminal kelch motifs through which they bind and regulate the actin cytoskeleton during cytoplasmic nutrient transfer between nurse cell and oocytes and facilitate long-term memory storage (Adams et al., 2000; Chen et al., 2002). Another kelch protein, α-Scruin has twelve WD motifs which bind actin and regulate the bundling of F-actin during the acrosomal reactions in sperm cells (Adams et al., 2000; Way et al., 1995). Therefore, the presence of kelch-like motifs within WDR1 together with the observations that WDR1 interacts with both itself and actin implies a role of WDR1 for actin turnover in human cells.

Protein expression analysis revealed the presence of two isoforms exhibiting approximately 10 kDa difference in size. The size of full length hWDR1 is currently consistent with the average size of known WDR1 proteins which range from 60-70 kDa; however no previous WDR1 studies have demonstrated the expression of a truncated isoform. Interestingly, Okada et al., (1999) identified several polypeptides in the cofilin-affinity column used to isolate the 65 kDa full length xAip1 including a 55 kDa peptide which could have represented the expression of the identified N-terminal truncated transcript, however further study is needed to confirm the identity of this protein (Okada, et al., 1999).

WDR1 expression studies with both chick and *Xenopus* showed WDR1 was expressed within embryos non-specifically, and adult chick tissue analysis confirmed the

98

conserved expression pattern within multiple tissue types including muscle, heart, liver, kidney, and brain (Konzok et al., 1999; Oh et al., 2002; Okada et al., 2002; Okada et al., 1999). However several reports also demonstrated tissue-specific functions of WDR1 which correlated to the location of cells containing high amounts of F-actin (Adler et al., 1999; Mohri and Ono, 2003). Chick WDR1 was identified as one of three genes up-regulated during tectorial membrane and hair cell regeneration within the auditory epithelium of acoustically damaged cochlea, and the WDR1 *C. elegans* ortholog localizes exclusively within body wall muscle, pharynx, and the spermatheca (Adler et al., 1999; Mohri and Ono, 2003).

Our investigation of hWDR1 tissue expression revealed both hWDR1 and hWDN534 are expressed in a conserved pattern since WDR1 cDNA for both isoforms were isolated from human lung, kidney, liver, heart, brain, and trachea total RNA. Further examination of WDR1 expression in rat brain supported the conserved pattern of expression as WDR1 was detected within the cerebellum, frontal cortex, post cortex, pons, spinal cord, medulla and hippocampus samples. These tissues represented a relatively limited collection of cell types. Therefore to determine the cellular expression of WDR1, rat pheochromocytoma, rat embryonic fibroblast, human embryonic kidney, breast adenocarcinoma, brain astrocytoma, and lung and prostate cancer cell lines RNA extracts were used to reveal the presence of a 3.0 kb WDR1 transcript in all cells. The analysis also revealed the presence of a smaller 2.2 kb transcript which is thought to encode truncated WDN534. Interestingly, Ichii et al., (2001) previously suggested hWDR1 was ~3.0 kb however cDNA analysis and northern blot analysis in *Xenopus* and chick (respectively)

99

have suggested the existence of two WDR1 transcripts ~3.0 kb and ~2.0 kb, therefore these results strongly suggest the existence of two WDR1 transcripts.

Further characterization of cellular WDR1 expression was performed using purified antibodies directed against a synthetically derived 17 amino-acid peptide as the attempted production of four recombinant GST-WDR1 proteins in *E. coli* yielded unstable protein fragments. Interestingly, both recombinant chick and *C. elegans* WDR1 fusion proteins were unstable and subsequently their characterization required the production of antibodies targeted against a synthetically-derived WDR1 epitope (Mohri and Ono, 2003; Oh et al., 2002; Ono, 2003). The successful production of bacterially generated stable recombinant *Xenopus* and yeast WDR1 suggested that some WDR1 fusion proteins are stable and can be produced with enough yield to be utilized for antibody production (Okada et al., 1999).

In vivo WDR1 was shown to localize to the barbed-ends of actin filaments both within areas undergoing active actin dynamics and within stable actin structures. The localization of WDR1 to the barbed-end of filaments appeared similar to vinculin FA expression. Additional investigation of the relative localization of two actin interacting proteins, cofilin and CAP1 demonstrated both co-localize with WDR1 to areas of dynamic actin remodeling, however both cofilin and CAP1 demonstrated a diffuse expression pattern and lack the distinct pattern of filament association displayed by WDR1. The difference in localization expression of the three proteins may indicate that any interaction between these proteins may be indirect or transient.

The ICC co-localization indicated that WDR1 and vinculin may be present within the FA complex; however a direct HA-WDR1-vinculin interaction was not detected using

IP analysis. A direct interaction between WDR1 and the two actin-interacting proteins cofilin and CAP1 was also not observed. Recently these proteins had been shown to interact with complexes isolated from *S. cerevisiae*, additionally all WDR1 currently characterized have been shown to interact with cofilin and actin (Balcer et al., 2003; Ono, 2003; Rodal et al., 1999). We were able to determine mammalian WDR1 was able to interact with actin which is a defining feature of all WDR1 proteins and additionally we identified novel oligomeric complex interactions between each of the two WDR1 isoforms as well as with WDR1 and WDN534. WDR1 homo and/or hetero oligomeric interactions have not been previously reported, and their formation may influence WDR1 function or potential binding partner interaction. These oligomeric interactions have been well established *in vivo* for several kelch proteins that are only able to interact with actin after dimerization, which may provide future insight into the functional purpose of the interaction (Adams et al., 2000; Gettemans et al., 2003; Robinson and Cooley, 1997). The kelch protein α-scruin has been established to form homodimers and enhance the structural stability of actin filaments bundled by the protein (Adams et al., 2000; Way et al., 1995).

To further characterize the function of WDR1 the *in vivo* endogenous expression patterns of WDR1 within rat embryonic fibroblast, human embryonic kidney, breast adenocarcinoma, brain astrocytoma, and lung and prostate cancer cell lines demonstrated dramatically different WDR1 and WDN534 expression patterns. Comparisons of the expression profiles of cofilin, CAP1, vinculin and actin revealed WDR1 was the only differentially expressed protein within each cell line, which could suggest a regulatory function of the oligomeric WDR1 protein complex as these cell lines display dramatically

different actin cytoskeletal properties. Further characterization of the interactions of WDR1 with both itself and other proteins within additional species is required. However, this data implicates a potential regulatory function of mammalian WDR1 proteins within essential and conserved actin-based cellular processes.

102

Chapter Three

Determination of WDR1 Proteins Functions during Cell Migration, Attachment, & Neurogenesis

Introduction:

Elucidating the complex cytoskeletal signal transduction pathways of cell attachment, adhesion and neurogenesis is important for understanding the basic mechanisms of cell behaviour and the numerous diseases that result from perturbations in these processes. Actin has been established to be a dominant cytoskeletal element essential for effecting a wide range of morphological changes such as endocytosis, exocytosis, cell cycle, neural extension and cell movement. Actin remodeling occurs through the activation of filament capping proteins, bundling proteins, severing proteins and monomer sequestering proteins in response to extra-cellular (EC) signals (Adjei, 2001; Kroeze et al., 2003). The recent focus of actin signaling has concentrated on the three main G-protein families of the Rho superfamily; the Rho, Rac and Cdc42 families which have all been shown to regulate actin rearrangement, neurogenesis, cell cycle progression and have all been implicated in cell transformation (Hall, 1998b; Nobes and Hall, 1999; Olivo et al., 2000). The Rho signaling proteins have additionally been classified as regulators of actin stress fiber formation and of focal adhesion formation and maintenance (Bishop and Hall, 2000). Rho is activated by adhesion of integrin receptors

103

and initiates FA formation through the activation and recruitment of essential linking proteins such as talin, vinculin, α-actinin and filamin (Bailly et al., 2003; Bass et al., 2002; Nobes and Hall, 1995). The FA linking proteins associate with Rho-recruited stress fibers and microtubules to localize the filaments to the FA protein complexes (Critchley, 2000; Critchley et al., 1999). The Rac and Cdc42 G-proteins have shown to cooperate within the leading edge of migrating cells interact to generate motility (Hall, 1998a; Nobes and Hall, 1999; Xu et al., 2003). Rac has been established to induce the formation of lamellipodia in migrating cells and recruit Cdc42 which has been proven to generate the filopodia and microvilli extensions required for motility (Bishop and Hall, 2000; Hall and Nobes, 2000; Machesky and Hall, 1997). Rac and Cdc42 proteins are also localized to the tips of neurites during neurogenesis and regulate the actin dynamics within the growth cone (P & T domains) (Gungabissoon and Bamburg, 2003; Sarmiere and Bamburg, 2004). Rho functions to bundle actin filaments to provide strength and extension force during neurogenesis at the base and shaft of the neurite (C domain) (Bishop and Hall, 2000; Sarmiere and Bamburg, 2004).

The function of actin interacting proteins can be elucidated by the cellular localization exhibited during these dynamic actin processes. We have shown WDR1 localizes to the leading edge of migrating cells and to the tips of neurites during neurogenesis. Additionally we have observed a novel role for WDR1 proteins functioning in cell adhesion at FA complexes.

104

Material & Methods:

WDR1 Protein Expression within Human and Rat Cell Lines:

The WDR1 protein expression patterns of MCF7, DU145, REF, Calu, U87, and HEK 293 human and rat cell lines were assayed using western blot analysis of total protein extracts. The cells were grown to ~80% confluency on 60 mm dishes and scraped off the plate in 0.5 ml of RIPA buffer (defined previously in chapter 2). The protein extracts were obtained by sonicating the cells in RIPA buffer and centrifugation and examined using an anti-WDR1 antibody (1:2000) for detection on a 10% PAGE followed by western blotting (as detailed in chapter 2). The blot was then striped for 1 hour at 37 ℃ with Restore Western Blot stripping buffer (Pierce), washed three times with 1X PBS and reprobed with the 12CA5 anti-HA antibody (1:5000) to target the HA-WDR1 protein controls (as described in chapter 2). The blot was stripped as described above and the pattern of vinculin expression was investigated using an anti-vinculin monoclonal antibody (1:500) (Cytoskeleton, Inc.).

Immunocytochemical Analysis:

The relative localization of WDR1 with actin and the other actin interacting proteins vinculin, cofilin, CAP1, and β-tubulin in REF 52 fibroblasts was investigated using ICC analysis performed as described in chapter 2 in the following assays.

Migration Analysis:

Fibroblast migration was stimulated through the removal of one half of ~95% confluent REF 52 cells from the CS using a cell scraper (Sarstedt). This stimulated the remaining cells to migrate into the vacant area of the CS. ICC confocal analysis was performed 12 hours after wounding.

105

Attachment Analysis:

Analysis of cell attachment was performed using ICC confocal analysis as detailed in chapter 2 with the exception that the REF 52 cells (~85%-90% confluent) were re-plated (1:5) on CS and fixed in 3.7% formaldehyde in 1X PBS at 6, 12, and 24 hour time points after splitting. ICC confocal detection of WDR1, vinculin, cofilin, CAP1, F- actin and β-tubulin proteins was performed as outlined in chapter 2.

The role of WDR1 protein during cell adhesion was investigated using the partial enzymatic removal of fibroblast cells with trypsin and subsequent ICC analysis of protein localization. REF 52 cells were grown on CS until cells were ~85%-90% confluent, then the CS were immersed in 37° C 1X Trypsin/EDTA (Sigma) for 3-5 minutes or for specific time points of 3, 4, 6 or 10 minutes. Immediately following the trypsin treatments the CS were fixed in 3.7% formaldehyde 1X PBS for ICC detection of WDR1, vinculin, cofilin, CAP1, F- actin and β-tubulin protein localizations.

Actin Disruption Analysis:

The influence of actin dynamics on the stability of the WDR1 barbed-end protein caps was examined using two G-actin sequestering agents known to inhibit *in vivo* actin polymerization and disrupt focal adhesion formation, latrunculin A (lat A, Sigma) and cytochalasin D (CD, Sigma) (Geiger et al., 2000; van Kooyk et al., 1999). The lat A treatments were performed on REF 52 cells (~65%-75% confluent) maintained in DMEM media (10% FBS + 1% P/S, Sigma) and supplemented with 2 nmol/ ml of lat A for 5, 10 or 20 minutes at 37 C before immediate 3.7% formaldehyde 1X PBS fixation. The localization of WDR1, vinculin, cofilin, CAP1, F- actin and β-tubulin proteins was then determined using ICC confocal microscopy. The CD assays were done in the same

106

manner using REF 52 cells maintained in DMEM media (10% FBS + 1% P/S, Sigma) and subjected to 8, 12, and 20 minute treatments of 5 μg /ml of CD (Sigma) at 37 °C before ICC fixation and staining as performed for the lat A treatments.

Neurogenesis:

The endogenous localization of WDR1, cofilin, CAP1, CAP2, tubulin and F-actin proteins during neurogenesis was investigated using the rat PC12 neural model of differentiation (described above). The cells were grown on acid washed CS (as described in chapter 2) which had been etched for approximately 2-3 minutes with sterile metal needle-tipped tweezers and washed briefly in 95% ethanol. The cells were maintained as described above and washed with Dulbeco's low serum media before the addition of Dulbeco's low serum media supplemented with NGF (as described). The cells were differentiated for 1, 3, 5 and 10 days before fixation in 3.7% formaldehyde 1X PBS for ICC analysis. The localization patterns of WDR1, cofilin, CAP1, CAP2, tubulin and F-actin were then examined using ICC confocal analysis with the previously described antibody concentrations (chapter 2).

Neural Differentiation and RT-PCR Analysis:

To examine the regulation of WDR1 during the actin driven process of neurogenesis, reverse transcriptase polymerase chain reaction experiments were performed on the RNA of rat pheochromocytoma (PC12) cells during neural growth factor (NGF) induced differentiation. The PC12 cells were maintained DMEM supplemented with 10% FBS, 5% horse serum and 100 units/ ml of penicillin/ streptomycin (P/S) and differentiated in Dulbeco's low serum media [1% FBS, 0.5% HS, and 1% P/S] supplemented with 100 ng/ml of murine submaxillary gland NGF. The cells

107

were differentiated on two sets of 10 cm plates for 0.5, 1, 2, 3, 4 and 5 day periods after which total RNA was isolated using a mammalian RNA isolation kit (Sigma) as per kit instructions with the exception that the RNA was concentrated in 30 µl during elution. The two control plates were prepared in Dulbeco's low serum media (above) without NGF for 5 days and the total RNA was collected as described above.

To examine any differential expression of WDR1 and WDN534 during neurogenesis the two primer sets detailed in chapter 2 were used to target the commonly shared 400 bp N-terminal sequence (#133F & #155R) and the unique 600 bp sequence of the WDR1 C-terminus (#156F & #139R) (appendix A). To quantify the expression of both of the WDR1 targets, the two amplicons were amplified in a triplex PCR with GAPDH, which functioned as an internal control. The PCR was performed using either a Robo Cycler PCR machine (Stratagene). The PCR was completed by initially using a 5 minute 95° C heating to disrupt any internal secondary or tertiary interactions of the template or primer nucleotides and a repetition of cycles consisting of a melting temperature of 94° C for 45 seconds, an annealing temperature of 50° C for 1.5 minutes, and an extension temperature of 70° C for 2 minutes each cycle. Prior to the final cycle the reactions were heated for an additional 10 minutes at 70° C then immediately cooled to 4° C before ethidium bromide agarose gel analysis. Saturation experiments were then performed to determine the number of cycles required to maximize the amplification of the most prevalent amplicon and saturate the pixel detection of the visualization system used. The maximum amount of cycles was determined to be 35 cycles and so each quantification PCR experiment was limited to 25 cycles and was repeated 14 times. The quantification of the three amplicons was performed using 7-10 µl of each reaction

108

separated on a 1.2% agarose gel and stained with ethidium bromide for 30 minutes followed by a 30-45 minute wash in ddH$_2$O to remove excess ethidium bromide. Using an Alpha Innotec gel imaging system, the WDR1 amplicon intensities of each sample were compared to the internal GAPDH control intensity.

Results:

WDR1 Localizes Along the Leading Edge during Cellular Migration:

The process of cellular motility requires the entire remodeling of the cytoskeleton which is accomplished through regulated actin filament rearrangement, including synthesis and depolymerization. Identifying the location of a protein relative to characterized proteins within a motile cell can allow for reasonable extrapolation of potential function. Therefore, to investigate the function of WDR1 within motile cells the localization of WDR1 and cofilin were examined using ICC confocal microscopy. Both proteins were observed to localize to the leading edge of migrating REF 52 fibroblast cells (Figure 3.1). WDR1 localized to the leading edge as thick filamentous structures associated the barbed-end of actin filaments (Figure 3.1, A-C). The localization pattern of cofilin was similar to WDR1 in that cofilin localized to areas of actin dynamics however cofilin exhibited diffuse distribution across the entire lamellae and did not appear restricted to filament ends as was observed for WDR1 (Figure 3.1, D-F). The localization of cofilin along the cortical leading edge actin pool corresponded with WDR1 expression during cell migration and may suggest an actin-based interaction between the two proteins (Figure 3.1, A & D). The localization of vinculin was not assayed in these experiments however it is known FA establishment (requiring vinculin localization)

109

Figure 3.1 Localization of WDR1 within migrating fibroblast cells.

The endogenous expression pattern of WDR1 during cell migration was examined in REF 52 cells using ICC confocal analysis. A, the localization of WDR1 (400X) is shown. B, details F-actin (400X). D, demonstrates the localization of cofilin (600X). E, shows the F-actin (600X). C (400X) & F (600X) detail the merged images.

110
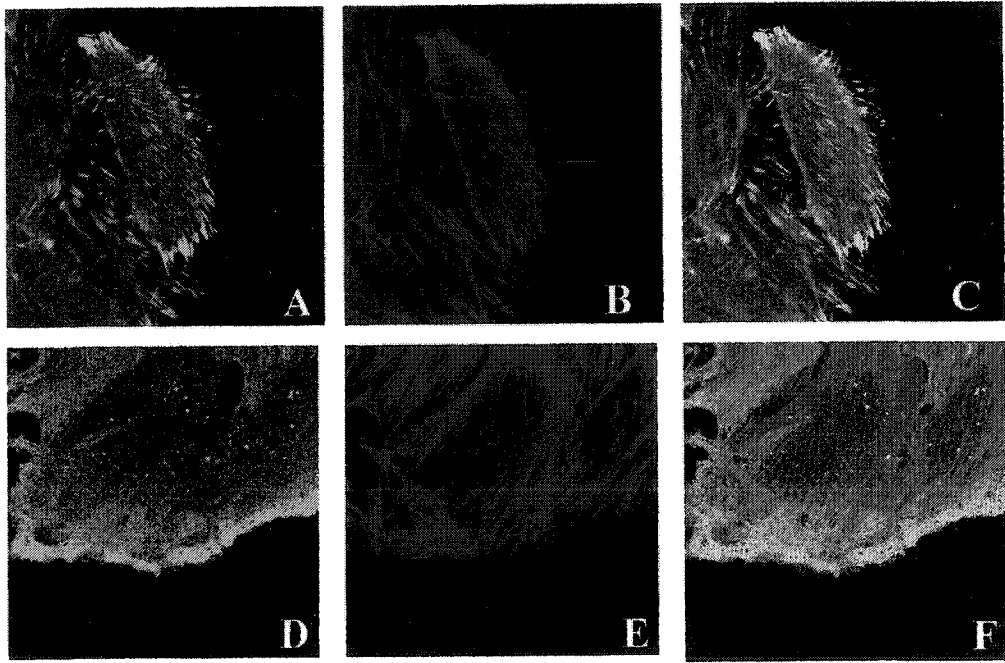
Figure 3.1

occurs at the leading edge of migrating cells (Bass et al., 2002; Critchley, 2000; Kaverina et al., 2002b; Pollard and Borisy, 2003; Rogers et al., 2003; Small et al., 2002).

Identification of a Novel Function of WDR1 during Cell Adhesion:

The process of cellular adhesion requires both the formation of stable actin structures for cell attachment and rapid remodeling and dissociation of those structures for cell migration and division and therefore requires the interaction of an abundance of actin interacting proteins. The *in vivo* localization pattern of WDR1 demonstrated the co-localization of WDR1 with the barbed-ends of actin filaments. Interestingly, the co-localization of WDR1 with vinculin suggested WDR1 may also interact at FA complexes to maintain cell adhesion. To determine whether WDR1 functions in cell attachment REF 52 cells were trypsinized for 3-4 minutes and fixed for ICC confocal analysis. The endogenous WDR1 pattern of localization with F-actin was confirmed (Figure 3.2, A, C, E) as it was observed WDR1 localized to the barbed ends of actin filaments as well as the peripheries of the filaments as described in chapter 2. The analysis of WDR1 location during attachment was determined from the ICC staining of trypsin treated fibroblasts. In detaching cells, WDR1 localized to the immediate cell periphery and demonstrated actin filament barbed-end binding. Interestingly, it was observed that WDR1 staining remained in specific areas on the CS after cell detachment (Figure 3.2, A, C, E). This was a repeatable observation and suggests the WDR1 protein provided an attachment function to the cell prior to trypsinization. This WDR1 staining pattern left on the CS will be referred to in this chapter as the WDR1 aggregate complexes (WACs). This pattern was compared to that displayed by actin which was shown to reveal two actin filament pools (Figure 3.2, B, D, F); the dynamic cortical leading edge of condensed filaments

112

Figure 3.2 Investigation of WDR1 using trypsin-treatment assays.

The localization of WDR1 during cell adhesion was explored using ICC confocal examination of detaching REF 52 cells. A (400X), C (600X), E (600X) detail the endogenous pattern of WDR1 localization. B (400X), D (1200X), F (2400X) show the *in vivo* F-actin pools.

113
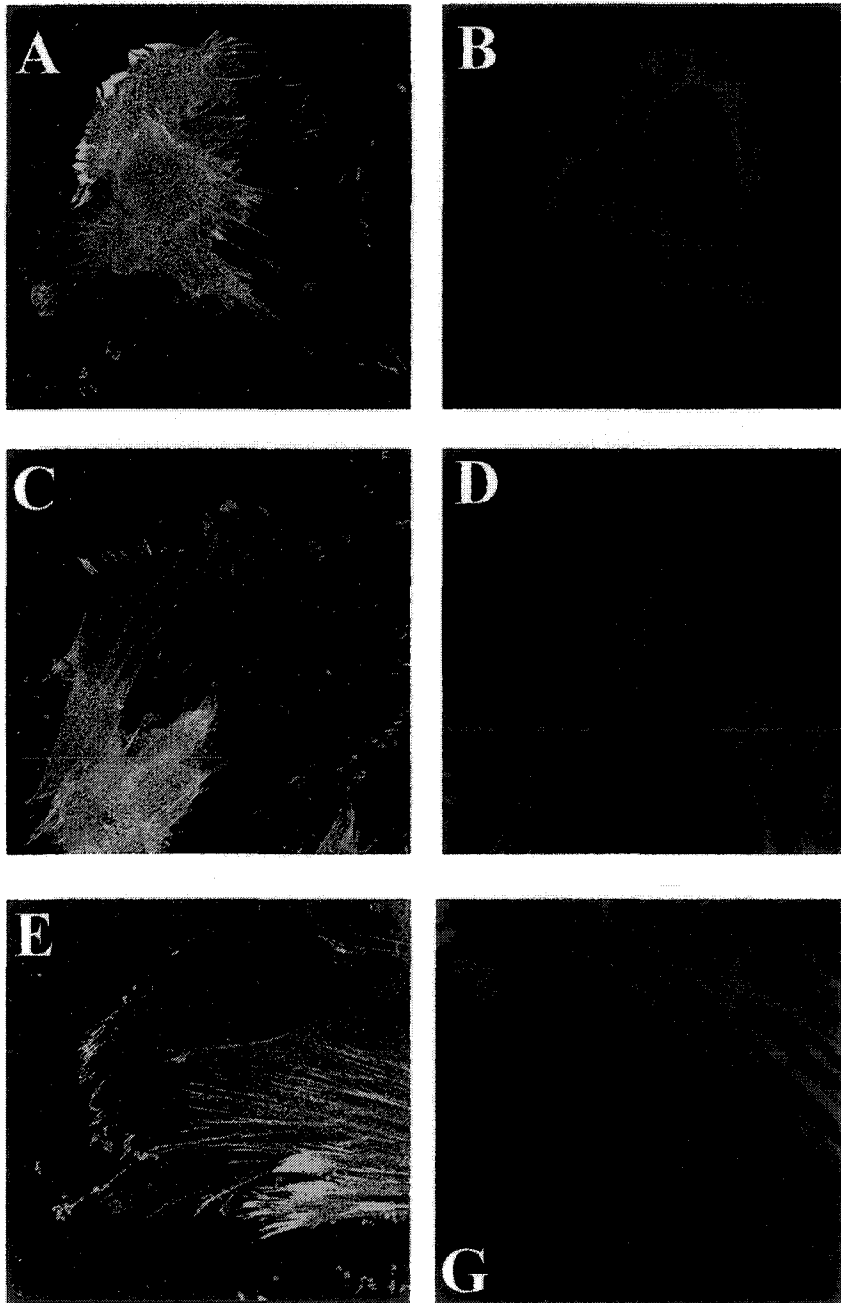
Figure 3.2

(corresponding to WDR1 localization, Figure 3.2, G, lower portion) and the stronger more stable interior F-actin stress fiber pool (Figure 3.2, G upper portion).

To further clarify the functional interaction between WDR1 and actin during cell attachment, REF 52 cells were trypsinized for 3-4 minutes and the relative localizations of WDR1 and actin was examined. WDR1 was observed to localize in thick microspikes at the immediate edge of adhering cells and remained attached to the CS after cell detachment as short filamentous-type structures described previously (WACs) (Figure 3.3, A, D, G). The staining of trypsinized REF 52 cells with phalloidin identified the presence of F-actin within both the cellular cortical WDR1 and to a notably lesser extent the attached WACs (Figure 3.3, A, B, D, E, G, H). Actin often appeared to be present only in small quantities and was not consistently localized with WDR1 as some WAC structures lacked phalloidin staining (Figure 3.3, A, B, D, E, G, H). These data suggest WDR1 interacts with either cortical actin or the barbed termini of stable F-actin fibers at the periphery of the cell to affect cell migration and attachment.

A dramatically different pattern was observed for the membrane-associated FA protein vinculin which appeared to dissociate from FA complexes prior to trypsin disruption and diffusely relocate deep within the cytosol (Figure 3.4, E & G). Vinculin is an established marker of FA complexes and the diffuse pattern within trypsinized cells is indicative of the dissociation of FA attachments (Critchley, 2000; Kaverina et al., 2002b; Small et al., 2002). The relative localization of vinculin with WDR1 was examined and confirmed the absence of vinculin from the WACs and the retracting cortical actin cytoskeleton (Figure 3.4, D-F). These data suggest WDR1 does not interact within FA complexes as vinculin localization was disrupted upon trypsin treatment, which is

115

Figure 3.3 Co-localization analysis of WDR1 with actin during cell detachment.

The relative localization of WDR1 with actin during cell detachment was examined in REF 52 cells through ICC confocal experimentation. A (400X), D (400X), G (400X) identify endogenous WDR1 localization. B (400X), E (400X), H (400X) detail the F-actin. C (400X), F (400X), I (400X) show the merged images.

116
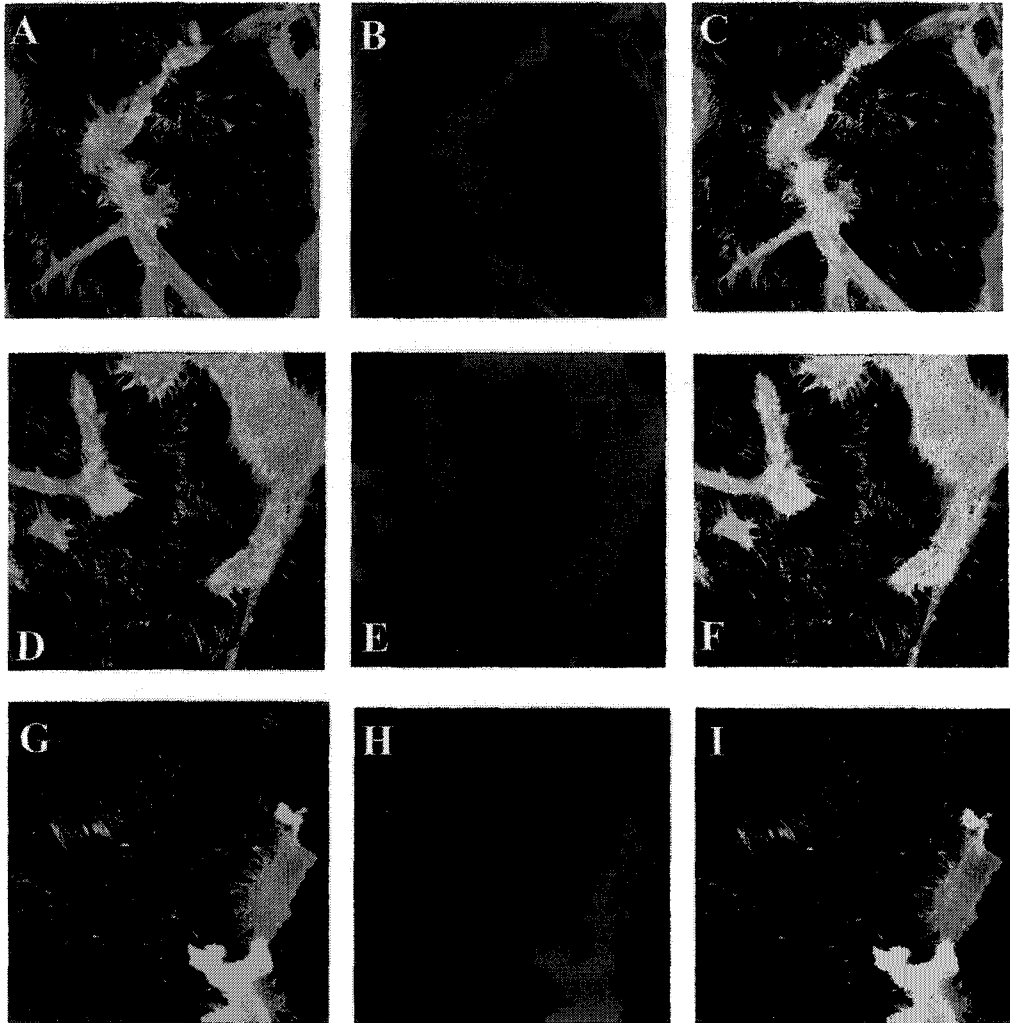
Figure 3.3

Figure 3.4 Co-localization analysis of WDR1 with vinculin during cell detachment.

The relative localization of WDR1 was compared with confocal analysis to vinculin localization during REF 52 trypsin-mediated cell detachment. A (400X), & D (400X) endogenous WDR1 localization. B (400X), & H (400X) show F-actin. E (400X), & G (400X) detail vinculin expression. C (400X), F (400X), I (400X) show the merged images.

118
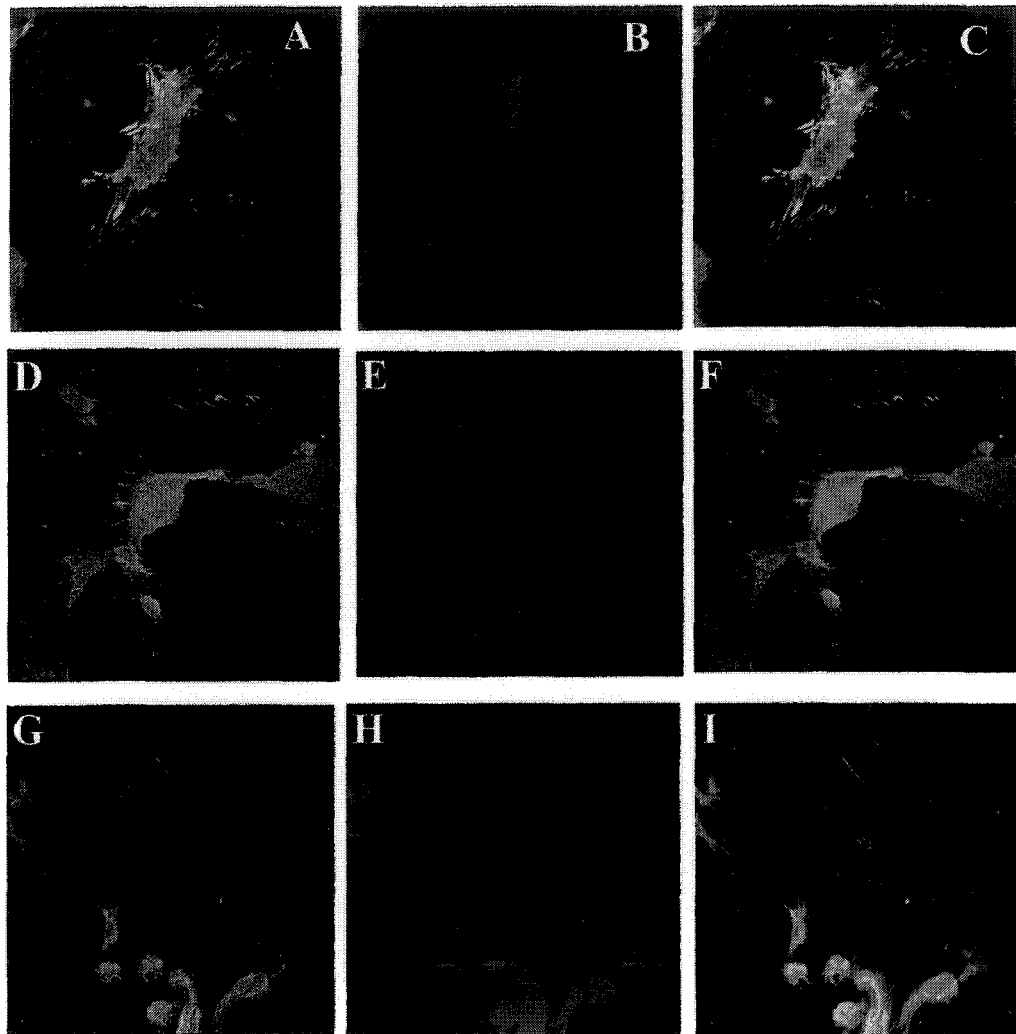
Figure 3.4

indicative of FA disassembly as vinculin only interacts with intact FA complexes (Bailly, 2003; Bass et al., 2002; Critchley, 2000). The difference between the loss of vinculin localization and the persistence of WDR1 filament localization after trypsin treatment suggests WDR1 is probably not a FA protein. The data for WDR1 localization however support a model of WDR1 barbed-end actin filament capping protein in conjunction with cell attachment.

To further investigate the attachment function of WDR1, the localization patterns of the actin interacting proteins CAP1 and cofilin within the WACs was contrasted to WDR1 expression. The ICC staining of trypsinized REF 52 cells revealed cofilin also localized at the retracting edges of detaching cells and associated in very slight amounts within WACs containing the small proportion of the attached actin filaments (Figure 3.5, A-C). A similar pattern was observed for CAP1 expression as CAP1 also localized to the retracting edges of cells and remained bound only within WACs containing actin filaments (Figure 3.5, D-F).

To further determine potential interactions of other FA complex proteins, the localization of β-tubulin during cell detachment was examined using the trypsin assay. The localization of β-tubulin after trypsin treatment was examined and observed to be similar to vinculin as β-tubulin also appeared to disperse diffusely within the cytosol as cell detached and was absent from the WACs (Figure 3.5, G-I). The lack of co-localization of β-tubulin with actin confirmed the lack of β-tubulin localization within the WACs (Figure 3.5, G-I).

To determine the persistence of the WDR1 staining within the WACs, a time course of trypsinization of REF 52 cells was performed. The cells were grown and treated

120

Figure 3.5 Co-localization analysis of WDR1 with actin associating proteins.

The relative localization of additional actin interacting proteins was investigated using trypsinization assays and confocal analysis of REF 52 cells. A (400X) shows the endogenous localization of cofilin. D (400X) details CAP1 expression. G (400X) demonstrates β-tubulin localization. B (400X), E (400X), H (400X) compare F-actin. C (400X), F (400X), I (400X) detail the merged images.

121
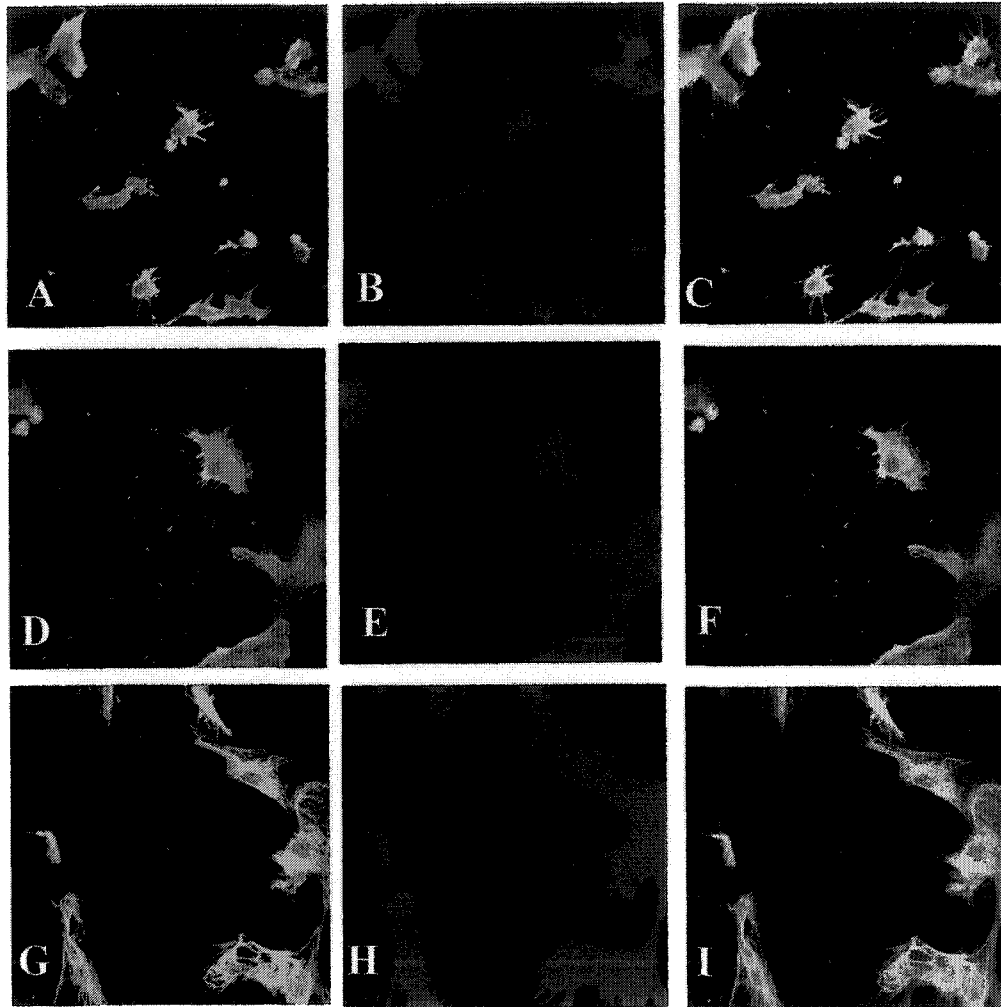
Figure 3.5

for either 3, 4, 6, or 10 minutes of trypsin before immediate formaldehyde fixation (Figure 3.6). After three minutes the cell contacts were enzymatically cleaved and the cells were beginning to retract with WDR1 remaining at the ends of actin filaments. The appearance of short thick WACs staining with a slight amount of F-actin was also visible (Figure 3.6, A-C). Four minutes of trypsin treatment increased the number of detaching cells and consequently resulted in an increase in the number of filamentous attachment structures that were left on the CS. However WDR1 was still localized within the cell at the end of retracting actin cables (Figure 3.6, D-F). After six minutes of treatment the cells were almost completely removed from the CS and exhibited a dramatic reduction in size and distinct actin filament visualization was difficult, but some WDR1 appeared to localize to the retracting cell edge while most WDR1 remained bound to the CS (Figure 3.6, G-I). After 10 minutes, the cells were completely removed from the CS and only WACs staining was visible in conjunction with a slight amount of actin (Figure 3.6, J-L).

WDR1 Localization to Cortical Actin of Adhering Cells

To investigate the function of WDR1 during cell attachment, confocal analysis of WDR1 localization during the settling and attachment of REF 52 cells on CS was performed. REF 52 cells were split into a tissue culture dish containing several CS and were stained for actin and WDR1 at 6, 12, and 24 hours after cell settling. Analysis of the cells after 6 hours of attachment revealed circular cells containing continuous lamellipodia with uniform thick filamentous microspike structures of WDR1 localized along cortical actin fibers (Figure 3.7, A-C). After 12 hours, WDR1 filamentous microspikes appeared to localize to distinct segregated attachment points (Figure 3.7, D-

123

Figure 3.6 Localization of WDR1 during trypsin treatments.

The effect of trypsin activity on the localization of WDR1 and the WAC structures was investigated in REF 52 cells using ICC confocal analysis of 3, 4, 6 and 10 minute trypsin treatments. A (400X), D (400X), G (400X), J (400X) show the endogenous localization of WDR1 examined after three minutes (A-C), four minutes (D-F), six minutes (G-I), and ten minutes (J-L). B (400X), E (400X), H (400X), K (400X) detail the corresponding F-actin. C (400X), F (400X), I (400X), L (400X) show the merged images.

124
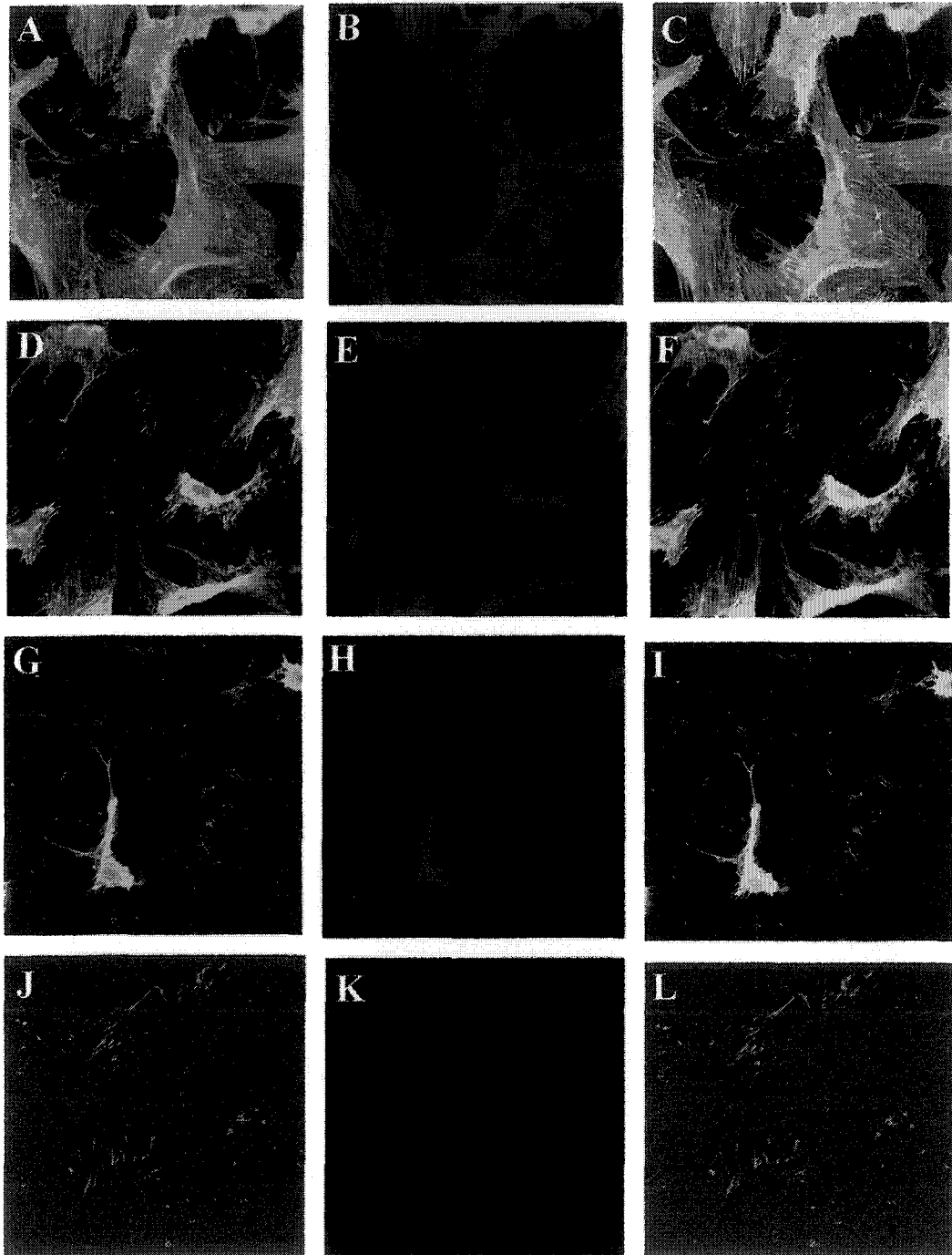
Figure 3.6

Figure 3.7 Localization of WDR1 during the attachment of settling fibroblast cells.

The further examination of the function of WDR1 during cell adhesion was investigated using ICC confocal examination of REF 52 fibroblast cells after six hours (A-C), twelve hours (D-F), and twenty-four hours (G-L) of adhesion. A (600X), D (600X), G (600X), J (400X) detail the endogenous localization of WDR1. B (600X), E (600X), H (600X), K (400X) display the corresponding F-actin. C (600X), F (600X), I (600X), L (400X) represent the merged images.

126
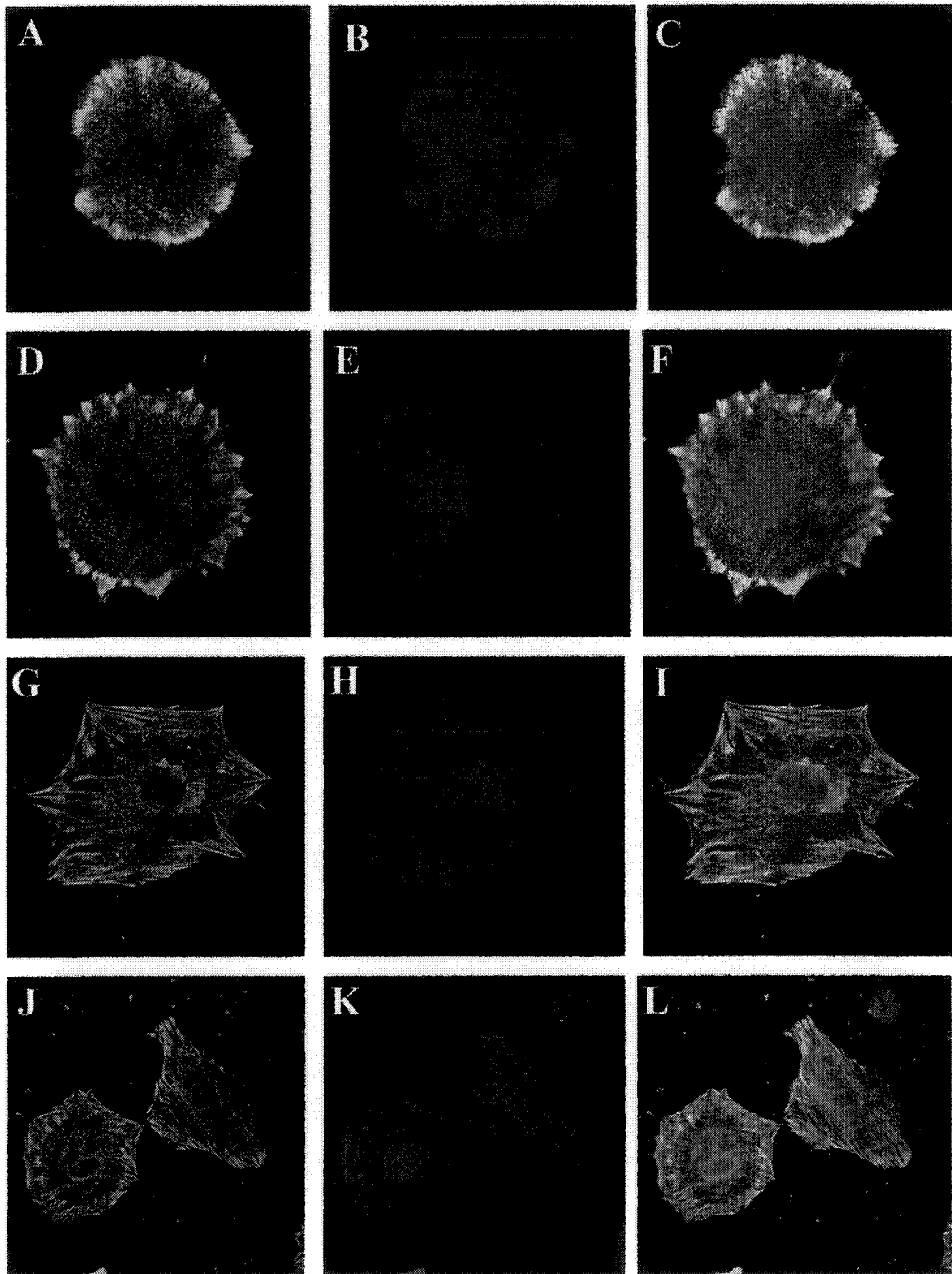
Figure 3.7

F). The upper portion of the cell in Figure 3.7 (D-F) demonstrates a long actin containing fiber extension co-stained with WDR1. Following 24 hours of attachment the majority of the cells attached to the CS displayed the typical structural architecture of established fibroblasts, indicated by the presence of stress fiber formation, and FA structures as formed in the upper cell in Figure 3.7 (J-L). Interestingly, after 24 hours of settling the localization of WDR1 appears less diffuse and is exclusive to the end of established actin filaments (Figure 3.7, J-L).

These results indicate the localization of WDR1 at the barbed-ends of actin filaments remains throughout the process of cell attachment. The process of FA establishment requires sequential protein recruitment and the persistence of WDR1 localization with actin throughout cellular detachment and attachment is not consistent with the expected pattern of temporal localization (as observed with vinculin). These data indicate the existence of a stable WDR1 barbed-end actin attachment and suggest a possible regulatory role of WDR1 within actin remodeling events.

Actin Filament Disruption Alters WDR1 Localization:

Cell survival critically depends on the initiation of rapid and unified responses to many changing environmental stresses. As actin is one of the most abundant cellular proteins the remodeling of the actin cytoskeleton requires the coordinated interactions of a plethora of actin interacting proteins. These proteins are typically responsive to many actin events such as depolymerization/polymerization, filament branching, and capping protein activity. To further define the relationship between WDR1 with F-actin, the localization of WDR1 was examined in the presence of actin disrupting agents.

128

Latrunculin A (lat A) is a G-actin binding agent which is able to prevent G-actin incorporation into growing actin polymers and block filament growth, and so lat A was used to assay the effect on actin polymerization on WDR1 localization. REF 52 cells were grown on CS and exposed to either 5, 10 or 20 minutes lat A treatments and the results are shown in Figure 3.8. After exposure to 5 minutes of lat A WDR1 barbed-end filament binding was still observed in cells, however it was diminished with the apparent loss of F-actin cables (Figure 3.8, A-C). Following 10 minutes of treatment the binding of WDR1 to actin filaments was dramatically reduced as compared with the presence of F-actin filaments; however regions retaining slight WDR1 staining also appeared to contain the most intact F-actin remnants (Figure 3.8, D-F). The 20 minute exposure of lat A to fibroblast cells disrupted almost all the F-actin however a few small fibrous patches remained with some WDR1 protein characteristically bound, indicating some WDR1 containing complexes were retained during actin polymerization inhibition (Figure 3.8, G-I).

To determine if the pattern of WDR1 expression was specific to lat A or was influenced by sequestration of monomeric actin, another G-actin binding agent was used to inhibit actin polymerization. Cytochalasin D (CD) binds and sequesters G-actin proteins similar to lat A, and inhibits filament extension and has also been shown to disrupt FA establishment and maintenance. REF 52 cells were treated with CD for either 5, 10 or 20 minutes and immediately prepared for ICC confocal analysis. Observations of the 5 minute cell exposure to CD resulted in a decrease of F-actin fiber presence and a corresponding reduction of WDR1 staining, which was similar but less dramatic to the effects of the 5 minute lat A treatments (Figure 3.9, A-C). Following 10

129

Figure 3.8 Effect of latrunculin A on WDR1 localization within fibroblast cells.

Examination of the interaction between WDR1 and actin was performed using ICC confocal analysis of REF 52 cells treated for five minutes (A-C), ten minutes (D-F) and twenty minutes (G-I) with the G-actin binding agent latrunculin A. A (600X), D (600X), G (600X) show the pattern of WDR1 localization. B (600X), E (600X), H (600X) demonstrate the F-actin staining. C (600X), F (600X), I (600X) detail the merged images.

130
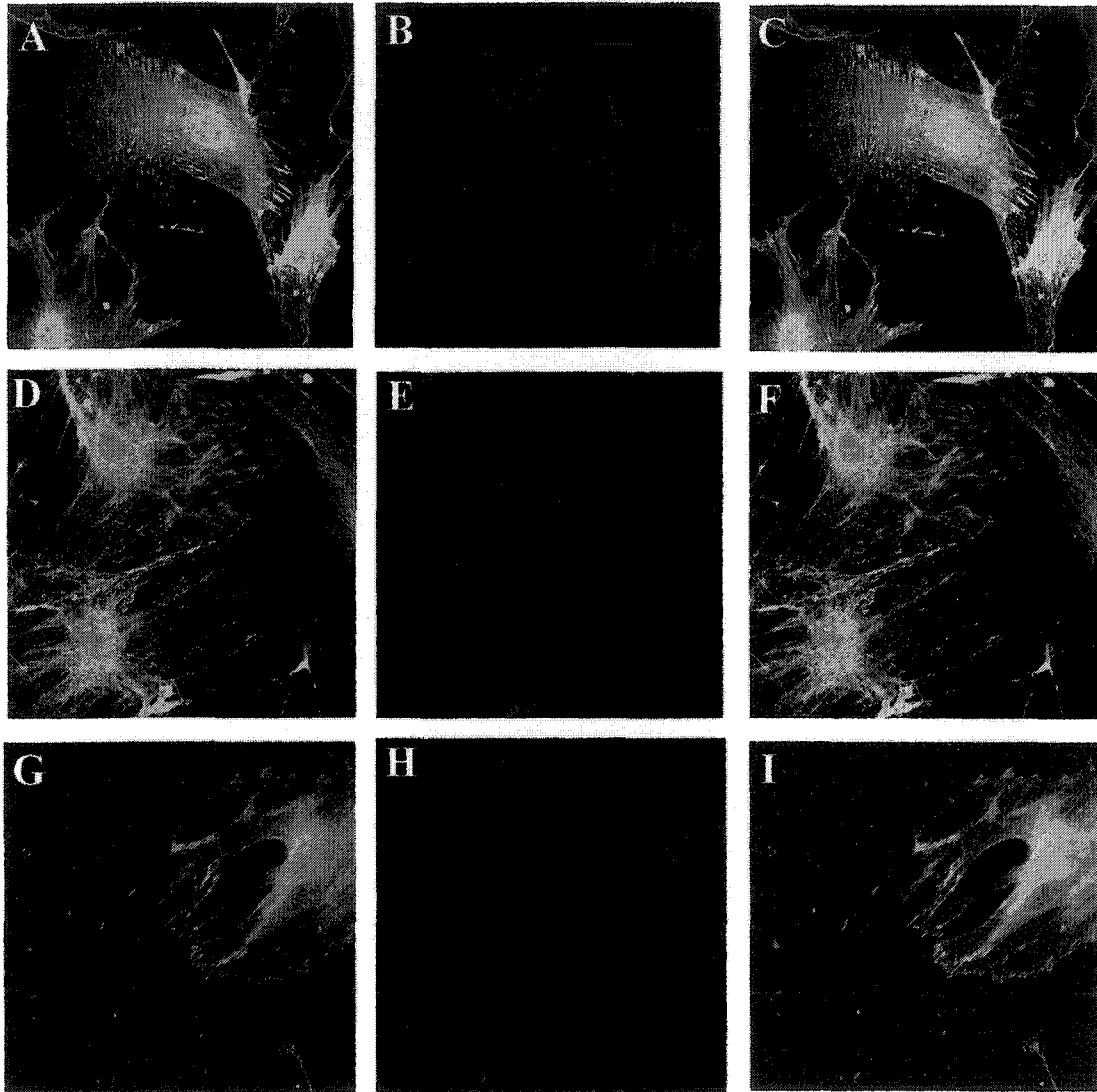
Figure 3.8

Figure 3.9 Effect of cytochalasin D on WDR1 localization within fibroblast cells.

Further investigation of the effects of actin on WDR1 localization was assayed in REF 52 cells which were treated with a second G-actin bind agent, cytochalasin D for five minutes (A-C), ten minutes (D-F) and twenty minutes (G-I). A (400X), D (600X), G (600X) detail the endogenous pattern of WDR1. B (400X), E (600X), H (600X) show the F-actin pattern. C (400X), F (600X), I (600X) are the merged images.

132
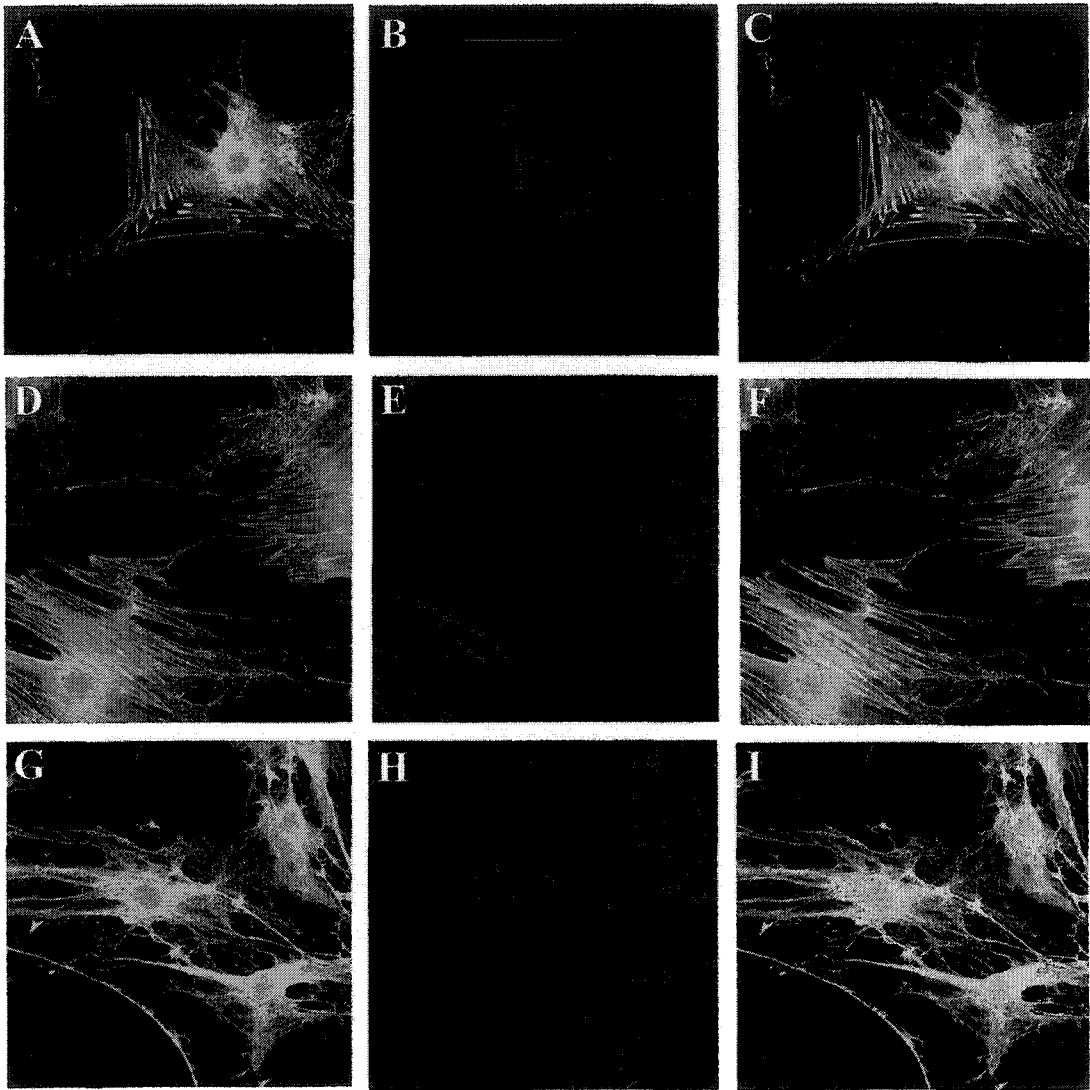
Figure 3.9

minutes of treatment a large amount of F-actin fibers remained intact within the cell and WDR1 was still observed to bind the barbed ends of filaments (Figure 3.9, D-F). The 20 minute CD treatment resulted in the substantial loss of F-actin staining; however some fibrous patches were observed which appeared co-localized with some diffuse WDR1 (Figure 3.9, G-I).

These data indicate the WDR1 actin filament cap was not immediately disrupted upon treatment which suggests the association of WDR1 with actin is not critically dependent on dynamic actin polymerization. However prolonged disruption of the actin polymerization increased filament depolymerization and resulted in the loss of WDR1 localization, implicating the structural integrity of actin filament is important for WDR1 interactions. A very interesting observation was the persistence of WDR1-associated F-actin fragments observed within the cells of both CD and lat A experiments. This data could support a function for WDR1 in stabilizing F-actin filaments as the presence of WDR1 appeared to confer protection from depolymerization to the associated filaments.

Localization of WDR1 and Actin Interacting Proteins during Neurite Extension:

Neurogenesis is a process that requires a dynamic actin cytoskeleton to generate neurite outgrowth. To examine the function of WDR1 during neurogenesis, the pattern of localization of WDR1 was compared to the relative expression of the actin-associated proteins cofilin, CAP1, CAP2, and the cytoskeletal protein β-tubulin during NGF induced neurogenesis in PC12 cells. Standard classification categorizes cells induced for < 7 days as containing young, immature neurites while NGF induction for > 7 days produces mature established neurons (Jacobs and Stevens, 1986). The analysis of relative protein

134

localization during early, intermediate and established NGF-induced PC12 neurite development and extension was examined at 1, 3, 5 and 10 days after induction of neurogenesis.

A major limitation of the PC12 cell line is their small size which can often increase the difficulty of obtaining detailed images however during neurogenesis ICC confocal analysis the majority of actin interacting proteins appeared to be present both at the peripheral edge of the cell body and within the tips of growing neurites. Throughout the 10 day NGF induction, cofilin appeared to remain localized within the immediate tip of growing neurites, while some protein was localized within the peripheral edges of the cell body (Figure 3.10, A-D). This pattern was similar to the pattern of CAP1 expression which demonstrated more diffuse localization within the tips and pads of growing neurites, and some peripheral localization within cell bodies (more established within early neurite formation) (Figure 3.11, A-E). The pattern of CAP1 expression was similar to the expression of CAP2 however CAP2 was more diffuse within the cell bodies and did not exhibit the same peripheral localization but was uniquely located at neural branch points throughout neurogenesis (Figure 3.12, A-F). The pattern of β-tubulin localization was also examined and observed to be very similar to actin, as β-tubulin was concentrated with actin within areas undergoing dynamic cytoskeletal rearrangement (data not shown). The pattern of WDR1 localization was the most dramatic of the proteins examined. Analysis of the one day NGF induced PC12 cells revealed WDR1 localized within the lamellipodia behind the actin growth cone of extending neuritis (Figure 3.13, A & B). However after three days WDR1 is remained localized to the peripheries of the cell body but also within the tips of growing neurites (Figure 3.13, C).

135

Figure 3.10 Localization of cofilin during neurogenesis.

The endogenous pattern of cofilin expression during NGF-induced PC12 neurogenesis was investigated using ICC confocal experimentation. The location of cofilin (green) and actin (red) was shown (merged) in PC12 cells exposed NGF for A (1200X) one day, B (1200X) three days, C (1200X) five days and D (600X) ten days of induction.

136
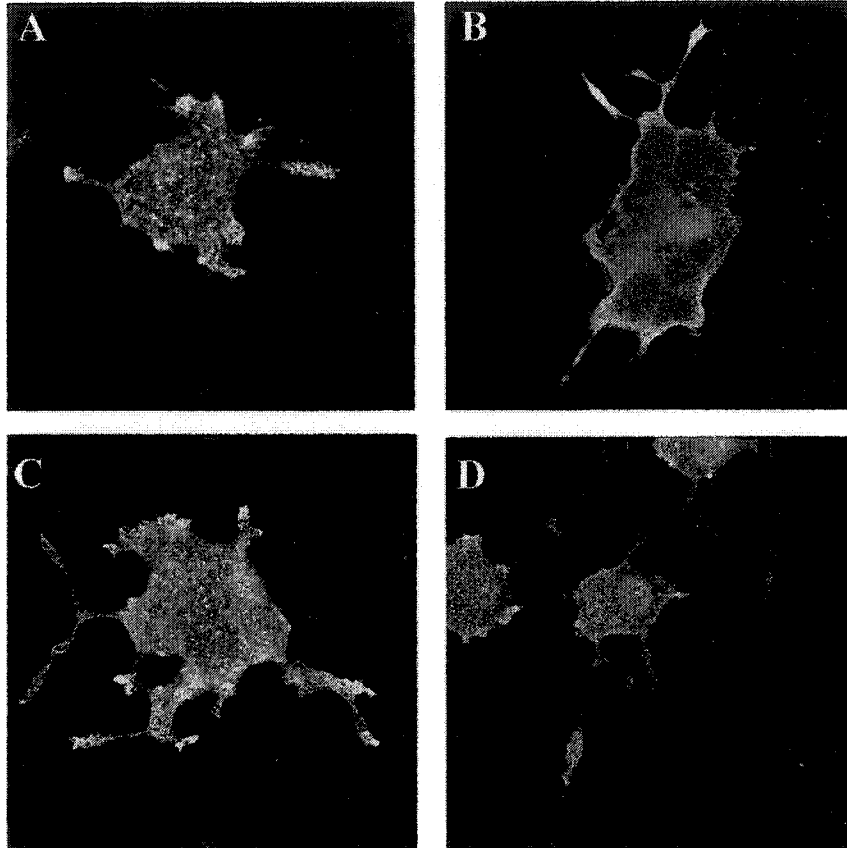
Figure 3.10

Figure 3.11 Localization of CAP1 during neurogenesis.

The localization of CAP1 through neurogenesis of PC12 was investigated using confocal investigation. The localization of CAP1 (green) and actin (red) was demonstrated (merged) at A (1200X) one day, B (1200X) three days, C (1200X) & D (2400X) five days, and E (600X) ten days after the addition of NGF.

138
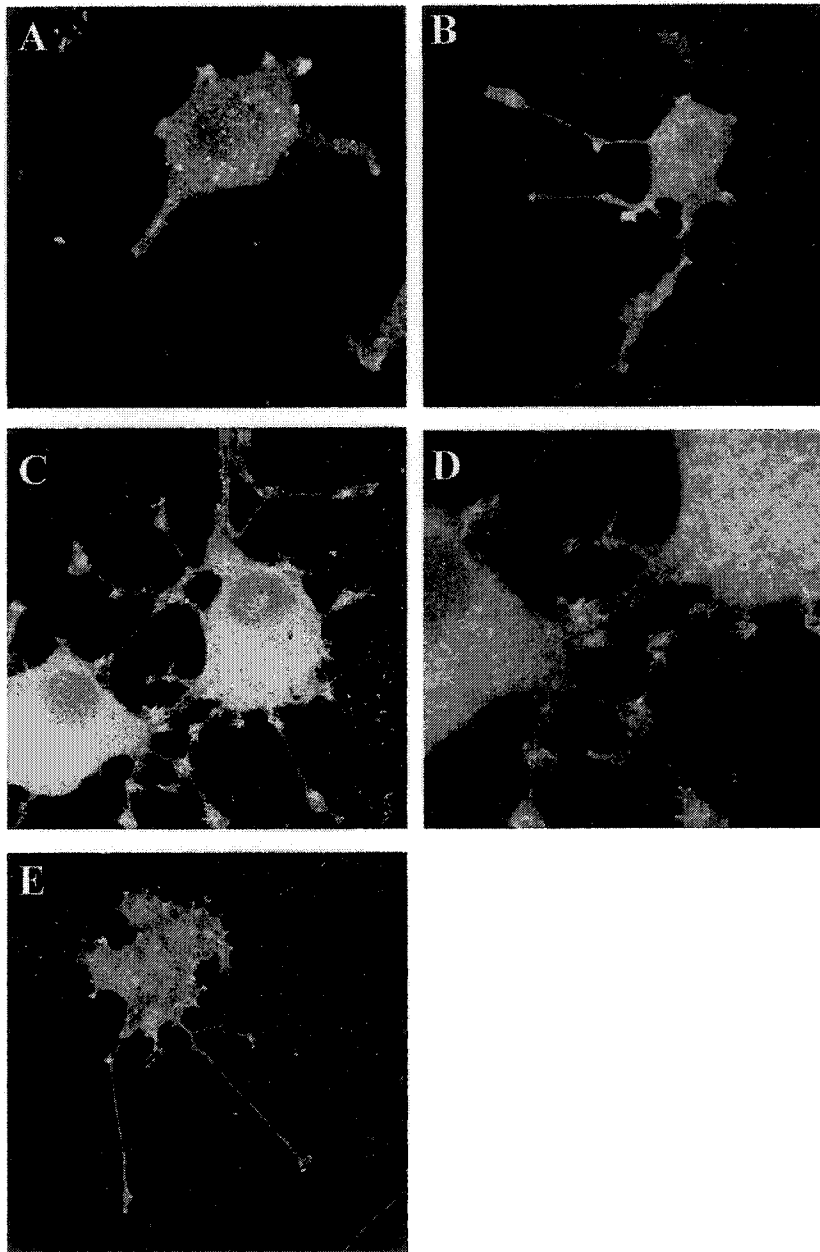
Figure 3.11

Figure 3.12 Localization of CAP2 during neurogenesis.

The investigation of the endogenous localization of CAP2 throughout PC12 neurogenesis was assessed using ICC confocal examination. The localization pattern of CAP2 (green) and actin (red) was demonstrated (merged) at A (1200X) & B (1800X) one day, C (2400X) three days, D (600X) five days, and E (600X) & F (1800X) ten days after induction.
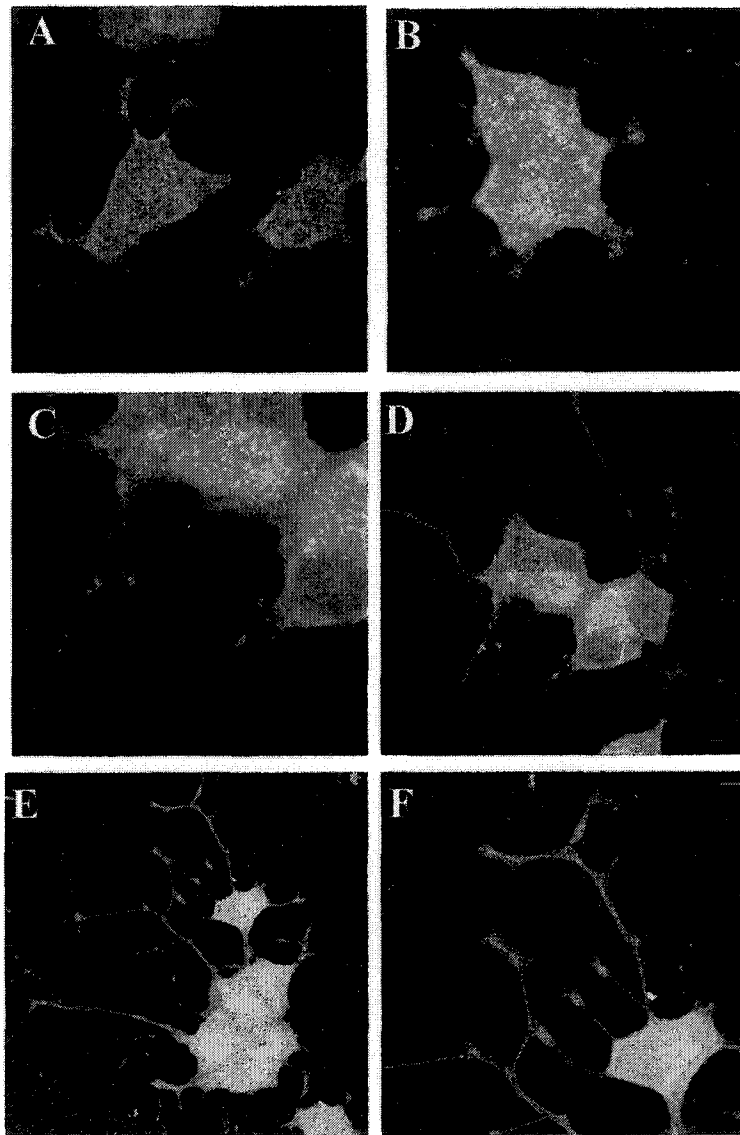
Figure 3.12

Figure 3.13 Localization of WDR1 during PC12 neurogenesis.

The endogenous localization of WDR1 during NGF-induced PC12 neurogenesis was investigated through ICC confocal analysis. The location of WDR1 (green) and actin (red) was shown (merged) in PC12 cells exposed NGF for A (1200X) & B (2400X) one day, C (600X) three days, D (600X), E (1800X), F (3000X) five days and G (600X) & H (600X) ten days.

142
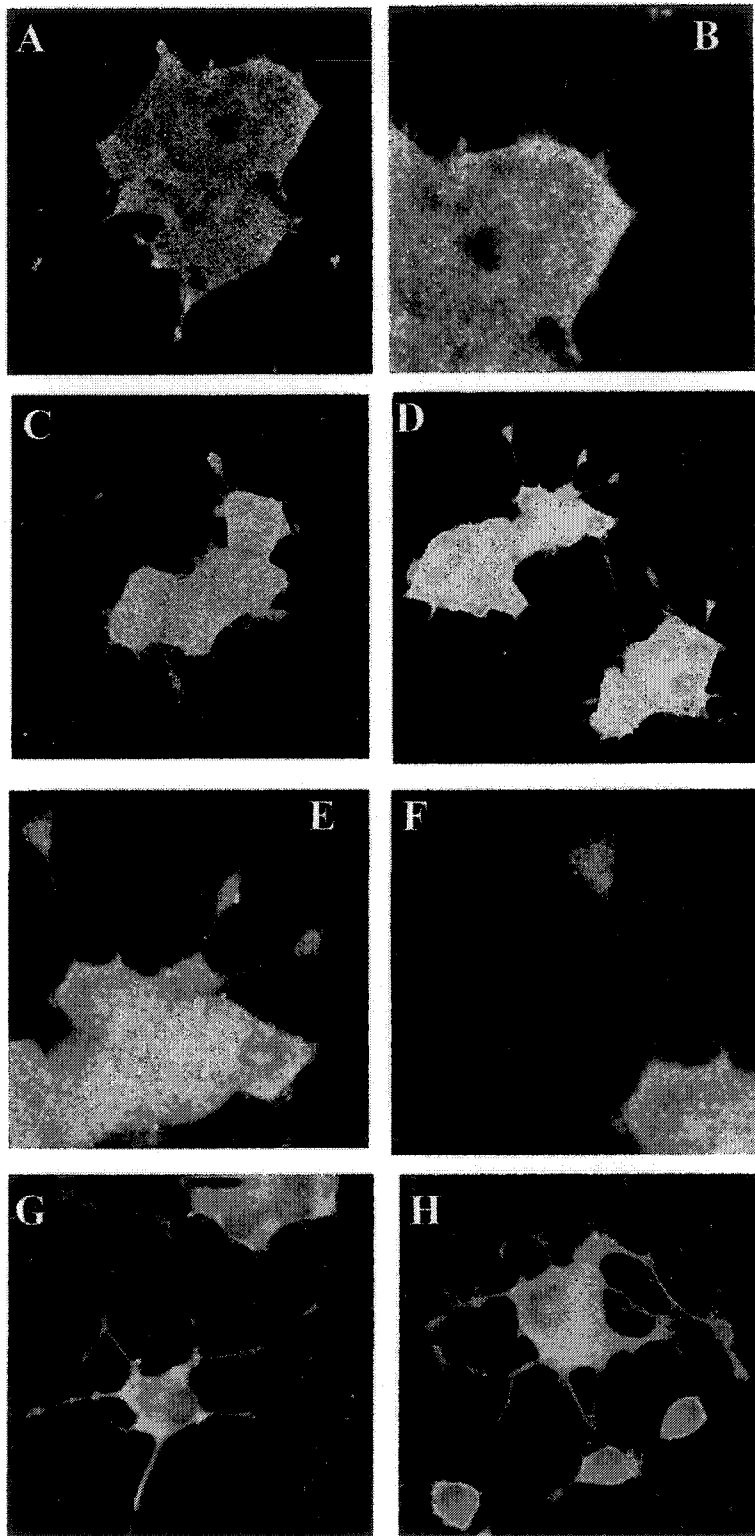
Figure 3.13

Figure 3.14 Localization of only WDR1 during PC12 neurogenesis.

The endogenous localization of WDR1 during NGF-induced PC12 neurogenesis was shown merged with actin in Figure 3.13. The WDR1 ICC confocal data demonstrated in Figure 3.13 is shown. The location of WDR1 (green) within PC12 cells at A (1200X) & B (2400X) one day, C (600X) three days, D (600X), E (1800X), F (3000X) five days and G (600X) & H (600X) ten days of NGF-induction.

144
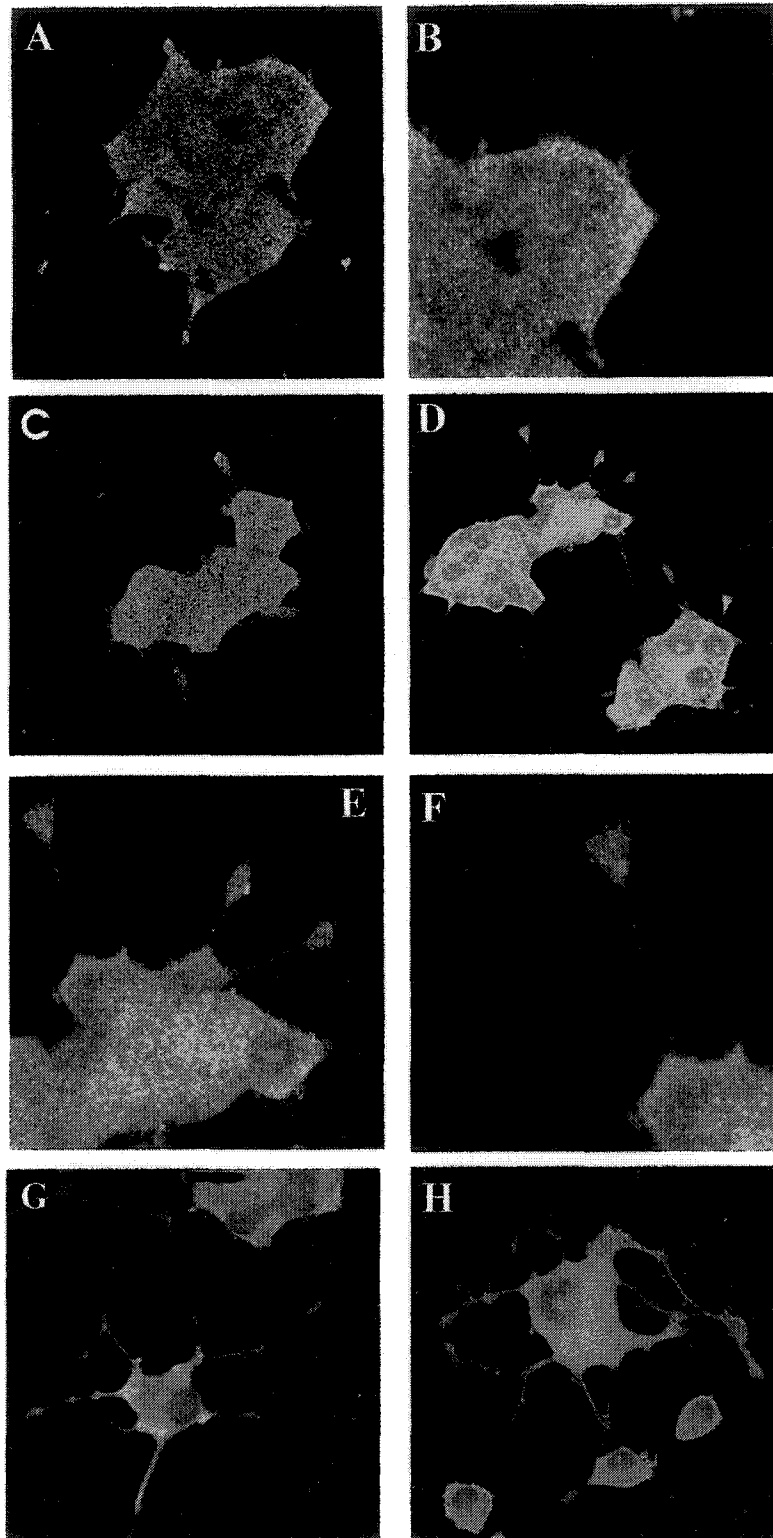
Figure 3.14

Figure 3.15 Localization of only actin during PC12 neurogenesis.

The confocal observations of F-actin filaments within the NGF-induced PC12 cells shown in Figure 3.13 are shown. The location of F-actin (red) in PC12 cells after A (1200X) & B (2400X) one day, C (600X) three days, D (600X), E (1800X), F (3000X) five days and G (600X) & H (600X) ten days of induction.

146
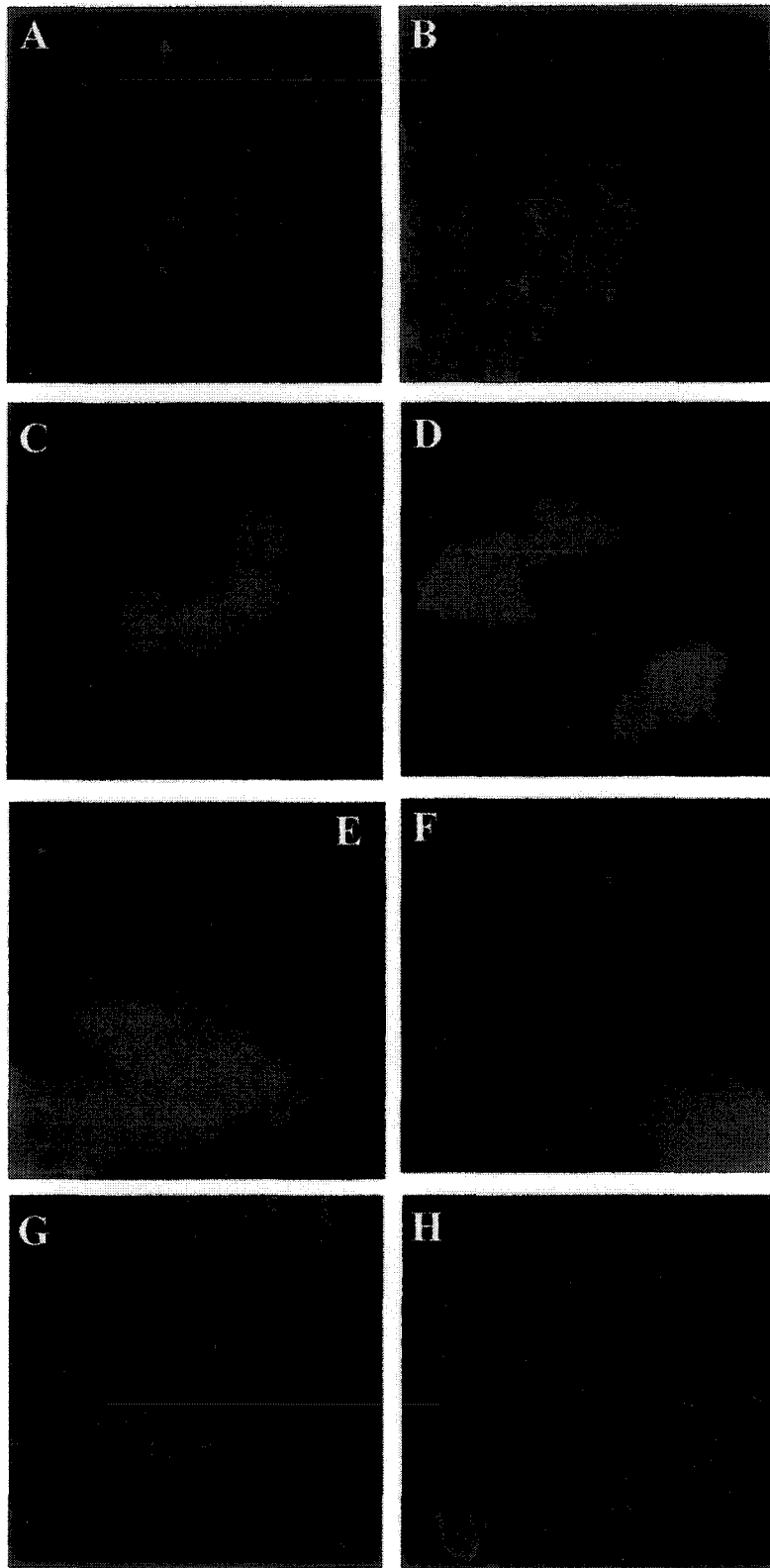
Figure 3.15

The expression of WDR1 remained consistent in both intermediate (5 days after NGF) and mature (10 days after NGF) PC12 cells as WDR1 expression continued within neurite tips and cell body peripheries (Figure 3.13, D-F, & G-H). Figure 3.14 demonstrates the WDR1 staining at one day (A & B), three days (C), five days (D-F) and ten days (G & H) after NGF-induction while the actin localization is shown in Figure 3.15. These results demonstrate an active role of WDR1 during the PC12 actin remodeling of neurogenesis, and further confirmed the involvement of cofilin and CAP (CAP1 & CAP2) proteins during neural actin rearrangement.

WDR1 Isoforms Maintain Consistent Expression Throughout Neurogenesis:

To analyze the expression of WDR1 during NGF induced neurogenesis, RNA was collected and cDNA was produced from PC12 cells undergoing neurogenesis for 12, 24, 48, 72, 96, and 136 hours (Figure 3.16, lanes 1-6). The quantification of the RT-PCR analysis was preformed using the constitutively expressed GAPDH transcript co-amplification as an internal control to quantify the WDR1 amplicon expression. The expression analysis of both WDR1 and WDN534 was determined by the relative pixel intensity of an N-terminal 400 bp amplicon which is unique to WDR1 transcript and a C-terminal 600 bp amplicon common to both isoforms which reflects the presence of the two transcripts (as outlined in chapter 2). Interestingly, the analysis of 14 RT-PCR reactions demonstrated both amplicons exhibited a slight decrease in expression through out the course of 136 hours (Figure 3.17). The N-terminal 400 bp: GADPH ratio average was 20.5%; however expression declined from 25% at 12 hours to 17% at 136 hours

148

Figure 3.16 RT PCR analysis of hWDR1 expression during neurogenesis.

The expression of WDR1 during NGF-induced neurogenesis of PC12 cells was examined using RT PCR. The 400 bp N-terminal and 600 bp C-terminal WDR1 amplicons were co-amplified with an 800 bp GAPDH internal control. Quantitative triplex PCR data of NGF-induced neurogenesis in PC12 cells for 12 hours (lane one), one day (lane two), two days (lane three), three days (lane four), four days (lane five), and five days (lane six). The ratio of WDR1 amplicon was compared to the control GAPDH, which was further contrasted to the five day low-serum control (lane seven) plate expression.

149
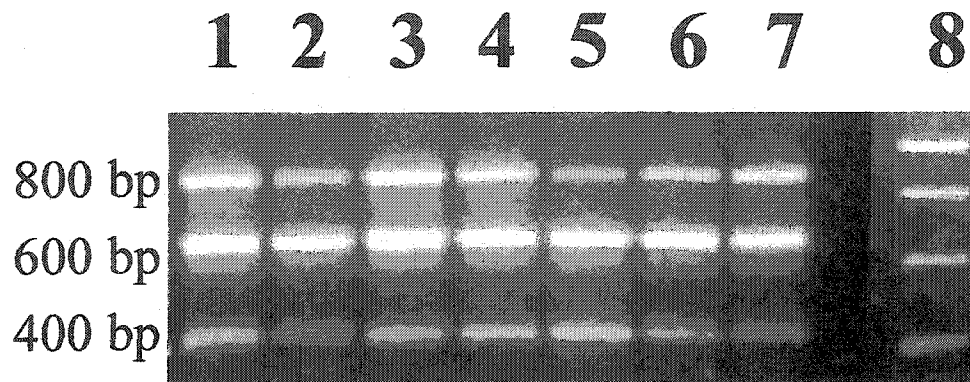
Figure 3.16

Figure 3.17 Ratio of WDR1 amplicon: GAPDH amplicon expression intensities.

The ratio of WDR1 N- (odd lanes 1, 3, 5, 7, 9, 11, 13) or C- (even lanes 2, 4, 6, 8, 10, 12, 14) amplicon intensities were compared to the amplification of the internal GADPH control transcripts in PC12 undergoing NGF-induced neurogenesis. The average relative expression data are shown indicating the relative statistical significance of expression.

150

The Relative Expression of WDR1 throughout PC12 Differentiation
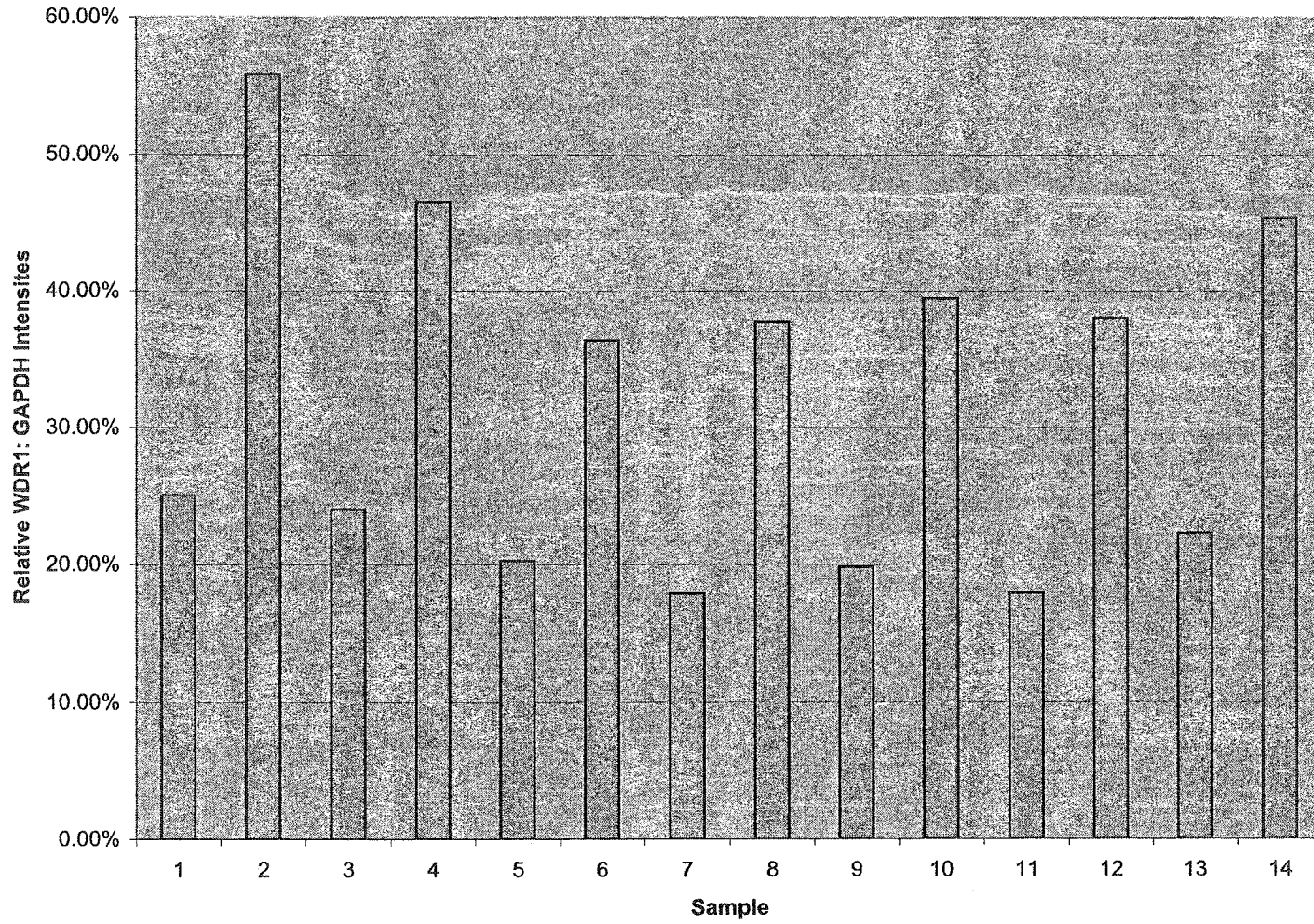
(with the low serum control ratio being 22%, Figure 3.17). The C-terminal 600 bp: GAPDH average expression ratio was 42% but exhibited a more substantial decrease as after 12 hours the ratio was 55% which declined to 38% after 136 hours (with the 136 hour low serum control demonstrating a 45% expression ratio, Graph 3.18). These data suggest WDR1 is not transcriptionally altered during PC12 differentiation although the relative protein levels still have to be examined.

Discussion:

Actin is a dominant effector of many vital cellular processes such as cellular adhesion to extra-cellular substrate, cellular migration and neural extension however many proteins regulating these essential behaviours still require characterization. Recently a novel family of actin-interacting WDR1 proteins has been shown to function during actin rearrangement with actin and the actin depolymerizing protein cofilin (Adler et al., 1999; Konzok et al., 1999; Oh et al., 2002; Rodal et al., 1999). However previous experimental evidence (chapter 2) did not identify an interaction with cofilin but did support one with actin.

However, *in vivo* co-localization studies (chapter 2) demonstrated a similar pattern of both vinculin and WDR1 expression and suggested WDR1 may be involved in cellular adhesion. The investigation of WDR1 localization during cell migration supported this function as WDR1 was observed to localize within both the leading edge lamellipodia as thick filamentous structures at the barbed-ends of actin filaments and to a lesser extent within the detaching uropodia. These data suggest a role for WDR1 in the establishment of the focal contacts structures required for the progression of motility, and additionally implicate WDR1 within the pathway of Rac signaling proteins which are

153

known to establish FA and lamellipodia through *de novo* filament generation (Bishop and Hall, 2000; Hall, 1998b). Additionally, cofilin was diffusely localized to the lamellipodia, however (as observed in static fibroblast cells) lacked distinct barbed-end association. These results suggest a barbed-end stabilizing or adhesion association with WDR1 during cell migration which is supported from studies within both *Dictyostelium* and *C. elegans* systems as WDR1 mutant cells have been shown to contain impaired cortical actin organization and inhibited motility, further implying that WDR1 may be controlled through the Rac signal pathway (Aizawa et al., 1999; Konzok et al., 1999; Mohri and Ono, 2003).

The elucidation of the novel function of WDR1 within cell adhesion was performed using a novel trypsin cleavage assay of REF fibroblast cells. Trypsin is a proteolytic enzyme isolate from pancreatic tissue which uses a serine residue to specifically cleave the peptide bonds of arginine and lysine residues. During trypsin-mediated cleavage of cell adhesion two distinct types of F-actin filaments were confirmed to exist within the cell. A small peripheral cortical actin layer containing short and dynamic actin fibers exists surrounding the thicker more stable inner structure of stable actin stress fibers. Localization of WDR1 demonstrated it was present at the barbed-ends of cortical actin filaments, and also identified the presence of interesting WDR1 aggregated complex structures (WACs) which remained attached to the CS during and after cell retraction. WDR1 participating within cell adhesion is a novel function of WDR1, however several studies within *Dictyostelium* and *Xenopus* have implicated WDR1 as regulators of cell division yet the mechanism of action remains unknown (Gerisch et al., 2004; Konzok et al., 1999; Okada et al., 2002; Okada et al., 1999).

154

Further confocal examination of the composition of the WACs demonstrated the presence of only a slight amount of F-actin. Interestingly, the FA proteins vinculin and β-tubulin were absent as vinculin localization was disrupted immediately upon trypsin treatment and became diffuse within the cell as the FA complex was disrupted. A similar pattern was observed for β-tubulin, which exhibited a slightly more diffuse cellular localization after trypsin disruption. Since vinculin is an established component of the FA adhesion complex and β-tubulin containing microtubules are localized prior to FA establishment, the absence of these two proteins within the WACs structures indicates the absence of FA complex within the adhered structures (Critchley, 2000). Interestingly, the actin interacting proteins cofilin and CAP1 are only slightly present within the WACs along with a small amount of F-actin, suggesting these two proteins are not interacting with WDR1 within the WACs and therefore are not true components of the adhered structures. However the slight amount of both cofilin and CAP1 with actin within the WACs may suggest the existence of an actin-regulating complex involving the interaction of the WDR1, cofilin and CAP1 proteins, as suggested by Balcer et al (2003).

Interestingly, the slight amount of actin within the WACs did not appear to fluctuate throughout the trials further defining the stability of the adhesive structures. The identification of the WAC structures represents the characterization of a method of cellular attachment, which when combined with the differential protein expression data of human transformed and non-transformed cell lines strongly implicates a functional role of WDR1 within cell adhesion. However, the analysis of WDR1 localization during cell attachment demonstrated high, uniforms amounts of WDR1 were present bound to the barbed-ends of actin filaments after 6 hours of substrate re-attachment within the

155

lamellipodia, and remained highly expressed within the peripheral lamellipodia as the cell settled-out for an additional 6 hours. After 24 hours of cell adhesion the amount of WDR1 protein appears consistent although more dispersed within the larger established cell to the ends of actin filaments within the edges of cells. The consistent expression and localization of WDR1 to the barbed-ends of actin filaments confirms previous reports classifying WDR1 as exclusive F-actin-binding proteins yet does not clarify the cellular function of this interaction (Adler et al., 1999; Konzok et al., 1999; Okada et al., 1999; Rodal et al., 1999).

The effect of actin polymerization on WDR1 localization was assayed using two G-actin sequestering agents, CD and Lat A. Both agents were shown to dramatically disrupt the actin cytoskeleton and resulted in loss of the associated barbed-end WDR1 structures, and a diffuse pattern of WDR1 cellular dispersal. These results were more dramatic with the lat A treatments, however both agents cause some fragments of F-actin to persist and WDR1 was co-localized with these remnants suggesting WDR1 may impart a stabilizing or protective function when bound to the barbed-filament ends.

The function of WDR1 was investigated during the active actin remodeling within extending neurites during NGF induced PC12 differentiation. The localization of several actin interacting proteins was established to confirm the dynamic actin remodeling occurring at both the bases of growing neurites, and the T and P domains of extending neurite tips (Gungabissoon and Bamburg, 2003; Sarmiere and Bamburg, 2004). The expression of cofilin was restricted within the cell to the lamellipodia of actively developing neurites and within the P domain of extending neurons and indicated the localization of active actin depolymerization within NFG-induced PC12 cells. The

156

expression of CAP1 was similar to both CAP2 and cofilin, however CAP1 appeared more diffuse then cofilin within the tips of extending neurites, and was additionally detected further back within the T domain (the neurite pad). CAP1 also demonstrated a diffuse localization within the cell body but was concentrated within extending lamellipodia, thus the similar localization of CAP1 and cofilin expression patterns confirm the locations of actively remodeled actin. CAP2 was diffusely located within the cytoplasm and appeared to only slightly localize to developing lamellipodia, however CAP2 was uniquely expressed within the branches of PC12 neurites.

The expression pattern of WDR1 displayed the most dramatic localization throughout NGF-neurogenesis. Initially WDR1 localized within the lamellipodia of developing neurites immediately posterior to the actin growth cone, in which a slight amount of WDR1 was observed, indicating responsiveness to the Rac/ Cdc 42 G-protein transduction pathways (Bishop and Hall, 2000; Hall, 1998b). Throughout neurite extension WDR1 expression was observed within both the P and T domains, further implicating the regulatory influence of Rac/ Cdc 42 pathways and also within the lamellipodia of the cell body (Hall, 1998b; Sarmiere and Bamburg, 2004). Expression in developed neurites remained localized within the P and T domains and cellular lamellipodia of extending neurites, which further implies the existence of a potential interaction between WDR1, CAP1, cofilin and CAP2 as each is localized within the same areas of actin rearrangement during neurogenesis, however CAP2 is the only protein which exhibited a unique expression pattern within the PC12 cells.

Further analysis of WDR1 NGF-induced transcript expression was assayed using RT-PCR amplification which revealed that both isoforms were slightly down-regulated

through the course of five day PC12 NGF-induction as compared to the expression pattern of the low serum control cells. The decrease in WDR1 expression compared to control expression was not significant and did not indicate a function for WDR1 proteins during neurogenesis independent of actin regulation. However WDR1 proteins were observed to function with cofilin during Rac/ Cdc42 regulated actin rearrangement within the neural P zone and the leading lamellipodia of PC12 and REF52 cells, which may suggest a mechanism of activation for WDR1 proteins (Bailly, 2003; Cotteret and Chernoff, 2002; Kaverina et al., 2002b). This data is currently supported by several reports from the dynamic actin events of yeast, *Dictyostelium* and *Xenopus* which demonstrate WDR1 localizing to cortical actin areas undergoing cell division (Konzok et al., 1999; Okada et al., 2002; Okada et al., 1999; Rodal et al., 1999). However, the observation of WDR1 FA-like expression at the ends of actin filaments could also suggest WDR1 responds to Rho-mediated transduction pathways, which have been shown to regulate cofilin activity through the LIM kinase pathway (via LIMK2) (Birkenfeld et al., 2003; Cotteret and Chernoff, 2002; Hall, 1994). Yet the novel WDR1 attachment and localization data provided in this thesis, combined with additional observations from studies of chick, mouse, and human systems may suggest a more complex mechanism of regulation of WDR1 which is independent of cofilin mediating pathways (Ichii et al., 2001; Oh et al., 2002; Verma et al., 2004a). Despite the discrepancies, the final conclusions drawn from the current collection of WDR1 data is that the function of WDR1 within the cell requires further investigation before the mechanism of *in vivo* WDR1 regulation and cytoskeletal function can be further understood.

158

Chapter Four

Conclusions and Future Directions

General Conclusions:

The work presented in this thesis initiated the characterization of the human homologue of yeast Aip1p and suggested several novel functions of mammalian WDR1. The sequence analysis demonstrated the WDR1 proteins may be classified as kelch proteins as three WD motifs are shown to be highly homologous to the *Drosophila* kelch-like motifs. Additionally hWDR1 protein interaction experiments appeared to demonstrate a few kelch-like functions such as the ability to bind actin and form hetero-multimer complexes, in addition to functioning in active actin filament dynamics. Expression data of both hWDR1 and hWDN534 transcripts were shown to be conservatively expressed within a variety of human tissues types such as brain kidney, liver, lung, trachea, heart. Both isoforms were shown to be expressed in several rat brain rat structures such as the cerebellum, frontal cortex, post cortex, pons, spinal cord, medulla, and hippocampus. Further examination of protein expression across several non-transformed and transformed human and rat cell lines were also assayed and indicated a differential expression of WDR1 proteins between the transformed and non-transformed cell lines. Transcript analysis through northern blot assays demonstrated the presence of both a 3.0 kb transcript and a less prevalent 2.2 kb transcript. The *in vivo* localization of WDR1 revealed that WDR1 localized to the barbed ends of actin filaments and was

159

present along with cofilin and CAP1 within areas of dynamic actin rearrangement such as the leading edge of migrating fibroblasts and the base and tips of extending neurites of PC12 cells undergoing neurogenesis. Investigation of the regulation of both WDR1 isoforms during neurogenesis indicated a slight down regulation of both transcripts; however no significant patterns correlated to NGF neural induction.

Similarities between hWDR1:

Several previous studies with other WDR1 orthologues have indicated an interaction with WDR1 and cofilin, CAP1 and actin. However our studies described a novel function of WDR1 during cell adhesion as WDR1 was found to localize in a manner similar to the FA vinculin, but unlike vinculin WDR1 was shown to remain attached to CS within a WDR1 aggregated complex (WACs) during and after trypsin mediated cell detachment. Latrunculin A and cytochalasin D treatments indicated WDR1 may protect and stabilize actin filaments during depolymerizing events.

These data have provided basic insight into the classification and function of hWDR1 proteins, however further study investigating the regulation and function of WDR1 proteins within several actin based processes is still required. Interestingly, data reported from numerous WDR1 orthologues indicates a general characterization pattern which differs from that displayed by hWDR1. Typically WDR1 orthologues have been shown to localize with cofilin and function synergistically to enhance the disassembly of actin filaments *in vitro* (Adler et al., 1999; Konzok et al., 1999; Matsumoto et al., 1998; Mohri and Ono, 2003; Oh et al., 2002; Okada et al., 2002; Rodal et al., 1999). Additionally, several WDR1 orthologues have been shown to be synthetically lethal with cofilin null-mutants, however WDR1 null-phenotypes differ from those of cofilin null

160

cells. The WD null- phenotypes of yeast and *Dictyostelium* included impaired cortical actin dynamics affecting the processes of endocytosis, cell motility, cytokinesis, phagocytic cup formation (Gerisch et al., 2004; Konzok et al., 1999; Rodal et al., 1999). WDR1 has also been shown to have distinct functions in both *Dictyostelium* and *Drosophila* mediating cytokinesis and lamellipodia formation, and has been shown to localize to cleavage furrow of Xenopus embryos (Gerisch et al., 2004; Okada et al., 2002; Rogers et al., 2003). These data indicate WDR1 proteins typically interact with cofilin during active actin dynamics and enhance regulation of several critical actin dependent processes.

The data collected in this thesis demonstrate hWDR1 shares a common feature of WDR1 proteins and interactively binds F-actin. However it is currently unique amongst WDR1 proteins as no interaction with cofilin was observed. The characterization of hWDR1 suggests the function of WDR1 proteins during cell migration may be through the establishment of cell adhesion and attachment. However, hWDR1 is the first higher eukaryotic WDR1 protein reported to express multiple isoforms (with the exception of the muscle and non-muscle WDR1 genes of *C. elegans*) and so the data collected from both the rat and human cell lines may be reflective of differential isoform expression and not represent a conserved WDR1 function (as indicated by the REF 52 cell system) (Mohri and Ono, 2003). However, since these data also confirmed a conserved pattern of WDR1 expression (as both hWDR1 isoforms were detected in a wide variety of human and rat cell types), an overall conserved function of WDR1 is suggested.

161

<u>Future Experiments:</u>

Owing to the essential functions WDR1 proteins have been implicated in (such as cell adhesion, neurogenesis, cytokinesis, and migration), the work presented in this thesis identified and characterized mammalian WDR1. However, as many aspects of hWDR1 function are still unknown and will require further experimental investigation, the results presented in this thesis can be expanded in several ways.

<u>Isoform Detection:</u>

The investigation of proteins capable of interacting with hWDR1 and hWDN534 would provide further data for the processes requiring WDR1 function, and may additionally provide evidence of novel WDR1 isoforms. The identification of novel hWDR1 isoform multimer interactions could be determined by the use of anti-WDR1 protein A beads using immunoprecipitation experiments. Identification of potential isoforms could then be assayed using anti-WDR1 antibody detection and protein sequence analysis. The demonstration of the two tissue specific WDR1 gene expression in *C. elegans* and the isolation of multiple polypeptides during the *Xenopus* Aip1 affinity column experiments indicate the possible existence of multiple isoforms (Okada et al., 1999). Strong supporting data for this possibility in mammalian systems was obtained from the identification of the presence of hWDR1 and WDN534 isoforms, and their differential expression within transformed and non-transformed human cell lines and the presence of the unique ~70 kDa protein was detected in REF 52 cells using anti-WDR1 antibodies. The sequence identification of this protein and those of additional WDR1 isoforms may provide insight into their transcriptional regulation. Examination of the

162

localization patterns of different WDR1 isoforms and analysis of the cytoskeletal effects from their over-expression in cells will be helpful for determining isoform functions.

Novel WDR1 Interacting Proteins:

Identification of novel proteins interactions (including additional isoforms) could be assayed in a similar manner using sequence analysis or direct antibody detection. The interaction established in yeast between WDR1 (Aip1), cofilin, CAP1 and actin would be of extreme interest to validate in mammalian systems. It is possible that the lack of interaction between these proteins and hWDR1 could be due to inappropriate experimental conditions. Therefore, the repetition of the IP interactions experiments should be performed using protein extracts from cells treated with actin remodeling agents such as Latrunculin A (binds G-actin and inhibits actin polymerization), Cytochalasin D (similarly blocks actin polymerization), Forskolin (stimulator of adenylyl cyclase), Phorbol 12-myristate 13-acetate (PMA, stimulates lamellipodia formation), Lysophosphatidic acid (LPA, induces stress fiber formation), as well as expressing constitutively active mutants of the Rho effectors Rho, Rac, and Cdc42 to induced different mechanisms of actin remodeling events. These experiments would augment the identification of transient or dynamic protein binding interactions. Immunoprecipitation experiments for the detection of possible multimer protein complexes could also be performed using actin disrupting agents.

WDR1 and Cell Migration:

The identification of WDR1 (and potential interacting proteins) within the WACs could be performed using mass spectrometry analysis. The effect of WDR1 proteins during cell attachment and migration could also be assessed using both endogenous and

163

exogenous protein expression and temporal ICC localization techniques. The effect of WDR1 within motile cells could be investigated using either ICC imaging of several motile cell types employing different adhesion complexes such as keratinocyte and fibroblast cell lines. Additionally, the effects of several actin disrupting compounds could be employed to further characterize the mechanism through which WDR1 associates with actin to form adhesion complexes.

Furthermore, disruption of hWDR1 expression could be performed through inhibitory RNA technology (RNA*i*) and the effect of decreasing WDR1 expression on these processes could be examined.

Examination of Isoform Expression:

To further explore the function of WDR1 proteins and their mechanisms of expression, the regulation of WDR1 transcripts within different cell types should be investigated using northern blot analysis. Particularly, the differential regulation of WDR1 transcripts within non-transformed and transformed cell lines and their corresponding WDR1 protein expression patterns should be compared. The exogenous manipulations of the endogenous expression levels of WDR1 proteins should be assayed, with particular attention to cell CS adhesion. Additional investigation could employ RNAi to disrupt the expression of WDR1 within both the transformed and non-transformed cell lines. The function of WDR1 proteins during neurogenesis, cell division, and cell migration could also be investigated using RNA*i* studies, and may further support distinct functions of WDR1 isoforms.

164

Final Considerations:

The recent identification of WDR1 proteins has identified a family of proteins characterized by the presence of multiple WD motifs, which also show strong homology to the kelch motifs identified in *Drosophila* kelch proteins. WDR1 proteins, similar to kelch proteins have been shown to interact with actin and other actin-associated proteins such as cofilin and CAP1 during dynamic cortical actin rearrangement events. The proteins have also been shown to regulate membrane dynamics, cytokinesis, cell migration, and in this thesis cell adhesion. Additionally, the differential display of hWDR1 proteins between transformed and non-transformed cell types has been demonstrated. These results clearly indicate potential regulatory functions for WDR1 proteins during several critical cellular behaviours implicated in many mechanisms of disease. Further study of these proteins should hopefully not just embellish our current understanding of cellular processes, but also provide a potential target for novel molecular therapies and medical treatments.

References

Abe, T., Kato, M., Miki, H., Takenawa, T. and Endo, T. (2003) Small GTPase Tc10 and its homologue RhoT induce N-WASP-mediated long process formation and neurite outgrowth. *J Cell Sci*, 116, 155-168.

Adams, J., Kelso, R. and Cooley, L. (2000) The kelch repeat superfamily of proteins: propellers of cell function. *Trends Cell Biol*, 10, 17-24.

Adams, J.C. and Schwartz, M.A. (2000) Stimulation of fascin spikes by thrombospondin-1 is mediated by the GTPases Rac and Cdc42. *J Cell Biol*, 150, 807-822.

Adjei, A.A. (2001) Ras signaling pathway proteins as therapeutic targets. *Curr Pharm Des*, 7, 1581-1594.

Adler, H.J., Winnicki, R.S., Gong, T.W. and Lomax, M.I. (1999) A gene upregulated in the acoustically damaged chick basilar papilla encodes a novel WD40 repeat protein. *Genomics*, 56, 59-69.

Aizawa, H., Katadae, M., Maruya, M., Sameshima, M., Murakami-Murofushi, K. and Yahara, I. (1999) Hyperosmotic stress-induced reorganization of actin bundles in Dictyostelium cells over-expressing cofilin. *Genes Cells*, 4, 311-324.

Amberg, D.C., Basart, E. and Botstein, D. (1995) Defining protein interactions with yeast actin in vivo. *Nat Struct Biol*, 2, 28-35.

Bailly, M. (2003) Connecting cell adhesion to the actin polymerization machinery: vinculin as the missing link? *Trends Cell Biol*, 13, 163-165.

Bailly, M., Craig, S.W. and Chen, H. (2003) Connecting cell adhesion to the actin polymerization machinery: vinculin as the missing link?

Lamellipodia protrusion: moving interactions of vinculin and Arp2/3. *Trends Cell Biol*, 13, 163-165.

Bailly, M., Ichetovkin, I., Grant, W., Zebda, N., Machesky, L.M., Segall, J.E. and Condeelis, J. (2001) The F-actin side binding activity of the Arp2/3 complex is essential for actin nucleation and lamellipod extension. *Curr Biol*, 11, 620-625.

Balcer, H.I., Goodman, A.L., Rodal, A.A., Smith, E., Kugler, J., Heuser, J.E. and Goode, B.L. (2003) Coordinated regulation of actin filament turnover by a high-molecular-weight Srv2/CAP complex, cofilin, profilin, and Aip1. *Curr Biol*, 13, 2159-2169.

Bamburg, J.R. (1999) Proteins of the ADF/cofilin family: essential regulators of actin dynamics. *Annu Rev Cell Dev Biol*, 15, 185-230.

Bamburg, J.R., McGough, A. and Ono, S. (1999) Putting a new twist on actin: ADF/cofilins modulate actin dynamics. *Trends Cell Biol*, 9, 364-370.

Bamburg, J.R., Minamide, L.S., Morgan, T.E., Hayden, S.M., Giuliano, K.A. and Koffer, A. (1991) Purification and characterization of low-molecular-weight actin-depolymerizing proteins from brain and cultured cells. *Methods Enzymol*, 196, 125-140.

Bamburg, J.R. and Wiggan, O.P. (2002) ADF/cofilin and actin dynamics in disease. *Trends Cell Biol*, 12, 598-605.

Bass, M.D., Patel, B., Barsukov, I.G., Fillingham, I.J., Mason, R., Smith, B.J., Bagshaw, C.R. and Critchley, D.R. (2002) Further characterization of the interaction between the cytoskeletal proteins talin and vinculin. *Biochem J*, 362, 761-768.

Belmont, L.D. and Drubin, D.G. (2001) Actin structure function relationships revealed by yeast molecular genetics. *Results Probl Cell Differ*, 32, 103-121.

Birkenfeld, J., Betz, H. and Roth, D. (2003) Identification of cofilin and LIM-domain-containing protein kinase 1 as novel interaction partners of 14-3-3 zeta. *Biochem J*, 369, 45-54.

Bishop, A.L. and Hall, A. (2000) Rho GTPases and their effector proteins. *Biochem J*, 348 Pt 2, 241-255.

Blanchoin, L. and Pollard, T.D. (2002) Hydrolysis of ATP by polymerized actin depends on the bound divalent cation but not profilin. *Biochemistry*, 41, 597-602.

Blanchoin, L., Pollard, T.D. and Mullins, R.D. (2000) Interactions of ADF/cofilin, Arp2/3 complex, capping protein and profilin in remodeling of branched actin filament networks. *Curr Biol*, 10, 1273-1282.

Blangy, A., Vignal, E., Schmidt, S., Debant, A., Gauthier-Rouviere, C. and Fort, P. (2000) TrioGEF1 controls Rac- and Cdc42-dependent cell structures through the direct activation of rhoG. *J Cell Sci*, 113 (Pt 4), 729-739.

Brieher, W.M., Coughlin, M. and Mitchison, T.J. (2004) Fascin-mediated propulsion of Listeria monocytogenes independent of frequent nucleation by the Arp2/3 complex. *J Cell Biol*, 165, 233-242.

Chan, A.Y., Bailly, M., Zebda, N., Segall, J.E. and Condeelis, J.S. (2000) Role of cofilin in epidermal growth factor-stimulated actin polymerization and lamellipod protrusion. *J Cell Biol*, 148, 531-542.

Chang, F. and Peter, M. (2002) Cell biology. Formins set the record straight. *Science*, 297, 531-532.

Chen, H., Bernstein, B.W. and Bamburg, J.R. (2000) Regulating actin-filament dynamics in vivo. *Trends Biochem Sci*, 25, 19-23.

Chen, Y., Derin, R., Petralia, R.S. and Li, M. (2002) Actinfilin, a brain-specific actin-binding protein in postsynaptic density. *J Biol Chem*, 277, 30495-30501.

Clayton, L., Hall, A. and Johnson, M.H. (1999) A role for Rho-like GTPases in the polarisation of mouse eight-cell blastomeres. *Dev Biol*, 205, 322-331.

Condeelis, J.S., Wyckoff, J.B., Bailly, M., Pestell, R., Lawrence, D., Backer, J. and Segall, J.E. (2001) Lamellipodia in invasion. *Semin Cancer Biol*, 11, 119-128.

Cooper, J.A. and Schafer, D.A. (2000) Control of actin assembly and disassembly at filament ends. *Curr Opin Cell Biol*, 12, 97-103.

Cotteret, S. and Chernoff, J. (2002) The evolutionary history of effectors downstream of Cdc42 and Rac. *Genome Biol*, 3, REVIEWS0002.

Critchley, D.R. (2000) Focal adhesions - the cytoskeletal connection. *Curr Opin Cell Biol*, 12, 133-139.

Critchley, D.R., Holt, M.R., Barry, S.T., Priddle, H., Hemmings, L. and Norman, J. (1999) Integrin-mediated cell adhesion: the cytoskeletal connection. *Biochem Soc Symp*, 65, 79-99.

Dawe, H.R., Minamide, L.S., Bamburg, J.R. and Cramer, L.P. (2003) ADF/cofilin controls cell polarity during fibroblast migration. *Curr Biol*, 13, 252-257.

Drechsel, D.N., Hyman, A.A., Hall, A. and Glotzer, M. (1997) A requirement for Rho and Cdc42 during cytokinesis in Xenopus embryos. *Curr Biol*, 7, 12-23.

Evangelista, M., Pruyne, D., Amberg, D.C., Boone, C. and Bretscher, A. (2002) Formins direct Arp2/3-independent actin filament assembly to polarize cell growth in yeast. *Nat Cell Biol*, 4, 32-41.

Falck, S., Paavilainen, V.O., Wear, M.A., Grossmann, J.G., Cooper, J.A. and Lappalainen, P. (2004) Biological role and structural mechanism of twinfilin-capping protein interaction. *Embo J*, 23, 3010-3019.

Freeman, N.L. and Field, J. (2000) Mammalian homolog of the yeast cyclase associated protein, CAP/Srv2p, regulates actin filament assembly. *Cell Motil Cytoskeleton*, 45, 106-120.

Geiger, C., Nagel, W., Boehm, T., van Kooyk, Y., Figdor, C.G., Kremmer, E., Hogg, N., Zeitlmann, L., Dierks, H., Weber, K.S. and Kolanus, W. (2000) Cytohesin-1 regulates beta-2 integrin-mediated adhesion through both ARF-GEF function and interaction with LFA-1. *Embo J*, 19, 2525-2536.

Gerisch, G., Faix, J., Kohler, J. and Muller-Taubenberger, A. (2004) Actin-binding proteins required for reliable chromosome segregation in mitosis. *Cell Motil Cytoskeleton*, 57, 18-25.

Gettemans, J., Meerschaert, K., Vandekerckhove, J. and De Corte, V. (2003) A kelch beta propeller featuring as a G beta structural mimic: reinventing the wheel? *Sci STKE*, 2003, PE27.

Goode, B.L., Drubin, D.G. and Barnes, G. (2000) Functional cooperation between the microtubule and actin cytoskeletons. *Curr Opin Cell Biol*, 12, 63-71.

Goode, B.L. and Rodal, A.A. (2001) Modular complexes that regulate actin assembly in budding yeast. *Curr Opin Microbiol*, 4, 703-712.

Gungabissoon, R.A. and Bamburg, J.R. (2003) Regulation of growth cone actin dynamics by ADF/cofilin. *J Histochem Cytochem*, 51, 411-420.

Hahne, P., Sechi, A., Benesch, S. and Small, J.V. (2001) Scar/WAVE is localised at the tips of protruding lamellipodia in living cells. *FEBS Lett*, 492, 215-220.

Hall, A. (1994) Small GTP-binding proteins and the regulation of the actin cytoskeleton. *Annu Rev Cell Biol*, 10, 31-54.

Hall, A. (1998a) G proteins and small GTPases: distant relatives keep in touch. *Science*, 280, 2074-2075.

Hall, A. (1998b) Rho GTPases and the actin cytoskeleton. *Science*, 279, 509-514.

Hall, A. and Nobes, C.D. (2000) Rho GTPases: molecular switches that control the organization and dynamics of the actin cytoskeleton. *Philos Trans R Soc Lond B Biol Sci*, 355, 965-970.

Hall, P.F. (1995) The roles of microfilaments and intermediate filaments in the regulation of steroid synthesis. *J Steroid Biochem Mol Biol*, 55, 601-605.

Higgs, H.N. and Pollard, T.D. (2001) Regulation of actin filament network formation through ARP2/3 complex: activation by a diverse array of proteins. *Annu Rev Biochem*, 70, 649-676.

Ho, J. and Bretscher, A. (2001) Ras regulates the polarity of the yeast actin cytoskeleton through the stress response pathway. *Mol Biol Cell*, 12, 1541-1555.

Hubberstey, A., Yu, G., Loewith, R., Lakusta, C. and Young, D. (1996) Mammalian CAP interacts with CAP, CAP2, and actin. *J Cell Biochem*, 61, 459-466.

Hubberstey, A.V. and Mottillo, E.P. (2002) Cyclase-associated proteins: CAPacity for linking signal transduction and actin polymerization. *Faseb J*, 16, 487-499.

Ichii, T., Koyama, H., Tanaka, S., Kim, S., Shioi, A., Okuno, Y., Raines, E.W., Iwao, H., Otani, S. and Nishizawa, Y. (2001) Fibrillar collagen specifically regulates human vascular smooth muscle cell genes involved in cellular responses and the pericellular matrix environment. *Circ Res*, 88, 460-467.

Iida, K. and Yahara, I. (1999) Cooperation of two actin-binding proteins, cofilin and Aip1, in Saccharomyces cerevisiae. *Genes Cells*, 4, 21-32.

Jacobs, J.R. and Stevens, J.K. (1986) Changes in the organization of the neuritic cytoskeleton during nerve growth factor-activated differentiation of PC12 cells: a serial electron microscopic study of the development and control of neurite shape. *J Cell Biol*, 103, 895-906.

Kaverina, I., Krylyshkina, O., Beningo, K., Anderson, K., Wang, Y.L. and Small, J.V. (2002a) Tensile stress stimulates microtubule outgrowth in living cells. *J Cell Sci*, 115, 2283-2291.

Kaverina, I., Krylyshkina, O. and Small, J.V. (2002b) Regulation of substrate adhesion dynamics during cell motility. *Int J Biochem Cell Biol*, 34, 746-761.

Kedes, L., Ng, S.Y., Lin, C.S., Gunning, P., Eddy, R., Shows, T. and Leavitt, J. (1985) The human beta-actin multigene family. *Trans Assoc Am Physicians*, 98, 42-46.

Kelso, R.J., Hudson, A.M. and Cooley, L. (2002) Drosophila Kelch regulates actin organization via Src64-dependent tyrosine phosphorylation. *J Cell Biol*, 156, 703-713.

Kim, I.F., Mohammadi, E. and Huang, R.C. (1999) Isolation and characterization of IPP, a novel human gene encoding an actin-binding, kelch-like protein. *Gene*, 228, 73-83.

Kong, K.Y. and Kedes, L. (2004) Cytoplasmic nuclear transfer of the actin-capping protein tropomodulin. *J Biol Chem*, 279, 30856-30864.

Konzok, A., Weber, I., Simmeth, E., Hacker, U., Maniak, M. and Muller-Taubenberger, A. (1999) DAip1, a Dictyostelium homologue of the yeast actin-interacting protein 1, is involved in endocytosis, cytokinesis, and motility. *J Cell Biol*, 146, 453-464.

Kowalczynska, H.M. and Nowak-Wyrzykowska, M. (2003) Modulation of adhesion, spreading and cytoskeleton organization of 3T3 fibroblasts by sulfonic groups present on polymer surfaces. *Cell Biol Int*, 27, 101-114.

Krendel, M.F. and Bonder, E.M. (1999) Analysis of actin filament bundle dynamics during contact formation in live epithelial cells. *Cell Motil Cytoskeleton*, 43, 296-309.

Kroeze, W.K., Sheffler, D.J. and Roth, B.L. (2003) G-protein-coupled receptors at a glance. *J Cell Sci*, 116, 4867-4869.

Kuhn, T.B., Brown, M.D. and Bamburg, J.R. (1998) Rac1-dependent actin filament organization in growth cones is necessary for beta1-integrin-mediated advance but not for growth on poly-D-lysine. *J Neurobiol*, 37, 524-540.

Kuhn, T.B., Meberg, P.J., Brown, M.D., Bernstein, B.W., Minamide, L.S., Jensen, J.R., Okada, K., Soda, E.A. and Bamburg, J.R. (2000) Regulating actin dynamics in neuronal growth cones by ADF/cofilin and rho family GTPases. *J Neurobiol*, 44, 126-144.

Little, K.D., Hemler, M.E. and Stipp, C.S. (2004) Dynamic regulation of a GPCR-tetraspanin-G protein complex on intact cells: central role of CD81 in facilitating GPR56-Galpha q/11 association. *Mol Biol Cell*, 15, 2375-2387.

Lomax, M.I., Gong, T.W., Cho, Y., Huang, L., Oh, S.H., Adler, H.J., Raphael, Y. and Altschuler, R.A. (2001) Differential Gene Expression Following Noise Trauma in Birds and Mammals. *Noise Health*, 3, 19-35.

Machesky, L.M. and Hall, A. (1996) Rho: a connection between membrane receptor signalling and the cytoskeleton. *Trends Cell Biol*, 6, 304-310.

Machesky, L.M. and Hall, A. (1997) Role of actin polymerization and adhesion to extracellular matrix in Rac- and Rho-induced cytoskeletal reorganization. *J Cell Biol*, 138, 913-926.

Matsumoto, S., Ogawa, M., Kasakura, T., Shimada, Y., Mitsui, M., Maruya, M., Isohata, M., Yahara, I. and Murakami-Murofushi, K. (1998) A novel 66-kDa stress protein, p66, associated with the process of cyst formation of Physarum polycephalum is a Physarum homologue of a yeast actin-interacting protein, AIP1. *J Biochem (Tokyo)*, 124, 326-331.

Medley, Q.G., Buchbinder, E.G., Tachibana, K., Ngo, H., Serra-Pages, C. and Streuli, M. (2003) Signaling between focal adhesion kinase and trio. *J Biol Chem*, 278, 13265-13270.

Mohri, K. and Ono, S. (2003) Actin filament disassembling activity of Caenorhabditis elegans actin-interacting protein 1 (UNC-78) is dependent on filament binding by a specific ADF/cofilin isoform. *J Cell Sci*, 116, 4107-4118.

Mohri, K., Takano-Ohmuro, H., Nakashima, H., Hayakawa, K., Endo, T., Hanaoka, K. and Obinata, T. (2000) Expression of cofilin isoforms during development of mouse striated muscles. *J Muscle Res Cell Motil*, 21, 49-57.

Mohri, K., Vorobiev, S., Fedorov, A.A., Almo, S.C. and Ono, S. (2004) Identification of functional residues on Caenorhabditis elegans actin-interacting protein 1 (UNC-78) for disassembly of actin depolymerizing factor/cofilin-bound actin filaments. *J Biol Chem*, 279, 31697-31707.

Mohri, T., Kameshita, I., Suzuki, S., Hioki, K., Tokunaga, R. and Takatani, S. (1998) Rapid adhesion and spread of non-adherent colon cancer Colo201 cells induced by the protein kinase inhibitors, K252a and KT5720 and suppression of the adhesion by the immunosuppressants FK506 and cyclosporin A. *Cell Struct Funct*, 23, 255-264.

Moriyama, K. and Yahara, I. (2002) The actin-severing activity of cofilin is exerted by the interplay of three distinct sites on cofilin and essential for cell viability. *Biochem J*, 365, 147-155.

Nakagawa, H., Miki, H., Ito, M., Ohashi, K., Takenawa, T. and Miyamoto, S. (2001) N-WASP, WAVE and Mena play different roles in the organization of actin cytoskeleton in lamellipodia. *J Cell Sci*, 114, 1555-1565.

Nakayama, A.Y. and Luo, L. (2000) Intracellular signaling pathways that regulate dendritic spine morphogenesis. *Hippocampus*, 10, 582-586.

Nobes, C.D. and Hall, A. (1995) Rho, rac, and cdc42 GTPases regulate the assembly of multimolecular focal complexes associated with actin stress fibers, lamellipodia, and filopodia. *Cell*, 81, 53-62.

Nobes, C.D. and Hall, A. (1999) Rho GTPases control polarity, protrusion, and adhesion during cell movement. *J Cell Biol*, 144, 1235-1244.

Nobes, C.D., Lauritzen, I., Mattei, M.G., Paris, S., Hall, A. and Chardin, P. (1998) A new member of the Rho family, Rnd1, promotes disassembly of actin filament structures and loss of cell adhesion. *J Cell Biol*, 141, 187-197.

Oh, S.H., Adler, H.J., Raphael, Y. and Lomax, M.I. (2002) WDR1 colocalizes with ADF and actin in the normal and noise-damaged chick cochlea. *J Comp Neurol*, 448, 399-409.

Ojala, P.J., Paavilainen, V. and Lappalainen, P. (2001) Identification of yeast cofilin residues specific for actin monomer and PIP2 binding. *Biochemistry*, 40, 15562-15569.

Okada, K., Blanchoin, L., Abe, H., Chen, H., Pollard, T.D. and Bamburg, J.R. (2002) Xenopus actin-interacting protein 1 (XAip1) enhances cofilin fragmentation of filaments by capping filament ends. *J Biol Chem*, 277, 43011-43016.

Okada, K., Obinata, T. and Abe, H. (1999) XAIP1: a Xenopus homologue of yeast actin interacting protein 1 (AIP1), which induces disassembly of actin filaments cooperatively with ADF/cofilin family proteins. *J Cell Sci*, 112 (Pt 10), 1553-1565.

Olivo, C., Vanni, C., Mancini, P., Silengo, L., Torrisi, M.R., Tarone, G., Defilippi, P. and Eva, A. (2000) Distinct involvement of cdc42 and RhoA GTPases in actin organization and cell shape in untransformed and Dbl oncogene transformed NIH3T3 cells. *Oncogene*, 19, 1428-1436.

Ono, S. (2001) The Caenorhabditis elegans unc-78 gene encodes a homologue of actin-interacting protein 1 required for organized assembly of muscle actin filaments. *J Cell Biol*, 152, 1313-1319.

Ono, S. (2003) Regulation of actin filament dynamics by actin depolymerizing factor/cofilin and actin-interacting protein 1: new blades for twisted filaments. *Biochemistry*, 42, 13363-13370.

Otterbein, L.R., Graceffa, P. and Dominguez, R. (2001) The crystal structure of uncomplexed actin in the ADP state. *Science*, 293, 708-711.

Paavilainen, V.O., Bertling, E., Falck, S. and Lappalainen, P. (2004) Regulation of cytoskeletal dynamics by actin-monomer-binding proteins. *Trends Cell Biol*, 14, 386-394.

Peraud, A., Mondal, S., Hawkins, C., Mastronardi, M., Bailey, K. and Rutka, J.T. (2003) Expression of fascin, an actin-bundling protein, in astrocytomas of varying grades. *Brain Tumor Pathol*, 20, 53-58.

Pollard, T.D. (2001) Genomics, the cytoskeleton and motility. *Nature*, 409, 842-843.

Pollard, T.D. (2002) Formins initiate new actin filaments. *Nat Cell Biol*, 4, E191.

Pollard, T.D. (2003) The cytoskeleton, cellular motility and the reductionist agenda. *Nature*, 422, 741-745.

Pollard, T.D. (2004) Formins coming into focus. *Dev Cell*, 6, 312-314.

Pollard, T.D., Blanchoin, L. and Mullins, R.D. (2000) Molecular mechanisms controlling actin filament dynamics in nonmuscle cells. *Annu Rev Biophys Biomol Struct*, 29, 545-576.

Pollard, T.D., Blanchoin, L. and Mullins, R.D. (2001) Actin dynamics. *J Cell Sci*, 114, 3-4.

Pollard, T.D. and Borisy, G.G. (2003) Cellular motility driven by assembly and disassembly of actin filaments. *Cell*, 112, 453-465.

Pruyne, D. and Bretscher, A. (2000) Polarization of cell growth in yeast. *J Cell Sci*, 113 (Pt 4), 571-585.

Ridley, A.J. and Hall, A. (1994) Signal transduction pathways regulating Rho-mediated stress fibre formation: requirement for a tyrosine kinase. *Embo J*, 13, 2600-2610.

Robinson, D.N. and Cooley, L. (1997) Drosophila kelch is an oligomeric ring canal actin organizer. *J Cell Biol*, 138, 799-810.

Rodal, A.A., Tetreault, J.W., Lappalainen, P., Drubin, D.G. and Amberg, D.C. (1999) Aip1p interacts with cofilin to disassemble actin filaments. *J Cell Biol*, 145, 1251-1264.

Rodriguez, O.C., Schaefer, A.W., Mandato, C.A., Forscher, P., Bement, W.M. and Waterman-Storer, C.M. (2003) Conserved microtubule-actin interactions in cell movement and morphogenesis. *Nat Cell Biol*, 5, 599-609.

Rogers, S.L., Wiedemann, U., Stuurman, N. and Vale, R.D. (2003) Molecular requirements for actin-based lamella formation in Drosophila S2 cells. *J Cell Biol*, 162, 1079-1088.

Rosenblatt, J., Agnew, B.J., Abe, H., Bamburg, J.R. and Mitchison, T.J. (1997) Xenopus actin depolymerizing factor/cofilin (XAC) is responsible for the turnover of actin filaments in Listeria monocytogenes tails. *J Cell Biol*, 136, 1323-1332.

Sagot, I., Rodal, A.A., Moseley, J., Goode, B.L. and Pellman, D. (2002) An actin nucleation mechanism mediated by Bni1 and profilin. *Nat Cell Biol*, 4, 626-631.

Sarmiere, P.D. and Bamburg, J.R. (2002) Head, neck, and spines: a role for LIMK-1 in the hippocampus. *Neuron*, 35, 3-5.

Sarmiere, P.D. and Bamburg, J.R. (2004) Regulation of the neuronal actin cytoskeleton by ADF/cofilin. *J Neurobiol*, 58, 103-117.

Small, J.V., Stradal, T., Vignal, E. and Rottner, K. (2002) The lamellipodium: where motility begins. *Trends Cell Biol*, 12, 112-120.

Soltysik-Espanola, M., Rogers, R.A., Jiang, S., Kim, T.A., Gaedigk, R., White, R.A., Avraham, H. and Avraham, S. (1999) Characterization of Mayven, a novel actin-binding protein predominantly expressed in brain. *Mol Biol Cell*, 10, 2361-2375.

Tseng, Y., An, K.M., Esue, O. and Wirtz, D. (2004) The bimodal role of filamin in controlling the architecture and mechanics of F-actin networks. *J Biol Chem*, 279, 1819-1826.

Tseng, Y., Schafer, B.W., Almo, S.C. and Wirtz, D. (2002) Functional synergy of actin filament cross-linking proteins. *J Biol Chem*, 277, 25609-25616.

Turner, A.M., Dowell, N., Turner, S.W., Kam, L., Isaacson, M., Turner, J.N., Craighead, H.G. and Shain, W. (2000) Attachment of astroglial cells to microfabricated pillar arrays of different geometries. *J Biomed Mater Res*, 51, 430-441.

Turner, C.E. (2000) Paxillin interactions. *J Cell Sci*, 113 Pt 23, 4139-4140.

Uruno, T., Liu, J., Li, Y., Smith, N. and Zhan, X. (2003) Sequential interaction of actin-related proteins 2 and 3 (Arp2/3) complex with neural Wiscott-Aldrich syndrome protein (N-WASP) and cortactin during branched actin filament network formation. *J Biol Chem*, 278, 26086-26093.

van Kooyk, Y., van Vliet, S.J. and Figdor, C.G. (1999) The actin cytoskeleton regulates LFA-1 ligand binding through avidity rather than affinity changes. *J Biol Chem*, 274, 26869-26877.

Verma, A. and Ihler, G.M. (2002) Activation of Rac, Cdc42 and other downstream signalling molecules by Bartonella bacilliformis during entry into human endothelial cells. *Cell Microbiol*, 4, 557-569.

Verma, R., Ramnath, J., Clemens, F., Kaspin, L.C. and Landolph, J.R. (2004a) Molecular biology of nickel carcinogenesis: identification of differentially expressed genes in morphologically transformed C3H10T1/2 Cl 8 mouse embryo fibroblast cell lines induced by specific insoluble nickel compounds. *Mol Cell Biochem*, 255, 203-216.

Verma, S., Shewan, A.M., Scott, J.A., Helwani, F.M., den Elzen, N.R., Miki, H., Takenawa, T. and Yap, A.S. (2004b) Arp2/3 activity is necessary for efficient formation of E-cadherin adhesive contacts. *J Biol Chem*, 279, 34062-34070.

Virel, A. and Backman, L. (2004) Molecular evolution and structure of alpha-actinin. *Mol Biol Evol*, 21, 1024-1031.

Voegtli, W.C., Madrona, A.Y. and Wilson, D.K. (2003) The structure of Aip1p, a WD repeat protein that regulates Cofilin-mediated actin depolymerization. *J Biol Chem*, 278, 34373-34379.

Way, M., Sanders, M., Garcia, C., Sakai, J. and Matsudaira, P. (1995) Sequence and domain organization of scruin, an actin-cross-linking protein in the acrosomal process of Limulus sperm. *J Cell Biol*, 128, 51-60.

Xu, J., Wang, F., Van Keymeulen, A., Herzmark, P., Straight, A., Kelly, K., Takuwa, Y., Sugimoto, N., Mitchison, T. and Bourne, H.R. (2003) Divergent signals and cytoskeletal assemblies regulate self-organizing polarity in neutrophils. *Cell*, 114, 201-214.

Appendix A

Forward Primer	Sequence
133	TTGAATTCATGCCGTACGAGATCAAGAG
163	TTGAATTCTTAACGTCCGCCTGTATTCCATC
143	TTGAATTCATGGCCTCCGGTGTGGCTG
144	TTGAATTCTAATGCCGTACGAGATCAAG
147	TTGAATTCTGGACAGAAACAACCCCAGC
156	GTGTGCATTGGACAGATTGTCCT
149	CTCCTTGGAGGCCATGTGGGCC

Reverse Primer	Sequence
139	TTGCGGCCGCTCAGTAGGTGATTGTCCAC
132	TTGCGGCCGCTTATTTTTCATGGTGTCCATA
141	TTGCGGCCGCTCAAAAGGCTTGCCCTCC
145	TTCTCGAGTCAGTAGGTGATTGTCCACTC
146	TTCTGAGTCAGTACCCGGACAGGGAGACAC
162	TTCTCGAGTCAGTACCCGGACAGGGAGACAC
155	GACCACGGCGATCCTCTTACTGT
150	CTCCTTGGAGGCCATGTGGGCC

174

VITA AUCTORIS

Tenley E. Noone, Department of Biological Sciences,
University of Windsor

Education:
University of Windsor: Master's of Biological Sciences degree
Duration: September 2002- July 2004
Supervisor: Dr. Andrew Hubberstey
Thesis: 'The Isolation and Characterization of the Mammalian Actin Interacting Protein WDR1'
Focus: Regulation of the Mammalian Actin Cytoskeleton
Additional Interests: Mammalian Signaling Transduction pathways, the Regulation of
Apoptotic pathways, the Biochemistry of Tertiary Protein structure

University of Windsor: Bachelor of Science Honors degree (with Chemistry Minor)
Duration: September 1998 – August 2002
Contact: Dr. David Cotter
Focus: Anatomy, Biochemistry, Chemistry, Immunology, Physiology, Microbiology,
Molecular Biotechnology.

Graduate Experience:
Publications:
Noone, T, E., and Hubberstey, A.V
Mammalian WDR1, an Actin-Binding Protein, Associates at Focal Adhesion Complexes within Rat Embryonic Fibroblast cells. (in preparation)

Published Abstracts:
Conference: 19th Annual International Congress of Biochemistry and Molecular
Biology
Abstract: 'Characterization of the Role of Mammalian WDR1 Proteins in Cell
Growth and Differentiation'
Accepted: June 2003, Conference Scheduled July 21st-25th, 2003

Conference: 43rd Annual American Society for Cell Biology Conference
Abstract: 'Functional Characterization of Mammalian WDR1 Proteins in Actin
Cytoskeletal Rearrangement'
Accepted: August 2003, Conference Scheduled December 13-17th, 2003

Awards:
Graduate Travel Award 2003-2004
University of Windsor Student Alliance Science Award 2001-2002 (Undergraduate)

175

University of Windsor Residence Entrance Scholarship Award 1998-1999
(Undergraduate)

Academic Accomplishments:
Dynamics of Protein Folding and Structure 03-59-663   Grade: +A
Winter 2004, University of Windsor
>   I will present a lecture on the regulation of tertiary
>   protein structure dynamics and submitted a paper
>   comparing the biological functions of selected groups
>   of isomers and potential biotechnological therapies.
Contact: Dr. Sirnart Ananvoranich

Selected Readings in Biology (Signal Transduction) 03-55-521   Grade: +A
Winter 2003, University of Windsor
>   I presented a seminar discussing the possibility of
>   inhibiting bacterial virulence factor transcription
>   *in vivo* through the novel quorum sensing pathway to
>   suppress biofilm formation within the lungs of CF
>   patients and submitted a paper further discussing this
>   novel antimicrobial mechanism.
Contact: Dr. Adan Ali

Principles of Disease (Apoptosis) 03-59-684   Grade: A
Fall 2002, University of Windsor
>   I presented a lecture on the suspected role of
>   G-actin during the cellular process of Apoptosis
>   and submitted a NSERC style research proposal
>   detailing the work that requires further completion
>   on the same topic and the relevance of that knowledge
>   to the fields of cellular and molecular biology.
Contact: Dr. Siyaram Pandey

Instructing and Lecturing Accomplishments:
Guest Lecturer for 03-55-460 'Molecular Biotechnology'
Winter 2004
>   I have been invited to introduce the field of Stem Cell research and discuss current
>   issues impeding research within that field.

**Graduate Seminar 'The Current Role of WDR1 during Actin Tread-milling and
Actin Signaling within Focal Adhesion Complexes'**
Winter 2004
>   I provided an overview of the currently known functions of WDR1 proteins across
>   species, and provided a functional model supplemented my results of WDR1 and
>   actin remodeling, and discussed my novel data demonstrating WDR1 at the focal

adhesion complex of fibroblast cells.

Graduate Teaching Assistant 03-55-202 Human Anatomy
Winter/ Fall 2003, Winter 2004

I instructed two sections of the undergraduate human anatomy
laboratory for the last three semesters which included guiding students through a
complete feline dissection and a partial dissection of selected sheep organs.

Graduate Seminar 'Characterization of Actin Interacting Protein WDR1'
Winter 2003

I delivered a lecture detailing the previously published support for my thesis and
the novel contribution my work presents to the field of cellular biology in addition
to discussing techniques utilized for my thesis.

Guest Lecturer for 03-55-238 'Introduction to Microbiology and Techniques'
Fall 2002

I discussed a novel method of bacterial cell signaling
which governs the expression of many bacterial processes such as
virulence factor regulation, metabolic regulation and biofilm
formation and architecture.

Graduate Teaching Assistant 03-55-238 Introduction of Microbiology and Techniques
Fall 2002

I instructed two sections of the undergraduate microbiology
laboratory in which I taught basic microbial laboratory techniques
procedures to secondary year biology, biotechnology and biochemistry
students.

<u>Current Medical Experience:</u>
Post-*Mortem* Medical Anatomy
Fall 2003

I have performed a lecture and dissection of a porcine model for
the citizens of the Windsor-Essex community, the St. Clair college community as
well as University patrons in which I detailed basic anatomical organ structure and
function, and introduced commonly associated diseases in efforts to promote public
health awareness and to provide funding for two non-profit Volunteer groups
focused on providing community medical services.
Contact: Dr. Richard Caron, Dean of Science, University of Windsor

University of Windsor's Emergency Response Team Responder
1999-current

I am an active responder for the university's emergency response team,
and have been so since 1999. I am certified in First-aid, CPR, Emergency
Oxygen Administration, and Emergency Automated Defibrillation
Administration. I am responsible for responding to any emergency medical

177

requirements on campus.
Contact: Jeffry Bilyck, Dir. Emergency Response Team, University of Windsor

University of Windsor Emergency Responder Volunteer of the Year Award
Awarded for the 1999-2000 Year

     I was awarded this award of excellence for my contributions to
     the team and the patients I treated. I have volunteered to assist professional
     paramedics on active duty with in Windsor- Essex community and have
     assisted paramedics on life-threatening medical calls in addition to
     serving the university's student and non-student population with medical
     assistance.
Contact: Jeffry Bilyck, Dir. Emergency Response Team, University of Windsor

Department of Biological Sciences Service:
Biological Sciences Departmental Council Graduate Student Representative
2003-2004
Biological Sciences Departmental Promotion and Tenure Committee Graduate Student Representative
2003-2004
Undergraduate Curriculum Committee Graduate Student Representative
2002-2003

Professional Associations:
American Society for Cellular Biology
2003-Current
University of Windsor Graduate Student Society
2002-Current

Additional Extra-Curricular Volunteer Work and Awards:
Windsor-Essex Regional Secondary School Science Fair Judge
Winter 2003

178